MULTI-OBJECTIVE DESIGN FOR EMC SOLUTIONS BY USING PREFERENCE SET-BASED DESIGN METHOD

BUI DUC CHINH

A dissertation submitted for the degree of

Doctor of Engineering

DEPARTMENT OF COMPUTER AND NETWORK ENGINEERING

GRADUATE SCHOOL OF INFORMATICS AND ENGINEERING

THE UNIVERSITY OF ELECTRO-COMMUNICATIONS

December 2023

Multi-Objective Design for EMC Solutions

by Using Preference Set-Based Design Method

Advisor: Associate Professor Yoshiki Kayano

Secondary Advisor: Professor Fengchao Xiao

SUPERVISORY COMMITTEE:

Professor Koji Wada

Professor Fengchao Xiao

Associate Professor Yoshiaki Ando

Associate Professor Satoshi Ono

Associate Professor Yoshiki Kayano

I would like to dedicate this dissertation to all my family and friends, who have always been supportive and encouraging during the challenges of graduate school and life.

Acknowledgments

First and foremost, I am deeply grateful to Associate Professor Yoshiki Kayano, my Ph.D. advisor, for his exceptional guidance throughout my program. Over the course of three years, his mentorship has been invaluable. Prof. Kayano taught me how to identify critical research issues, develop a structured schedule, and effectively disseminate my findings through academic publications. His visionary advice, unwavering support, and insightful feedback have played a pivotal role in my development. Furthermore, his industry experience has broadened my perspective beyond academia. His passion for impactful research has been a constant source of motivation. Prof. Kayano's research insight, technical expertise, and dedication to his students are truly irreplaceable.

I sincerely thank Professor Fengchao Xiao, my secondary advisor and mentor in Electromagnetic Compatibility at The University of Electro-Communications. Prof. Xiao's ambition and foresight have inspired me to bridge gaps in the field. I am having him as my co-advisor has been an immense privilege.

I would also like to express my deep appreciation to Professor Emeritus Yoshio Kami for his excellent guidance and valuable insights about Electromagnetic field and Preference Set-base Design method.

Furthermore, I extend my heartfelt gratitude to the committee members: Professor Koji Wada, Associate Professor Yoshiaki Ando, and Associate Professor Satoshi Ono. Their thoughtful comments and suggestions were instrumental in helping me complete this dissertation.

My heartfelt thanks go to my lab mates, Mr. Taiki Yamagiwa and Mr. Ren Kitahara. It has been a pleasure collaborating with each of you.

In addition, I am indebted to my parents, wife, and son. Your unwavering support when I arrived in Japan, thousands of miles away from home, has been instrumental in my achievements. I am grateful for your care and for making me the person I am today.

Lastly, I wish to acknowledge the Vietnam Government Information Security Committee scholarship for funding my Ph.D. course.

概要

現代の電子機器は性能だけでなく，電磁的適合性（Electromagnetic Compatibility: EMC），速度，安定性，コスト，サイズなどの多くの要件を満たさなければならない．電子機器の EMC は，複雑な電磁環境での安定性と正常な機能を確保するために重要であり，そのため電子機器の電磁妨害を制御し，電子機器の耐性を向上させるために EMC 対策を実装することがますます重要となっている．

主に使用される EMC 対策には，フィルタ法とシールド法がある．例えば，フィルタ法の一例として，電磁干渉（Electromagnetic Interference: EMI）フィルタは，電子機器に十分な電流と電圧を供給しながら，主回線に伝達されるあらゆる種類の干渉放射を低減する．シールド法は，周囲に発せられる電磁放射の減衰を確保し，外部の電磁妨害から電子機器を保護する．

このような EMC 設計では，しばしば相反する要件を含む複数の目標を同時に満たす対策が求められる．選好度付きセットベース設計（Preference Set-based Design: PSD）アプローチは，複数目標の設計手法として開発されており，すべての性能が要件を満たす場合，最高の満足度と堅牢性指数を持つ最終設計パラメータの許容範囲を得ることができる．さらに，実際の設計においてさらなる考慮が必要な問題は，不確かなパラメータの存在である．ランダムパラメータの統計的な問題を解決するために最も一般的に使用される方法は，モンテカルロ（Monte Carlo: MC）法である． MC 法は多数のサンプルから高精度な統計情報を直接得ることができるが，サンプル数が増えるにつれて多くの計算を必要とし，計算効率が低下するという欠点がある．

本論文では，上記の問題を解決するために， MC 法と比較して適切な精度を保ちながら計算効率を向上させる多項式カオス（Polynomial Chaos: PC）法による統計解析と，PSD 法による多目的満足度設計の新しい組み合わせを提案している．PC 法は不確かなパラメータをシミュレートし，PSD 法の初期フェーズのための初期データを生成するために利用される．その後，PSD 法を用いて要求に応じた設計パラメータが得られる．論文で研究されているアプリケーションは，EMI フィルタや筐体の金属板などの電磁装置の一般的な EMC 対策であり，複数の要素や不確実なパラメータを含む実践的なケースを想定している． PSD 法によって要求される性能を満たす EMC 対策の設計パラメータは範囲解で得られる．提案された手法の妥当性は，PSD 法で得られた範囲内の 1000 の設計パラメータの組み合わせを評価することで実証している．結果は，統計的手法を用いた多目的 PSD アプローチを適用することで、電子設計における製品開発の時間とコストを削減するために使用できることを示している．

本論文は 5 つの章で構成されている．第 1 章では，EMC 問題の多目的満足化設計の必要性と解決すべき課題を整理している．第 2 章では，EMC 対策，PSD 法，PC 法の基本原理及び課題点を整理している．第 3 章では PC 法と PSD 法の組み合わせ法について提案している．第 4 章では穴あき筐体を対象とした PSD 法による設計，並びに電源，負荷インピーダンスにバラツキがある場合の EMI フィルタの組み合わせ手法による設計を行っている．第 5 章は結論である．

Abstract

With the rapid development of science and technology, the number of electronic devices has increased sharply, and the operating frequency and power consumption of electronic devices (such as integrated circuits and power switching circuits) have also increased. Consequently, the electromagnetic environment surrounding these devices has become more complex and challenging. An electronic device is a system that can generate potential interference and be transmitted to the surrounding environment through conductive interference or electromagnetic radiation interference. Therefore, today's electronic devices must meet not only performance requirements but also many other requirements, such as electromagnetic compatibility, speed, stability, cost, size, etc.

Electromagnetic Compatibility (EMC) for electronic devices is essential to ensure stability and proper functioning in this complex electromagnetic environment. Therefore, implementing EMC solutions to control Electromagnetic Interference (EMI) and enhance the immunity of electronic devices has become increasingly important.

EMC solutions used are mainly the filter method and shielding method. These methods aim to attenuate the disturbances from power lines and cables or attenuate electromagnetic emissions from electronic devices to the surrounding environment and vice versa. For instance, the EMI filter, as an example of the filter method, supplies sufficient current and voltage to electronic devices while reducing any types of interference radiation that are transmitted to the main line. The shielding method ensures the attenuation of electromagnetic radiation emitted to the surrounding environment and protects electronic devices from external electromagnetic disturbances.

For such an EMC design, the requirement is to have a solution that simultaneously meets multiple objectives, sometimes including conflicting requirements. The Preference Set-based Design (PSD) approach was developed as a multi-objective design method. In this approach, when all performance meets the requirements, the allowable range of the final design parameters is obtained with the highest levels of satisfaction and robustness index.

In addition, an issue that needs further consideration in the actual design is the presence of uncertain parameters. The most common method used to solve the statistical problem of random parameters is the Monte Carlo (MC) method. The MC method can directly obtain highly accurate statistical information from many samples but has the disadvantages of

requiring many computations and poor computational efficiency as the number of samples increases. Therefore, the dissertation proposes using the Polynomial Chaos (PC) method, which enhances computational efficiency while maintaining appropriate accuracy compared to the MC method.

With the problems mentioned above, the dissertation proposes a new combination of statistical analysis by the PC method to handle the situation of randomness and multi-objective satisfactory design by the PSD method. The PC method is utilized to simulate uncertain parameters and generate the initial data for the preliminary phase of the PSD method. Subsequently, the PSD method is employed to obtain design parameters that satisfy the requirements of the application. The applications studied in the dissertation are common EMC solutions for electromagnetic equipment, including EMI filters and metal sheet of an enclosure. Applications are considered in practical cases, including plural element and uncertainty parameters. The design parameters of the EMC solutions, which satisfy required performances, are obtained in range by the PSD method. The validity of the proposed method is demonstrated with 1000 combinations of design parameters in the range obtained by the PSD method. The results indicate that applying the multi-objective PSD approach with statistical methods to handle uncertainty can reduce the time and cost of developing products in electronic designs.

This dissertation includes five chapters, as below.

Chapter 1 introduces the multi-objective design for EMC solutions, providing motivations, objectives, and an overview of the dissertation's organization.

Chapter 2 describes the problem and basic principles of the proposed method, including EMC solutions for electronics, the PSD method, and the PC method.

Chapter 3 provides an idea and the literature reviews related to the problem, and after that, proposes a method that combines the design method based on the PSD and the PC method.

Chapter 4 experiments with the proposed method with EMC solutions. The two most common EMC solutions are used: metal sheet of the enclosure and EMI filter. The validity of the proposed method is evaluated.

Chapter 5 summarizes as "Conclusion". Abstract of results and discussions in this dissertation is remarked on.

TABLE OF CONTENTS

LIST OF ABBREVIATIONS

CISPR	Comité International Spécial des Perturbations Radioélectriques
CM	Common Mode
DM	Differential Mode
DoE	Design of Experiments
EMC	Electromagnetic Compatibility
EMI	Electromagnetic Interference
EN	European Standards
IC	Integrated Circuit
IEC	International Electrotechnical Commission
I/O	Input/Output
ISO	International Organization for Standardization
MC	Monte Carlo
MIL-STD	Military Standards
PC	Polynomial Chaos
PCB	Printed Circuit Board
PCE	Polynomial Chaos Expansion
PSD	Preference Set-based Design
RF	Radio Frequency
RSM	Response Surface Methodology
SE	Shielding Effectiveness

LIST OF FIGURES

LIST OF TABLES

Chapter 1
General Introduction

Chapter 1 briefly introduces the multi-objective design for EMC solutions, providing motivations, objectives, and an overview of the dissertation's organization.

1.1. Multi-objective Design for EMC Solutions

Nowadays, the number of electronic devices has increased dramatically, and the operating frequency and power consumption of electronic devices (such as integrated circuits and power converter circuits) have increased. This creates a more complex electromagnetic environment around devices. These devices have the potential to generate interference, which can be transmitted to the surrounding environment through conductive or electromagnetic radiation interference. The issue of Electromagnetic Compatibility (EMC) for electronic devices is very important to ensure stability and proper functioning in this complex electromagnetic environment. EMC regulations, such as those set by CISPR, IEC, EN, and other standards, have become more stringent. Hence, applying EMC solutions to electronic devices to control Electromagnetic Interference (EMI) and enhance equipment immunity has become increasingly important.

Besides, electronic devices must meet many requirements, such as those related to performance, limits to the radiated electromagnetic field, size, etc. For such a design, the requirement is to have a solution that simultaneously meets multiple objectives that sometimes include conflicting requirements. Simultaneous design techniques to meet multiple performance requirements have been proposed, for example, some design methods such as the Taguchi method [1], set-based design [2], etc. On the other hand, in set-based design, the required performance and design parameters are expressed in a range, and the design parameters are narrowed to accommodate multiple performances. One of the specific methods of set-based design is the Preference Set-based Design (PSD) method [3], which has been proposed and is commonly used in the mechanical field. In the PSD method, design parameters are obtained within a range rather than an point value, so there is robust design capability, including deviations in actual production. The PSD method is not a performance optimization method but rather a design approach to meet multi-objective performance concurrently.

This dissertation focuses on two commonly studied EMC solutions: the shielding method and the EMI filter. The shielding method uses a sheet of material (usually metal) to control the propagation of electromagnetic fields between two spatial regions. It aims to prevent the transmission of electromagnetic signals from one area to another or enclose a source within a shield. Using an enclosure made of metal sheets prevents electromagnetic signals from inside to the outside and vice versa. The design of metal sheets often has to consider shielding effectiveness, including attenuation to magnetic and electric fields. The EMI filter is a fundamental EMC solution for noise suppression and is widely used in high-speed differential signal wires, power supply lines, and so on [4]. With the EMC problem, the design of the EMI filter should simultaneously satisfy the required performances for both Differential Mode (DM) and Common Mode (CM). Various EMI filter design methods have been studied, proposed, and tested, such as those using analytic electromagnetic fields, trial-and-error tests through experiments, and design using Particle Swarm Optimization, a super simulation method [5].

1.2. Motivation

The studies conducted in this dissertation explore the proposed multi-objective design options for EMC solutions. The motivation for these studies is explained as follows.

Firstly, with the traditional method (referred to as Point-based design in this dissertation) for electric systems, various trial-and-error point-based design methods are implemented. An optimal design solution is obtained by iteratively setting the initial values and continuously modifying the design variables. However, as the number of design variables and performance requirements increases, achieving values that satisfy actual specifications and performances becomes more challenging. Additionally, numerous uncertain parameters, such as bias, electromagnetic coupling, and parasitic factors, exist in the actual product, which makes the design more complex. Adopting a set-based design approach can solve multi-objective problems, reducing product development costs and time. The idea of a preference set is simple and unique, making the concurrent design process easy to understand and implement. In the PSD method, in addition to set-based characteristics, the designer's intent can be reflected in the required performances and design variables using a quantitative evaluation metric known as Preference expressed as a preference set and frequency. Because design variables are obtained in a range rather than an exact value, PSD provides robust design capabilities to include deviations in actual production. While PSD has been

successfully applied in mechanical engineering, its application in the electronics field has also yielded positive outcomes [6].

Secondly, when dealing with the EMC problem, such as the design of an EMI filter, it is crucial to simultaneously satisfy the required performances for both DM and CM. In practical cases, various issues need to be considered, including unnecessary coupling due to component miniaturization, element asymmetry, manufacturing tolerances, parasitic elements, and improper impedance matching. These factors introduce uncertain parameters that affect circuit performance in ways that are difficult or impossible to predict deterministically. Even with highly accurate simulation models, the actual performance may significantly deviate from predictions at an early stage due to this uncalculated variation. Therefore, the use of statistical simulation is necessary to evaluate the EMC performance with variations in characteristics due to unintended fluctuations of these uncertain numerical parameters. The Monte Carlo (MC) method is commonly used for simulating randomness in these cases. The MC method can directly obtain highly accurate statistical information from a large number of samples but has the disadvantages of requiring many computations and poor computational efficiency as the number of samples increases [7]. To enhance computational efficiency, this dissertation adopts another statistical method, the Polynomial Chaos (PC) method, to simulate uncertain parameters in EMC solutions. The data generated through the PC method is used as initial data for the PSD method to solve the multi-objective problem. The PC method looks for an approximate response to a system's performance as an expansion in orthogonal polynomials. Polynomial Chaos Expansion (PCE) coefficients can be calculated using various approaches, such as the stochastic testing method and stochastic Galerkin method [8], and directly provide relevant statistical information such as mean and variance. PCE is commonly used as a cheap but computationally accurate macro model. The PC method analyzes faster than the MC method, although it may be slightly less accurate. The PC method has also been applied and reviewed in circuit design [7, 8].

1.3. Objectives

The objectives identified in this dissertation align with the research purpose, which aims to establish a design method to ensure EMC in practical cases. These objectives are as follows:

+ Apply the PSD method to multi-objective design for EMC solutions. The PSD method, known for its set-based characteristics, will be utilized to address the simultaneous fulfillment of multi objectives in the design process.

+ Employ the PC method to solve the problem of uncertain parameters and generate initial data for the PSD method. By utilizing the PC method, the dissertation aims to handle uncertainties associated with parameters in EMC solutions, allowing for statistical analysis and obtaining reliable initial data for the subsequent design phase.

+ The proposed method helps to enhance calculation efficiency while ensuring accuracy. By combining the PC method with the PSD method, the dissertation seeks to improve computational efficiency compared to traditional approaches and satisfy the multi-objective requirements.

+ Apply the proposed method to two specific EMC solutions: EMI filters and metal sheets of the enclosure. The dissertation focuses on investigating and validating the effectiveness of the proposed method in the design of these common EMC solutions, considering their respective requirements and performance criteria.

By achieving these objectives, the dissertation aims to contribute to the development of a practical and efficient design method that can effectively ensure EMC in practical applications.

1.4. Dissertation Organization

The remainder of this dissertation is organized as follows:

Chapter 2 introduces the problem and basic principles of the proposed method, including EMC solutions for electronics, the PSD method, and the PC method. It begins by providing an overview of EMC and the causes of electromagnetic radiation signals, including conductive and radiated interference. The section also introduces solutions to ensure EMC for electronic devices, such as Printed Circuit Board (PCB) design, cable solutions, shielding methods, and filtering methods. Next, the multi-objective design approach is discussed, focusing on the PSD method and the main steps. Lastly, chapter 2 presents the PC method, including how to implement PCE and its advantages and disadvantages compared to the traditional MC method.

Chapter 3 provides an idea and the literature reviews related to the problem, and after that, proposes a method that combines the design method based on the PSD and the PC method

to solve the multi-objective design problem for EMC solutions. The PC method is employed to generate the initial data for the preliminary phase of the PSD. Then the PSD method is utilized with the required performance and design parameters to provide a final solution set for the application.

In Chapter 4, the proposed method is implemented with EMC solutions. The two solutions selected here are the two most commonly used EMC solutions: metal sheet of the enclosure and EMI filter. For instance, in the case of the EMI filter, the design specifications would be set, then apply the proposed method when fluctuations in the resistors of the source and load result in an imbalance. The proposed method is applied with attenuation of the DM voltage and CM current at the output terminal of an EMI filter as the required performances, and the results are obtained with the PSD method as range and verified. Subsequently, the results are compared with the results of the MC method as well as evaluate the validity of the combined method of PC and PSD.

Chapter 5 concludes the dissertation by summarizing the main points and discussing the limitations and future goals of the research.

Chapter 2
Background

In Chapter 2, the dissertation presents background information related to the research content of the dissertation. The first part focuses on EMC solutions. The second part describes the use of the PSD method for multi-objective design. In the set-based design method, the required performances and design parameters are expressed using set theory, and narrowing design parameter sets can lead to a common set that satisfies multiple required performances. The third part aims to solve the problem of uncertain parameters, ensuring that the application is as close to reality as possible.

2.1. EMC Solutions for Electronic Equipment

2.1.1. Overview of EMC

EMC is a crucial aspect of electronic devices and systems. Electronic devices, which consist of microprocessors and specialized circuits operating at high speeds, can generate EMI [9]. This interference can be transmitted outside the system through one or both distinct pathways: radiated interference energy as electromagnetic waves into space (radiation interference) and radiated interference energy through power lines, input/output (I/O) cables, or control cables (conductive interference). These cables may become secondary sources of radiation.

The goal of EMC is to ensure that electronic devices and systems can function properly in their electromagnetic environments. This involves limiting the unintentional generation, propagation, and reception of electromagnetic energy that could cause unwanted effects such as EMI or physical damage to operational equipment [9]. To meet the requirements for both radiation and conductive interference emission, electronic devices must comply with specific EMC standards like CISPR-22 [10], IEC EN 61000 [11], or MIL-STD-461F [12]. Achieving EMC compliance is a challenging task that requires the application of various modern technologies, including selecting appropriate materials for component manufacturing, advanced PCB design and manufacturing techniques, and effective device shielding design. It is a mandatory requirement for information systems with digital processing, enhancing system reliability, operational speed, and information transmission efficiency.

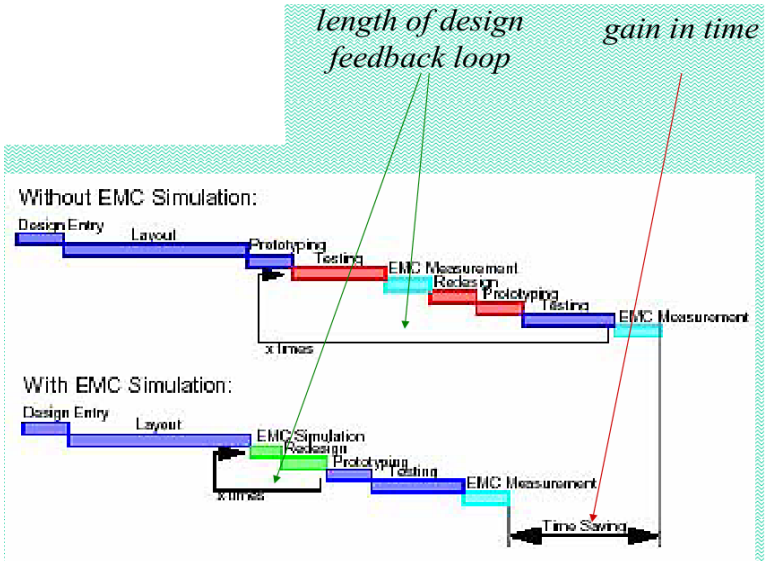

Figure 2.1. Comparison of design strategy time with EMC and without EMC [13]

Applying EMC design principles from the initial stages of research and device design can save costs and reduce the time required to develop a new product, as shown in Figure 2.1 [13]. It becomes increasingly challenging to achieve EMC standards once a product is completed because any interference with the device would necessitate significant changes to the entire structure and radiation characteristics of the device.

For effective EMC solutions, it is essential to consider and integrate them into the research and design process of electronic devices. Solutions should be incorporated at various levels, from component selection to PCB design, structural construction, the layout of protection points, and responses to leaks.

2.1.2. Sources and causes of electromagnetic radiation

To design a device with optimal EMC, it is crucial to understand the structure of electromagnetic radiation sources originating from electronic components and their underlying causes.

2.1.2.1. Sources of electromagnetic radiation

During operation, all electronic devices emit various types of noise into the surrounding environment. The primary sources of interference include disturbances within the PCB and interconnecting cables that comprise the device, as well as noise present in the signals on the I/O ports and the hidden radio frequency (RF) characteristics of passive components.

a. Radiation from the PCB and connecting cables

Many different sources and types of radiation can be classified, but it is quite difficult because most of these radiated noises are generated by unwanted CM currents flowing on the PCB or connecting cables. These CM currents occur when a voltage between the source circuit and ground induces pulsed disturbance currents to flow through parasitic inductances. The resulting noise voltage, influenced by the parasitic inductances, affects the cables connected to the PCB, effectively acting as antennas. Another cause of CM currents on interconnecting cables is the asymmetrical structure of the I/O devices, which is difficult to determine and unpredictable. Although CM currents are often significantly smaller in magnitude than the DM currents (µA compared to mA), they cause much higher radiation intensity and are essentially uncontrollable. On the other hand, DM currents pose a greater risk as they may contain sensitive information during processing. The radiated noise sources on PCB can be classified into three types, as described in Figure 2.2.

- From the integrated circuits (ICs) and components during operation, changing currents in the ICs and components create small loops.

- From the traces on the PCB during the operation of signal currents.

- From the connecting cables during the use of DM currents for signals or due to the presence of unwanted CM currents on the connecting cables when a noise voltage is generated between the power circuit and the ground on the PCB or due to the asymmetrical structure of the circuit.

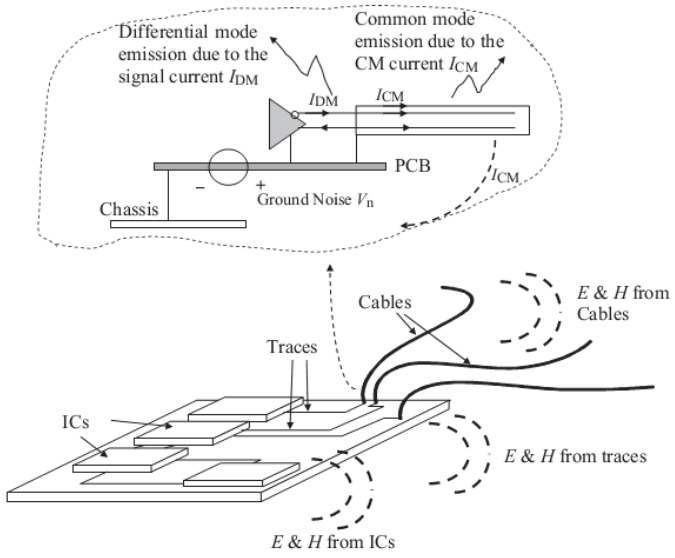

Figure 2.2. Description of sources of electromagnetic radiation from PCB [14]

b. Radiation from the signals on the I/O ports

The radiated noise at the signals on the I/O ports is caused by the following:

- The logic components of the I/O ports operate in common mode.

- Interference from parasitic elements in the I/O ports and cables.

- The clock signal parasitically enters the lead cable of the I/O port by both conductive and radio interference.

- Lack of data filter on the connector and associated signal, both in CM and DM.

- Improper connection of equipment chassis, signal, digital and analog ground.

- The use of incorrect types of I/O connectors (plastic, metal, non-metallic).

c. Hidden RF characteristics of passive components

Electromagnetic radiation occurs due to various causes, with one of the most significant factors being the inherent high-frequency characteristics found in the structural composition of components. The hidden RF characteristics of passive components have a considerable impact on the generation of radiated noise. These characteristics include [15]:

- High-frequency operating resistor is a combination of a series of inductance in the resistive conductor, in parallel with a capacitor between the two terminals.

- Capacitors operating at high frequencies act as inductors coupled with resistors and other elements on each side of the capacitor plates.

- Inductors operating at high frequencies act as inductors with capacitors between their terminals, accompanied by some impedance in the conductor.

Unpredicted problems arising from existing components with parasitic components at both high and low frequencies are shown in Figure 2.3.

When designing with passive components, it is essential to consider their parasitic elements and their behavior at high frequencies. Understanding the combinations of components and employing design techniques that account for these hidden characteristics becomes imperative to meet the original product requirements.

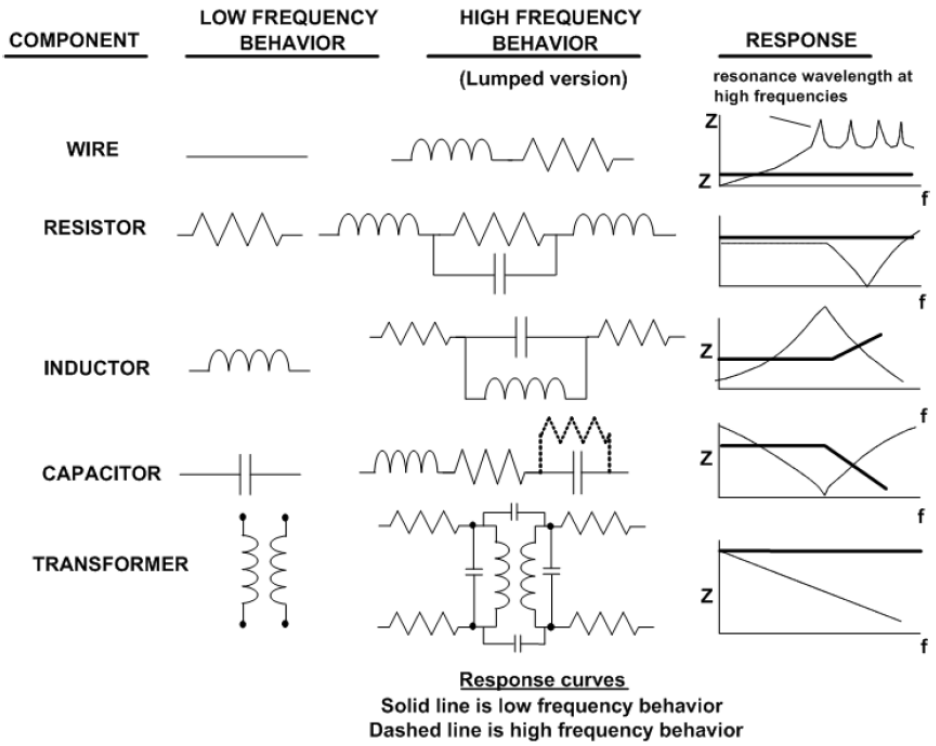

Figure 2.3. Component characteristics at RF frequencies [15]

However, relying on parasitic components based solely on low-frequency criteria without considering their characteristics in the high-frequency range can lead to serious issues, including non-compliance with EMC regulations. EMI issues may also arise when designers disregard or violate the rules governing parasitic components.

2.1.2.2. Causes of electromagnetic radiation

Once the effects of parasitic components are understood, designing products becomes a simpler process, ensuring EMC and signal integrity requirements. The impact of parasitic components must also consider the switching speed of all active components, along with their characteristic properties, such as resistive, capacitance, and inductance factors.

Due to the existence of parasitic elements, it is necessary to study how RF energy is generated on the PCB. Both active and parasitic electronic components produce unwanted RF energy. The field of EMC is described by a series of complex mathematical formulas called Maxwell's equations, which encompass the relationship between electric and magnetic fields. These equations are derived from Ampere's law, Faraday's law, and Gauss' laws.

Maxwell's equations explain the generation of EMI through time-varying currents. The distribution of static charges creates a static electric field, while constant current sources generate magnetic fields. Time-varying currents produce both electric and magnetic fields, accumulating energy. This accumulation of energy is analogous to the function of a capacitor, which accumulates and stores charge. For simplification, Maxwell's equations are related to Ohm's law, providing a concise representation of EMC principles [15].

Ohm's Law (time domain):

$$V = IR \tag{2.1}$$

Ohm's law (frequency domain):

$$V_{RF} = I_{RF}Z \tag{2.2}$$

with *V*: voltage, *I*: ampere, *R*: resistance, *Z*: impedance.

Relating the simple Maxwell's equation to Ohm's Law, if RF current exists in a path of a PCB having an impedance value, an RF voltage will be generated proportional to the RF current. Note that in the electromagnetic model, *R* is replaced by *Z*, a complex quantity that includes both resistance (real component DC) and reactance (complex component AC). Impedance *Z* is the resistance to energy flow in both time and frequency domains. Voltage and current are both units of measurement that describe the behavior of electrons, electromagnetic fields, and static electric fields. The standard impedance equation is expressed in several forms. For the conductor or path (trace) of the PCB, impedance is calculated with known impedance and inductance factors as Equation (2.3):

$$Z = R + jX_L + \frac{1}{jX_C} = R + j\omega L + \frac{1}{j\omega C} \tag{2.3}$$

where $X_L = 2\pi fL$, $X_C = \frac{1}{2\pi fC}$ and $\omega = 2\pi f$ with *f* is frequency.

Equation (2.4) can be applied taking into account the change of impedance with frequency.

$$|Z| = \sqrt{R^2 + jX^2} = \sqrt{R^2 + j(X_L - X_C)^2} \tag{2.4}$$

Inductance values often exceed resistance values for frequencies above a few kHz. In such cases, the current will prefer the path with the lowest impedance. Each trace on a PCB has a certain impedance value, and trace inductance is one of the factors contributing to RF energy generation. According to Ohm's law, if there is an RF voltage passing through an

impedance, an RF current will be generated. This RF current can lead to radiation and non-compliance with EMC requirements.

Another phenomenon that occurs in PCBs and cables is crosstalk, which represents energy transfer between paths [16]. Crosstalk can be either magnetic (inductive) or capacitive, depending on the changes in current or voltage. Rapid voltage changes between conductors and the ground layer, as well as between conductors themselves, can create an electromagnetic field that exhibits purely electric behavior (capacitive crosstalk, Figure 2.4). Similarly, changes in current within a conductor or cable can create an electromagnetic field that exhibits magnetic behavior (inductive crosstalk, Figure 2.5).

Crosstalk can occur in cable paths, especially between power cables used in digital networks, such as parallel or twisted pairs. The strength of crosstalk increases with the length of parallel conductors, shorter distances between wires or pairs, and higher operating frequencies. Shielded wire pairs or twisted pairs can help mitigate both capacitive and inductive coupling. As an example of capacitive crosstalk in Figure 2.4, the voltage coupling factor can be expressed as follows:

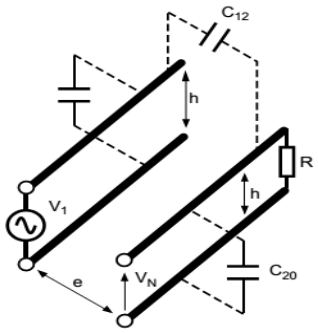

Figure 2.4. Formation of capacitive crosstalk [16]

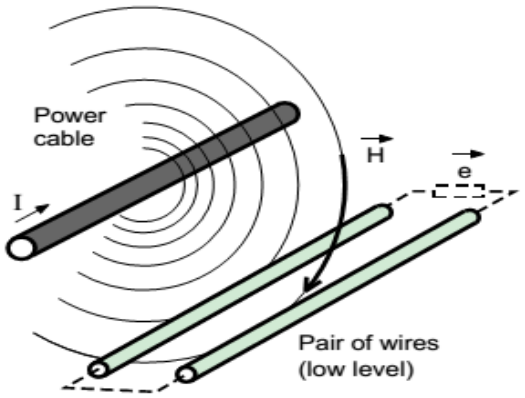

Figure 2.5. Formation of inductive crosstalk [16]

$$\left|\frac{V_N}{V_1}\right| = 2\pi f \frac{\frac{C_{12}}{C_{12}+C_{20}}}{\frac{1}{R(C_{12}+C_{20})}} = 2\pi f R C_{12} = \omega R C_{12} \quad (2.5)$$

with: V_1: Source voltage (signal).

V_N: Capacitive crosstalk voltage.

C_{12}: Parasitic capacitors between pairs of conductors, proportional to the conductor length and distance factor $\log_{10}[1+(h/e)^2]$ where h is the distance between two wires of the pair and e is the distance between two pairs.

C_{20}: Parasitic capacitor between two wires of the pair.

R: Load of the disturbed wire pair.

The above factors contribute to the electromagnetic radiation of electronic devices. Minimizing noise produced during operation is one way to ensure EMC for electronic equipment. In the next part, the dissertation will explore solutions for achieving EMC compliance in electronic devices.

2.1.3. EMC design for electronic devices

Figure 2.6 shows a design method that ensures good EMC for an electronic device or system [17]. A hierarchy is presented in the form of a pyramid.

This dissertation focuses on two main solutions, EMI filter and shielding method, so the remaining solutions only summarize the main ideas.

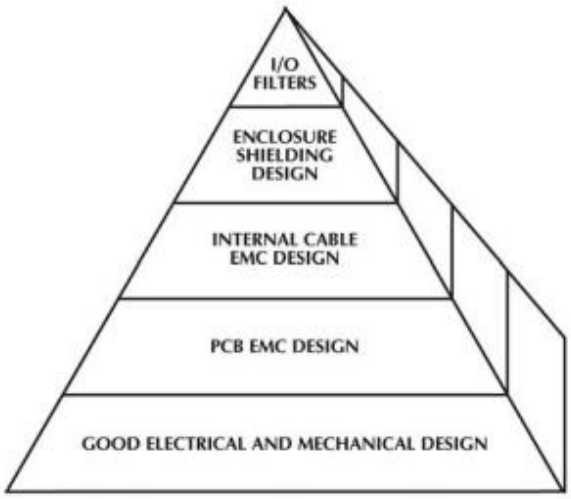

Figure 2.6. Pyramid model in the design of electronic equipment ensures EMC [17]

2.1.3.1. Electrical and mechanical design

A good EMC design is simply the application of good electrical and mechanical design principles. This includes reliability considerations like meeting design specifications within acceptable tolerances, good packaging and comprehensive development testing. The US military's standards MIL-STD are widely recognized and utilized as a foundation for designing both electrical and mechanical principles in various industries. These standards provide guidelines for achieving specific performance and reliability requirements.

Electrical design needs to consider grounding, power and signal integrity, filtering, layout and routing, and component selection. They are essential for minimizing electromagnetic emissions and susceptibility. Similarly, mechanical design aspects, including enclosure design, cable management, grounding and bonding, EMI gaskets and seals, thermal management, and mechanical isolation, contribute to effective EMC mitigation. These considerations help contain and shield electromagnetic radiation, prevent interference, manage heat dissipation, and isolate sensitive components from mechanical disturbances.

The early integration of EMC design considerations is crucial to address potential EMC issues from the outset and avoid costly redesigns later in the development process. Testing and verification, including EMC testing, play a vital role in validating the design measures and ensuring compliance with relevant EMC standards and regulations.

2.1.3.2. PCB design

Electronic device controls typically reside on one or more circuit boards, which include potential interferenc sources, as components and circuits sensitive to electromagnetic energy. Therefore, PCB EMC design is the next most important consideration in EMC design. PCB EMC design refers to the application of design techniques and principles to ensure that a PCB meets EMC requirements and minimizes EMI issues. The location of active components, routing of traces, impedance matching, grounding design, and circuit filtering are EMC considerations. Some PCB components may also require shielding. In order to reduce the potential radiation on the PCB, there are a lot of documents mentioned [18-21].

When designing a PCB ensure EMC, the design goal is to control the emissions from the PCB, susceptibility of PCB circuits to external interference, coupling between PCB and other nearby circuits in the device, and coupling between circuits on the PCB. Here are some key considerations for PCB EMC design:

1. Component Placement: Proper component placement is crucial for achieving good EMC performance. Place components strategically to minimize the length of high-speed traces, reduce signal coupling, and separate noisy components from sensitive ones. Group components according to their function and signal types to minimize interference [22].

2. PCB Layer Stackup: If clock frequencies above 10 MHz are used, in most cases, it will be necessary to use a multilayer design with an embedded ground layer [23]. The layer stack up of the PCB can impact EMC performance. Use appropriate ground planes and power planes to provide shielding and reduce noise coupling [24]. Consider implementing separate ground planes for analog and digital signals to prevent interference between them.

3. Signal Traces: Keep high-speed signal traces as short as possible to minimize their length and reduce the potential for electromagnetic radiation [25]. Use controlled impedance routing for high-speed signals to maintain signal integrity and minimize reflections. Clock runs should be minimized and oriented perpendicular to signal traces.

4. Grounding: Establish a solid grounding system on the PCB [25, 26]. Connect all ground planes, shields, and signal returns to a single, low-impedance ground point. Implement proper grounding techniques to minimize ground loops and reduce noise.

5. Power Distribution: Ensure proper power distribution on the PCB [14]. Use decoupling capacitors near power pins to suppress voltage fluctuations and provide clean power to the components. Employ a distributed decoupling strategy with a combination of bulk capacitors and smaller capacitors for different frequency ranges.

6. EMI Filtering: Incorporate EMI filters at critical points such as power supply inputs and high-speed signal lines [27-28]. Use ferrite beads, common-mode chokes, or RC filters to attenuate conducted and radiated emissions.

7. PCB Layout: Pay attention to PCB layout guidelines for EMI mitigation [18, 20]. Minimize the use of vias and avoid long or parallel traces that can act as antennas for radiated emissions. Minimize power bus loop areas by routing the power bus as close as possible to its return. Maintain appropriate spacing between traces and minimize the use of stubs and sharp corners. Keep clock traces, buses, and chip enables separate from I/O lines and connectors. If the clocks go off the board, then they should be located close to the connector. Otherwise, clocks should be centrally located to help minimize onboard distribution traces.

I/O chips should be located near the associated connectors. Circuit types (i.e., digital, analog, power) should be separated.

8. Ground Plane Splitting: In cases where sensitive analog and noisy digital components coexist, consider implementing ground plane splitting. This involves physically separating the ground planes for analog and digital sections and connecting them at a single point [15].

9. Shielding: If necessary, use shielding techniques to contain electromagnetic radiation. Utilize metal shielding cans, conductive coatings, or shielded enclosures to isolate sensitive components or sections from external interference [9, 17].

10. EMC Testing: Conduct EMC testing during the development process to validate the PCB design's compliance with EMC requirements and identify any potential issues. Test for radiated emissions, conducted emissions, and immunity to ensure proper EMC performance [10, 11, 12].

By incorporating these PCB EMC design principles, designers can minimize EMI issues, improve signal integrity, and ensure EMC for PCB. It is important to refer to relevant EMC standards and guidelines specific to application to ensure compliance.

2.1.3.3. Internal cable design

Internal cables are generally used to connect PCBs or other internal subassemblies. The internal cable EMC design, including routing and shielding, is very important to the overall EMC of any given device. To ensure EMC in internal cable design, several key considerations should be taken into account.

Firstly, internal cabling should be minimized as much as possible. When cables are required to connect assemblies and PCBs, the lengths should be minimized. Long service loops can be disastrous.

Secondly, proper shielding should be incorporated into the cable design. This involves using shielding materials such as braided copper or aluminum foil to protect the internal conductors from external EMI. If PCBs are properly designed, the requirement for shielding of internal cabling will be minimized. However, if it is found that cable shielding is required, the technique used to ground the shield is critical to the attenuation afforded by the shield. The shielding should be grounded effectively to provide a path for the EMI to dissipate. Cable shields should not be used as signal returns.

Thirdly, cable routing and separation are crucial in minimizing EMI. Careful planning should be employed to keep high-frequency and low-frequency cables separated to reduce the chance of cross-talk and interference. Additionally, routing cables away from potential sources of EMI, such as power cables or motors, can further enhance EMC.

Next, for certain unbalanced circuits, coaxial cables are often used. In this case, the shield of the coaxial cable is intentionally used for signal return. In this application, the shield is not intended for attenuation of electromagnetic energy emanating from the center conductor. If the circuits at each end of a coaxial cable are designed properly, the coaxial cable should not radiate. However, if circuit impedances are not properly matched and the coaxial cable does radiate, another shield must be added to the cable (triaxial). This outer ground would be then bonded to the chassis ground.

Next, the use of balanced transmission lines, such as twisted pair cables, can help reduce the impact of electromagnetic noise. Balanced lines have two conductors that carry equal and opposite signals, which cancel out common-mode noise. This configuration improves the immunity of the cable to external electromagnetic disturbances.

Lastly, it is essential to ensure proper grounding and bonding throughout the cable system. All metallic components should be connected to a common ground plane to maintain consistent reference potentials and minimize ground loops. Ground connections should be low impedance and capable of carrying high-frequency currents to prevent the buildup of voltage differentials that can lead to EMI.

By incorporating these principles into the internal cable design, it is possible to achieve a robust EMC performance, minimizing the potential for EMI and ensuring the reliable operation of electronic systems.

2.1.3.4. Shielding design

After the EMC design of the PCB and internal cables are complete, special consideration must be given to the enclosure shielding design. The treatment of apertures, penetrations, and cable interfaces is essential to maintain the integrity of the shielding.

The shielding method is used to eliminate electromagnetic signals, ensuring EMC for components or electronic devices within the shielding enclosure. The effectiveness of the shielding method depends on various factors, of which the choice of the shielding material and design method plays a vital role.

a. Shielding effectiveness

A metal shield is a sheet of material, typically metal, placed between two areas to control the propagation of an electromagnetic field, or it can enclose a source as shown in Figure 2.7 [9].

Using a sealed object made of metal shields prevents electromagnetic signals from the inside escaping to the outside and vice versa. The first need to look at how to calculate the shielding efficiency of a metal shield.

The effectiveness of electromagnetic shielding is measured by the shielding effectiveness (SE). *SE* is the ratio of magnitude of electric field E_0 without shielding (or magnitde of magnetic field H_0) to magnitude of electric field E_1 (or magnitude of magnetic field H_1) with shielding. The shielding effectiveness is expressed in decibels (dB) as follows [29]:

$$SE_e = 20 \log_{10} \left| \frac{E_0}{E_1} \right| \tag{2.6}$$

$$SE_h = 20 \log_{10} \left| \frac{H_0}{H_1} \right| \tag{2.7}$$

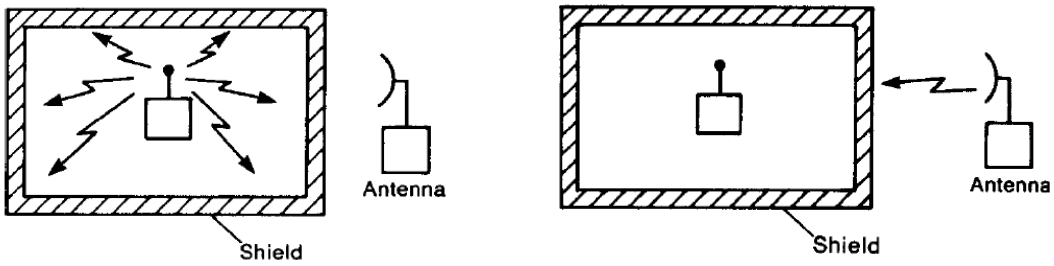

(a). Contain radiated emissions (b). Exclude radiated emission

Figure 2.7. The use of a shielded enclosure [9]

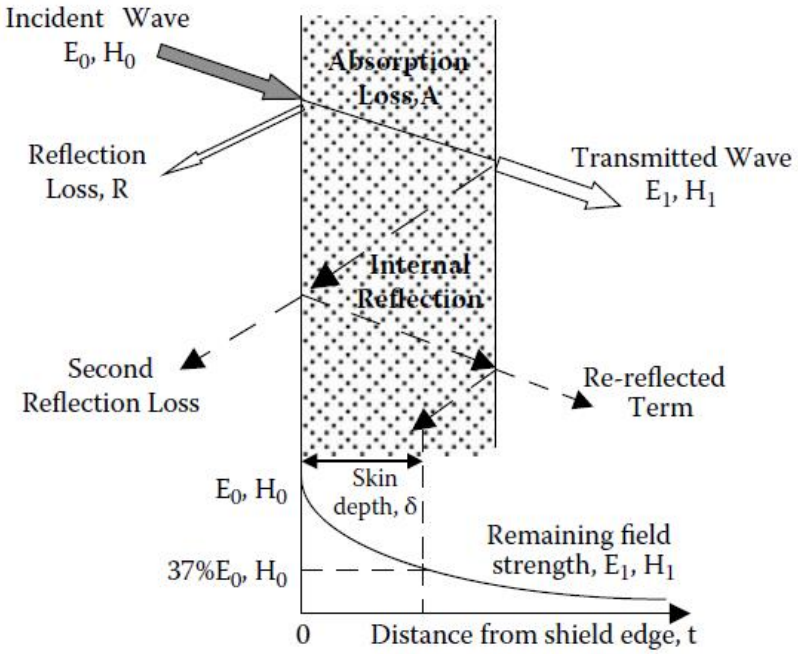

Figure 2.8. Components of an electromagnetic field when passing through a shield [30]

The attenuation of the electromagnetic signal from the metal shield is a combination of three factors, as illustrated in Figure 2.8 [9, 30, 31].

1. The incident wave is reflected by the left edge of the shield due to the impedance discontinuity at the air-metal boundary.

2. The wave that cross the shield surface is attenuated (absorbed by turning into heat energy) in passing through the shield.

3. The wave after passing through the shield, reach the opposite face of the shield, encountering another air-metal boundary. Some of it is reflected back into the shield. This reflection occurs multiple times inside the shield. If a shield is designed to have a thickness much greater than the skin depth of the material at the frequency of the incident wave, these multiple reflections occurs rarely at the edges of the shield and can be neglected.

The first factor is the reflection loss *R*, the second is the absorption loss through the shield *A*, and the last is the multiple reflection *M*. *M* is significant only if $A \leq 15$ dB (i.e. depends on the thickness of the shield) [30]. Thus, the *SE* of a metal shield is the sum of the attenuations of the first reflection, absorption and multiple reflections, expressed in dB as follows:

$$SE_{dB} = R_{dB} + A_{dB} + M_{dB} \tag{2.8}$$

- **Reflection Loss**

The reflection loss depends not only on the intrinsic impedance of the shield but also on the intrinsic impedance of the free space. It is related to the impedance difference between the two media through which the incident wave passes. Here assuming the incident wave direction is perpendicular to the metal shield. If the incident wave is not perpendicular to the shield, the electromagnetic field loss due to reflection will increase with the angle of incident wave. Thus, the dissertation consider the case of the incident wave with the smallest reflection loss.

- In the far field

In the far field, the lower the impedance of the metal shield, the greater the reflection loss. If the incident wave is a plane wave (far field), its wave impedance is equal to the impedance of free space, which is 377 Ω. The reflection loss in the far field is calculated as follows [9]:

$$R_{dB} = 168 + 10\log_{10}\left(\frac{\sigma_r}{\mu_{rf}}\right) \tag{2.9}$$

where: μ_r is the permeability relative of the material to that of free space.

σ_r is the conductivity relative of the material to that of copper.

- In the near field

The near field has a more complex structure compared to the far field. The field components not only vary simply with the distance inverse of $1/r$, but also depend on $1/r^2$ và $1/r^3$. $1/r$ equals $1/r^2$ and $1/r^3$ at $r = \lambda_0/2\pi$or approximate $\lambda_0/6$. The near field/far field boundary is where the ratio E/H ≈ η_0 (intrinsic impedance of the free space). This ratio is also known as wave impedance [9]:

$$Z_w = \frac{E}{H} \tag{2.10}$$

The magnitude of the wave impedance is expressed in terms of the distance from the source as shown in Figure 2.9. In the far field, the term $1/r$ predominates, it means $Z_w \approx \eta_0 = 377\ \Omega$.

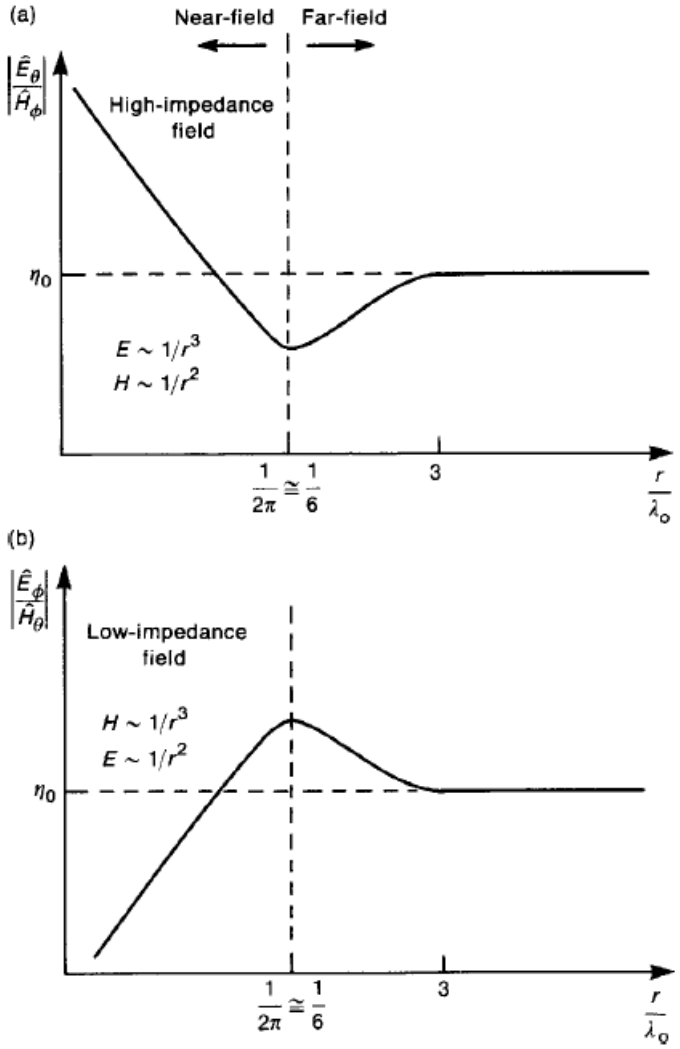

Figure 2.9. Wave impedance of the electric field (a) and the magnetic field (b) [9]

In the near field of a electric source, the electric field is proportional to $1/r^3$ and the magnetic field is proportional to $1/r^2$ (Figure 2.9a). Additionally, the wave impedance in the near field of the electric source is greater than the intrinsic impedance of the medium. Hence the electric source is referred to as a high-impedance source.

In the near field of a magnetic source, the magnetic field is proportional to $1/r^3$ and the electric field is proportional to $1/r^2$ (Figure 2.9b). The wave impedance in the near field of the magnetic source is less than the intrinsic impedance of the medium. Hence the magnetic source is referred to as a low-impedance source.

In the near field, the ratio between the electric and magnetic fields is not determined by the wave impedance of the medium but by the characteristics of the source. Depending on the characteristics of the emitter (high voltage and low current, low voltage and high current)

the wave impedance can be greater or less than 377 Ω. Since the reflection loss is a function of the wave impedance and the shield impedance, in the near field, this attenuation will vary with the wave impedance. The reflection loss in the near field is calculated as follows [9]:

+ With electric field:

$$R_{e,dB} = 322 + 10\log_{10}\left(\frac{\sigma_r}{\mu_r f^3 r^2}\right) \quad (2.11)$$

+ With magnetic field:

$$R_{m,dB} = 14.57 + 10\log_{10}\left(\frac{f r^2 \sigma_r}{\mu_r}\right) \quad (2.12)$$

- **Absorption loss**

Absorption loss occurs when part of the energy of the electromagnetic field passing through the shield is converted into the internal energy (heat) of the shield and is calculated as follows [9]:

$$A_{dB} = 1.314 t\sqrt{f \mu_r \sigma_r} \quad (2.13)$$

with *t* is thickness of metal sheet [cm].

Equation (2.13) shows that the absorption capacity of a metal shield depends on the frequency, the nature of the material and the thickness of the metal sheet. These factors should be considered when selecting shielding materials.

b. Shielding material

A shielded enclosure should be constructed using materials that exhibit the desired physical and electrical properties while also being resistant to unfavorable environmental conditions. Before selecting a material for electromagnetic shielding, it is important to consider the required properties of the material. Electromagnetic shielding involves the reflection and absorption of electromagnetic waves by an object acting as a shield. The primary shielding mechanism is reflection, which requires materials with free charge carriers (electrons or holes) that can interact with the incident electromagnetic field. Consequently, conductive materials are typically used for shielding, such as metal sheets commonly found in the walls of shielded rooms like Faraday cages or Anechoic chambers. These metal sheets, due to the presence of free electrons, serve the purpose of reflecting the electromagnetic waves.

The second shielding mechanism is absorption, which is best achieved with materials possessing electric and magnetic dipoles. The electric dipoles are present in materials with high dielectric constant values while magnetic dipoles are present in materials with high permeability.

According to the formulas from (2.9) to (2.13), the efficiency of absorption is evaluated by the product $\sigma_r \mu_r$ while the efficiency of reflection is evaluated by the ratio σ_r / μ_r. Table 2.1 [30] presents several common materials such as copper, silver, gold and aluminum, which exhibit good reflectivity due to their electrical conductivity. Materials with high permeability, such as a magnetic alloy of nickel (80%) and iron (20%), or soft ferromagnetic materials consisting of nickel (77%), iron (16%), copper (5%), and chromium (2%), have excellent absorption capacity. The efficiency of reflection decreases as the frequency of the incident wave increases, while the efficiency of the absorption increases as the frequency increases.

Table 2.1. Conductivity σ_r and permeability μ_r of shielding materials [30]

Material	σ_r	μ_r	$\sigma_r \mu_r$	σ_r / μ_r
Silver	1.05	1	1.05	1.05
Copper	1	1	1	1
Yellow	0.7	1	0.7	0.7
Aluminum	0.61	1	0.61	0.61
Magnesium	0.38	1	0.38	0.38
Zinc	0.29	1	0.29	0.29
Iron	0.17	1000	170	1.7×10^{-4}
Tin	0.15	1	0.15	0.15
Steel SAE 1045	0.1	1000	100	1×10^{-4}
Lead	0.08	1	0.08	0.08
Stainless Steel	0.02	1000	20	2×10^{-5}
Soft ferromagnetic	0.03	20,000	600	1.5×10^{-6}

c. Effect of leakage

In practical applications, shields often have leakages at seams or holes in shielding metal. The shielding effectiveness in dB, as described in Equation (2.8), can be calculated more accurately as follows [30]:

$$SE = A + R + M - \text{Leakage Effects} - \text{Standing Wave Effect} \quad (2.14)$$

Leakage effects can manifest in various situations, including:

- Welding seams, connecting parts, screws, bending edges, welds...

- Doors, air vents.

- Connection holes such as power lines, signal lines, control lines, etc.

- Nonhomogeneous areas, screens, cables, grids, and conductive buffers.

The shielding enclosure always require openings or holes for power supply, I/O signal transmission and ventilation... However, these holes can significantly compromise the enclosure shielding effectiveness due to leakage. Therefore, controlling vulnerabilities is crucial for achieving good enclosure shielding.

Typically, at low frequencies, the shielding effectiveness of the enclosure is primarily determined by the material used. However, at higher frequencies, the joints, openings, and ports on the enclosure become the primary factors affecting the shielding effectiveness. Discontinuities in the enclosure can degrade the shielding and therefore their design is crucial in maintaining the desired levels of shielding effectiveness, as they can allow for electromagnetic coupling through the openings and seams. The efficiency of this coupling depends on the size of the hole or seam relative to the wavelength of the interfering signal. Any openings in the enclosure can create a highly efficient coupling path at certain frequencies, and as the aperture size increases, the coupling efficiency also increases.

To reduce leakage through the holes, the following measures can be taken:

- Minimize the number of apertures.

- Reduce the size of the hole: Avoid making the hole larger than necessary. Instead, convert the required holes into multiple smaller holes to increase their resonant frequency above the operating frequency of the enclosure. A good rule of thumb to follow in general design practice is to avoid openings larger than l/20 for standard commercial products and l/50 for products operating in the microwave range.

- In situations where there are long seams or joints between metal structures, it is important to establish electrical connectivity by employing direct metal-to-metal bonding techniques at regular intervals along the seam or joint. Methods such as soldering or screwing can be utilized for this purpose. To reduce the size of holes, particularly when dealing with stretched gaps like covered doors or windows, conductive gaskets or EMC gaskets are highly recommended and widely used. These gaskets serve as effective solutions to minimize the size of openings, ensuring enhanced shielding effectiveness within the enclosure.

- Distribute the necessary holes as far apart as possible: When the gap between holes exceeds $\lambda/4$, some attenuation of the radiated signal will occur.

- Reduce near-field leakage: In cases where covering the hole with a conductive gasket is not possible, mitigate the effects of near-field leaks by ensuring that potential radiation sources within the enclosure are not located near the openings. The distance between the radiation source and the hole should generally be at least 1.5 times the size of the hole.

- Techniques for large holes: When dealing with large holes, such as doors or screens, there are additional techniques that can help achieve good shielding effectiveness. These techniques may involve the use of waveguides, screened windows, panel screens, shielded ventilation windows, or conductive cushions.

2.1.3.5. Filter design

The final part of the EMC design is the filter of input and output power and other cables. These filters can be integrated into the circuit board or located on the connectors of the I/O cables themselves.

Filtering is a technique that involves the utilization of electronic components to construct an electronic circuit aimed at eliminating or attenuating signals within a specific frequency range. In simpler terms, it divides the signal spectrum into frequency components that are allowed to pass through the filter and those that are blocked or attenuated. The filtering method has a wide range of applications as well as theory; this dissertation mainly focuses on applications in the field of EMC, particularly EMI filters.

One commonly used filtering method in EMC is the EMI filter. EMI filter is a fundamental solution for noise suppression and is widely used in high-speed differential signal wires, power supply lines, and other applications [4]. They are designed to suppress

both differential mode (DM) and common mode (CM) noise, with the effects varying depending on the intended use. EMI filters are typically employed for input power or signal conductor pairs. Figure 2.10 depicts a schematic diagram of a typical EMI filter.

Basically, the EMI filter needs to fulfill several technical requirements, including::

- Frequency: The passband frequency is the frequency range that ensures the operation of the device, while the stopband frequency is the frequency range at which the device can emit electromagnetic signals.

- Attenuation: The attenuation is expressed in dB and represents the ratio between the input voltage/current and the output voltage/current across the filter within the specified frequency range.

With an EMI filter, it is necessary to determine the design specifications (required performances) of the DM and CM in a defined real frequency region to find the values of the circuit's components (design variables) satisfying the requirements. The design method is based on the Insertion Loss method [32], and attenuation of the DM voltage and CM current are considered as required performances of the EMI filter. The attenuation can be increased proportionally to size and weight of filter as the number of components increases.

Filter attenuation is highly dependent upon source and load impedances. Manufacturers' data is generally published for 50 Ω source and load impedances, while actual impedances are generally reactive and vary considerably over the frequency range of interest, resulting in variations in the attenuation factor for the entire system.

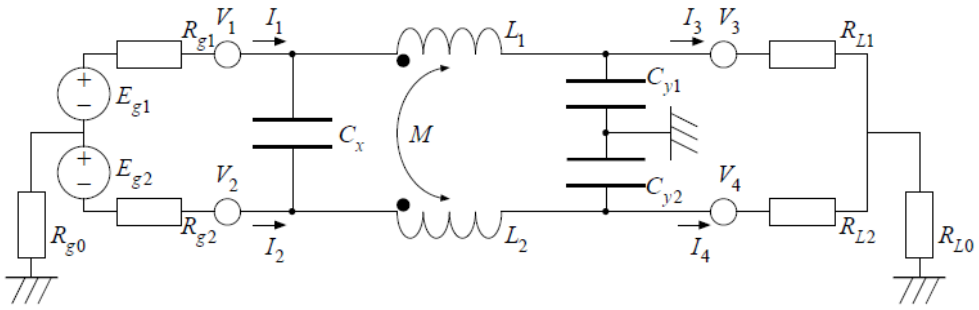

Figure 2.10. Circuit model for EMI filter

This section will analyze how an EMI filter works as shown in Figure 2.11 [33]. EMI conduction noise on lines is usually divided into two components, common mode noise (CMN) and differential mode noise (DMN). CMN, also known as asymmetric noise, occurs in both lines (signal or source) compared to the line-to-ground noise. The direction of the CMN current is directed from the 2 wires to the ground wire. DMN, also known as symmetric interference, occurs between lines, without DMN current in the ground wire. For example, with an EMI source filter with a source and load impedance of 50 Ω, these noise currents are shown in Figure 2.11.

In the provided diagram, the components L_{c1}, L_{c2} are two double blocking coils on a shared core, combined with capacitors to form a filter in both modes. L_{c1}, L_{c2}, L_{d1}, L_{d2}, C_{y1} and C_{y2} form a CM filter that reduces noise from the lines generated with the ground wire. The parasitic inductance of L_{c1}, L_{c2}, L_{d1}, L_{d2} and capacitors C_{x1}, C_{x2} form a DM filter that reduces noise between the supply lines. Resistors R_{x1}, R_{x2}, R_{y1}, R_{y2} discharge the capacitors when the device is powered off, contributing to the stable operation of the filter and assisting with the input and output impedance matching. of the filter. During the design process, it is common to select values such as $L_{c1} = L_{c2} = L_c$, $L_{d1} = L_{d2} = L_d$, $C_{x1} = C_{x2} = C_x$, $C_{y1} = C_{y2} = C_y$. In DM, the inductor L_c will generate an L_{leak} detector. The corresponding filters for the two modes CM and DM are shown in Figures 2.12 and 2.13, respectively.

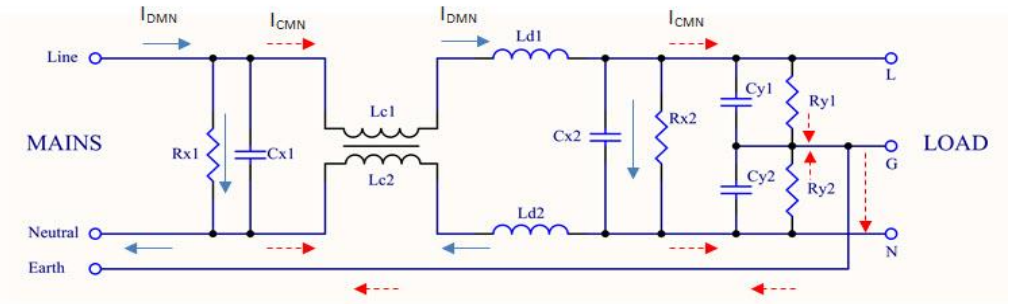

Figure 2.11. Example diagram of an EMI filter designed for AC power [33]

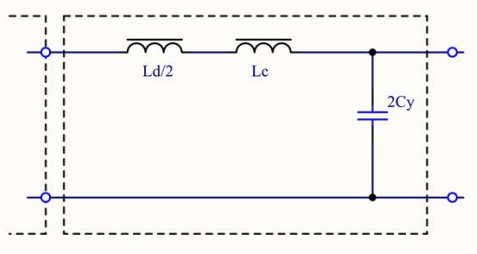

Figure 2.12. Equivalence circuit in CM [33]

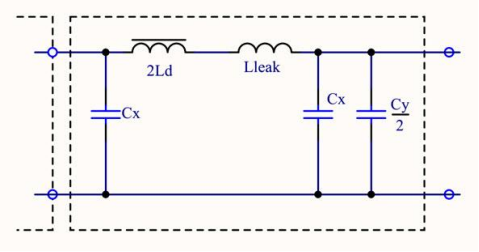

Figure 2.13. Equivalence circuit in DM [33]

The values in the above diagram are calculated from the cut-off frequency in the two modes CM and DM as follows [28]:

$$f_{RCM} = \frac{1}{2\pi\sqrt{L_{CM}.C_{CM}}} = \frac{1}{2\pi\sqrt{(L_c+\frac{1}{2}L_d).2C_y}} = \frac{1}{2\pi\sqrt{L_c.2C_y}} \quad (2.15)$$

where f_{RCM} is the cut-off frequency in CM, normally $L_d << L_c$.

$$f_{RDM} = \frac{1}{2\pi\sqrt{L_{DM}.C_{DM}}} = \frac{1}{2\pi\sqrt{(2L_d+L_{leak}).C_{DM}}} = \frac{1}{2\pi\sqrt{(2L_d+L_{leak}).C_X}} \quad (2.16)$$

where f_{RDM} is the cut-off frequency in DM, normally $C_y << C_x$.

note that L_{leak} = (0,5% ÷ 2%)L_c.

As the EMI filter's required performances, the frequency ranges of the passband and stopband and the attenuation values in each band should be given. Here, when designing an EMI filter, the required performances for DM are set as follows:

- $f \leq f_p$ (passband): Attenuation $A \leq A_{DM,p}$ [dB],
- $f \geq f_s$ (stopband): Attenuation $A \geq A_{DM,s}$ [dB].

where, p means passband and s means stopband.

In designing a filter in the real frequency region, it is difficult to know the range of element values without prior knowledge. However, the filter's attenuations in the normalized frequency region are the same as the characteristics in the real frequency region, and the filter element values are between 0.1 and 2.0 in the normalized frequency range [34]. Thus, the difficulty of selecting element values in the real frequency region can be avoided. The relationship between the attenuation characteristics and the circuit element values can be effectively displayed as approximate expressions, called meta-modeling expressions [35]. Since it is possible to study within a limited scope in Ref. [36], it is suggested to design using PSD from the normalized frequency region. The specific frequency that defines the

normalized frequency in the normalized filter design is specified by the filter for the DM component and applies the appropriate modifications to the CM component. As a result, the filter for CM components will be designed with the same normalized frequency.

In general, when the impedance of the source/load circuit is multiplied by m after designing the passive network, the operating characteristics do not change if the inductance and resistance of the network are both multiplied by m and the capacitance is multiplied by $1/m$. Therefore, if the network is designed with the impedance of the source/load circuit set to 1 Ω, the L, C, and R values of the network with the same characteristics will be the values of the impedance R_0 of any source/load circuit. If an element value of the original network is expressed in a lowercase letter, it can be obtained by setting $L = R_0 l$, $C = c/R_0$, and $R = R_0 r$. Also, for the impedance of L and C at a given angular frequency ω_0 to be the same as the impedance at another angular frequency ω_1, the corresponding element values have the relation $L' = \frac{\omega_0}{\omega_1} L$ and $C' = \frac{\omega_0}{\omega_1} C$. Therefore, if the network's L and C are multiplied by ω_0/ω_1, the network's operating characteristics will match the frequency obtained by multiplying the frequency axis by ω_1/ω_0. Using this property, in filter design, the normalized frequency $\Omega = f/f_0$ is obtained by dividing the real angular frequency $\omega = 2\pi f$, which is determined based on the specific angular frequency $\omega_0 = 2\pi f_0$, and the attenuation characteristic is determined in this processing of the normalized frequency region.

When filter design is considered at normalized frequencies, a Wagner prototype LPF is used [37], and the frequency is normalized by f_p, the reference frequency is $\Omega = \frac{2\pi f}{2\pi f_p} = \frac{\omega}{\omega_p}$, and the converted factor is $k = k_p/k_s$. The frequency is converted from the real region to the normalized region:

- $\Omega \leq \Omega_p = 1 : A \leq A_p$,
- $\Omega \geq \Omega_s = \frac{2\pi f_s}{2\pi f_p} = \frac{1}{k} : A \geq A_s$.

The require order N_w of the filter can be estimated as:

$$N_w = \frac{1}{2} \frac{\ln\left(10^{\frac{A_S}{10}} - 1\right) - \ln\left(10^{\frac{A_p}{10}} - 1\right)}{\ln\left(\frac{1}{k}\right)} \tag{2.17}$$

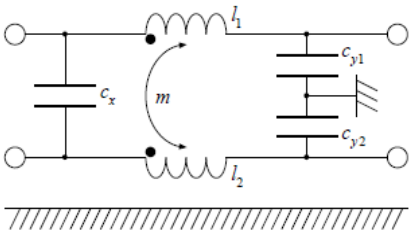

(a). Lowpass prototype filter

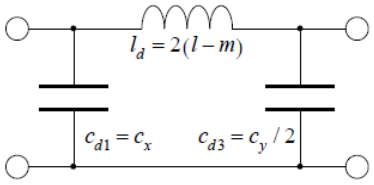

(b). Third-order equivalent circuit model for DM

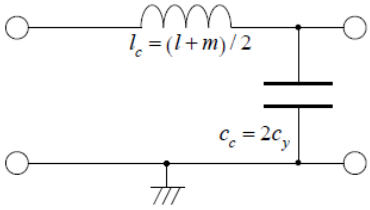

(c). Second-order equivalent circuit model for CM

Figure 2.14. Equivalent circuit model for EMI filter: $l = l_1 = l_2$, $c_y = c_{y1} = c_{y2}$, $m = k\sqrt{l_1 l_2}$, where k is coupling coefficient

The circuit topology of the lowpass prototype filter in Figure 2.14a is expressed in two equivalent circuit components, DM as shown in Figure 2.14b, which is an independent orthogonal mode of a balanced system, and CM as shown in Figure 2.14c, is a component in the equivalent phase so that the effect of EMI filter can be seen more clearly. If the mutual induction circuit is an ideal transformer, the circuit itself acts as a CM filter, but when the frequency is high, the inductance is high, and a tightly coupled element is difficult to fabricate. For this reason, X capacitor is often added to remove DM noise, and Y capacitor is often added to remove CM noise [2]. From the equivalent circuit, the equivalent circuit for DM is a third-order filter, and the equivalent circuit for CM is a second-order filter. The theoretical properties of the filter are numerically calculated to generate initial data for a meta-modeling formula and verify the obtained range solution.

The *F* matrix (ABCD matrix) of the EMI filter diagram in Figure 2.14 is defined as follows:

$$\boldsymbol{F_x} = \begin{bmatrix} \boldsymbol{U} & \boldsymbol{O} \\ \boldsymbol{Y_x} & \boldsymbol{U} \end{bmatrix} \quad \text{with } \boldsymbol{Y_x} = j\omega C_x \begin{bmatrix} 1 & -1 \\ -1 & 1 \end{bmatrix} \tag{2.18}$$

$$\boldsymbol{F_{ch}} = \begin{bmatrix} \boldsymbol{U} & \boldsymbol{Z_{ch}} \\ \boldsymbol{O} & \boldsymbol{U} \end{bmatrix} \quad \text{with } \boldsymbol{Z_{ch}} = j\omega \begin{bmatrix} L_1 & M \\ M & L_2 \end{bmatrix} \text{ and } M = k\sqrt{L_1 L_2} \tag{2.19}$$

$$\boldsymbol{F_y} = \begin{bmatrix} \boldsymbol{U} & \boldsymbol{O} \\ \boldsymbol{Y_y} & \boldsymbol{U} \end{bmatrix} \quad \text{with } \boldsymbol{Y_y} = j\omega \begin{bmatrix} C_{y1} & 0 \\ 0 & C_{y2} \end{bmatrix} \tag{2.20}$$

$$\boldsymbol{F} = \boldsymbol{F_x F_{ch} F_y} = \begin{bmatrix} \boldsymbol{A} & \boldsymbol{B} \\ \boldsymbol{C} & \boldsymbol{D} \end{bmatrix} \tag{2.21}$$

where $\boldsymbol{U}$ is a unit matrix and $\boldsymbol{O}$ is a zero matrix.

The current at the output of filter is calculated using the following equation:

$$\begin{bmatrix} \boldsymbol{I_i} \\ \boldsymbol{I_o} \end{bmatrix} = \begin{bmatrix} \boldsymbol{Z_g} & \boldsymbol{AZ_l + B} \\ \boldsymbol{-U} & \boldsymbol{CZ_l + D} \end{bmatrix}^{-1} \begin{bmatrix} \boldsymbol{E_g} \\ \boldsymbol{0} \end{bmatrix} \tag{2.22}$$

The current and voltage in CM and DM at the output of filter are calculated as follows:

$$\boldsymbol{I_{m,o}} = \boldsymbol{T_i^{-1} I_o} \text{ with } T_i = \begin{bmatrix} 1 & 1/2 \\ -1 & 1/2 \end{bmatrix} \tag{2.23}$$

$$\boldsymbol{V_{m,o}} = \boldsymbol{Z_{m,l} I_{m,o}} \tag{2.24}$$

Then, some required performances of EMI filter such as the attenuation of the DM voltage A_{VDM}, the attenation of the CM voltage A_{VCM}, and CM current I_{CM} are calculated as follows:

$$A_{V_{DM}} = -20 \log_{10} \left| \frac{V_{dm,o}}{V_{dm,ref}} \right| \tag{2.25}$$

$$A_{V_{CM}} = -20 \log_{10} \left| \frac{V_{cm,o}}{V_{cm,ref}} \right| \tag{2.26}$$

$$I_{CM} = I_3 + I_4 \tag{2.27}$$

where $V_{dm,o}$ and $V_{dm,ref}$ are DM voltages in cases with and without an EMI filter at the output terminal. $V_{cm,o}$ and $V_{cm,ref}$ are CM voltages in cases with and without an EMI filter at the output terminal. I_3 and I_4 are the output current at the output terminal of the EMI filter.

2.2. Preference Set-based Design Method

2.2.1. Overview of PSD

Electronic design is often used with concepts based on circuit theory. Electromagnetic fields emitted in devices and components need to be considered in order to achieve expected performance and meet EMC rules. In such a design, it is necessary to pursue a solution that simultaneously meets multiple performance that sometimes include conflicting requirements. In electronic systems, initial values have been established for many variables designs and their values have been used many times. Point-based design methods are used to repeatedly correct values.

As shown in Figure 2.15a, the traditional point-based design approach rapidly develops a "single solution", evaluating it against multiple target, and then iteratively setting the initial values and modifying the design variables until it reaches an optimal design solution [38]. This iterative design practice is indeed a popular and widely accepted design approach in the engineering design community. However, this approach severely reduces the effort of concurrent product and process design. The more design variables and the higher the performance requirements, the harder it is to find a value that satisfies the specifications. In addition, many uncertain parameters such as misalignment, unnecessary electromagnetic coupling, and parasitic factors occur in the actual product, making the design more difficult. In this iterative process, there is no theoretical guarantee that the process will converge and produce an optimal solution [39]. In the electric system, many design methods based on trial-and-error that repeat the initial values and modify the design variables for many design variables have been implemented and this should be eliminated.

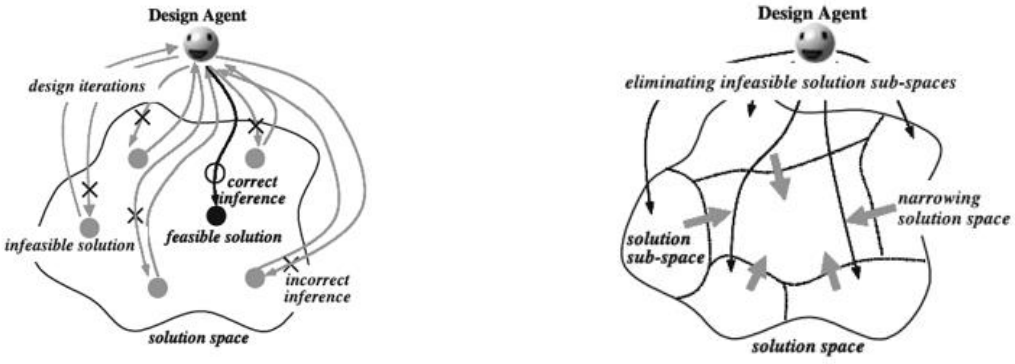

(a). Point-based Design

(b). Set-based Design

Figure 2.15. Point-based versus Set-based design [38]

To solve such problems and to reduce product development costs and time, concurrent design techniques for meeting multiple performance requirements have been proposed, for example, several design methods, such as the Taguchi method [1] and set-based design [2]. SBD considers a range of design possibilities from the outset by dividing the solution space into relatively equal volumes (Figure 2.15b). Then the designers communicate explicitly and consider the set of design alternatives. The sets are gradually narrowed through the elimination of inferior alternatives until the final solution remains. On the other hand, in set-based design, required performances and design variables are expressed in a range, and the range of design variables is narrowed to accommodate multiple performances.

Many design methods have been proposed to reduce the time and cost of product development, such as the concurrent design approach, for example, the fuzzy set-based design method [2]. Fuzzy set-based design, proposed as a design method for satisfying multi-objectives, has renewed the traditional point-based design concept. Point-based design is based on the use of a point-to-point process between required parameters and performance. Therefore, the method requires a large amount of computation (and/or testing). In contrast, the required performances and design parameters in fuzzy set-based design methods are expressed in set theory, and narrowing design parameter sets can lead to a common set that satisfies many required performances.

One of the specific methods for set-based design is the Preference Set-based Design (PSD) method [3], which has been proposed and is commonly used in the field of mechanical engineering. PSD has been proposed and developed as a practical procedure for the fuzzy set-based design method [3], [38].

The PSD method is proposed and developed by Emeritus Professor Haruo Ishikawa of the University of Electro-Communications. This method was initially applied as a mechanical design method, and many results were obtained and announced. Efforts to apply this method to electrical systems have been reviewed by the Gigabit Research Group of the "PSD Subcommittee" since 2015.

The PSD method is a type of composite technique for simultaneous optimization of multiple purposes. The idea of a preference set is quite simple and unique, making the concurrent design process easy to understand and implement. In the PSD method, in addition to set-based characteristics, the designer’s intent can be reflected in the required performances and design variables using a quantitative evaluation metric known as

Preference expressed as a preference set. Because design variables are obtained in a range rather than an point value, it is a robust design ability to include deviations in actual production [6]. In the PSD method, when all performance meets the requirements, the allowable range of the final design parameter is obtained with the highest levels of satisfaction and robustness index. At the core of PSD is a set-theoretic (set-based) design algorithm that can be applied in many different fields.

While the PSD method has been successfully applied to the mechanical field, auto/automotive field, its application to electric and electronic design is also being tested. The utility of which suggests that a design solution (within range) can be obtained that satisfies many performance requirements at the same time.

Figure 2.16 shows a flowchart of the PSD procedure. The main elements of the PSD process include three phases of "set representation," "set propagation," and "set narrowing" [38].

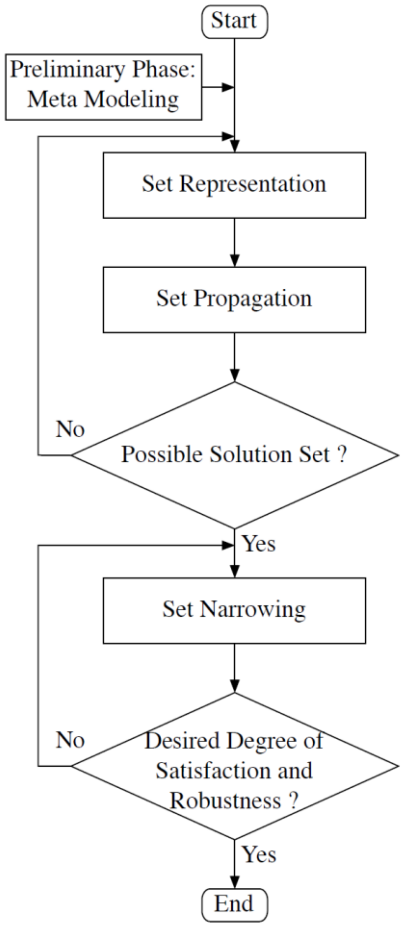

Figure 2.16. Flowchart of PSD

2.2.2. Phases of PSD

2.2.2.1. Preliminary Phase

In the preliminary phase, it is necessary to prepare computational models regarding the relationship between design parameters and required performances. One of the computational models, the meta-modeling, i.e., an approximation model, is used. A response surface methodology (RSM) is used in the Design of Experiments (DOE) to obtain the meta-modeling in this dissertation [40] - [42]. RSM is a collection of mathematical and statistical techniques useful for modeling and analyzing a problem in which a response of interest (required performance) is influenced by several variables (design parameters), and the objective is to optimize this response. Therefore, the initial data for RSM is required. First, the associated performances are calculated or simulated by combining discrete points for each design parameter as initial data. Then using RSM to conclude the approximate expressions. The approximate formula is then inferred from discrete data obtained from calculation, simulation such as FDTD or experiment.

The basic idea behind RSM is to apply linear regression techniques to create a statistical model that predicts response (output) of the system when the inputs are different [43]. This is achieved by generating a set of observed outputs in response to specific sets of input conditions, defined through a design experiment (initial data). The system model is constructed as a linear equation by fitting the observed and input responses using the least squares fitting technique. Once the model is created, it becomes possible to predict the system's output for arbitrary combinations of inputs.

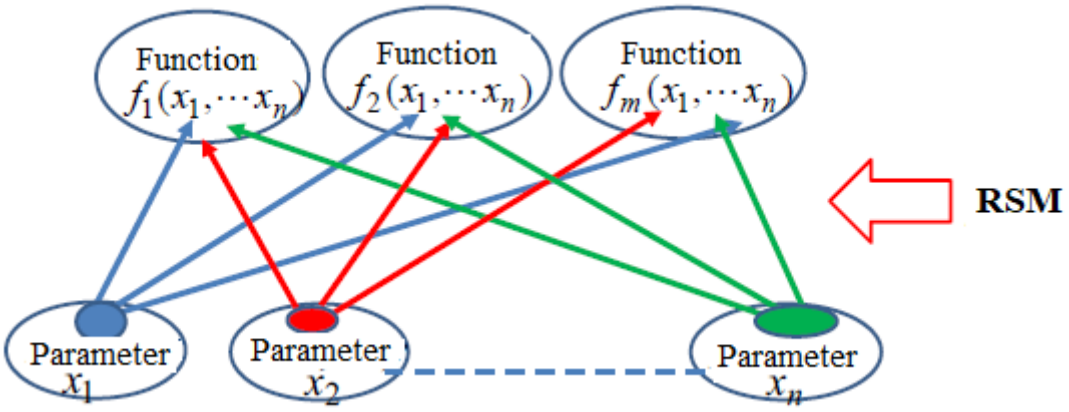

Figure 2.17. Response Surface Method

The response surface model is a linear function of the fit coefficients. This linearity provides flexibility, allowing to fit curved response surfaces by incorporating higher-order input variables. In general, second-order models are often sufficient for high-speed signal links and PSD applications. The general form of such a response surface model has the form:

$$y = \beta_0 + \sum_{i=1}^{n} \beta_i x_i + \sum_{i=1}^{n} \beta_{ii} x_i^2 + \sum_{i=1}^{n} \sum_{j\#i}^{n} \beta_{ij} x_i x_j \quad (2.28)$$

where *y:* the system response (output),

β_i: the model fit coefficients,

x_i: the systems inputs,

n: the number of independent input variables.

Details of the RSM method are presented in [40 - 43]. In this dissertation, RSM will be created using available PSD software with initial data; this will be presented in Chapter 4.

2.2.2.2. Set representation phase

The "set representation" phase is to configure the region or range of design parameters and required performances. Preference, the basis of the PSD approach, is expressed using a set (i.e., a range) and a "Preference Number (PN)" to reflect the designer's intent for design parameters and required performances. PN is introduced in a quantified number from zero to one and is used to estimate the optimum set for performance. It is a quantitative processing index that evaluates and determines the design parameters range [6]. An example of a preference set of parameters and performance is shown in Figure 2.18, where trapezoidal functions serve as an example. The value of PN = 0 is the allowable range. The value of PN = 1 corresponds to the most proper region meeting the needs and desires of the designer. Figure 2.19 shows another example of a set representation of parameter X_1 and X_2 and performance *Y*.

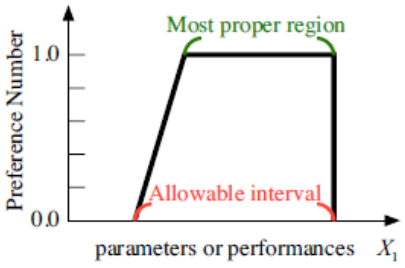

Figure 2.18. Preference set of parameters and performance

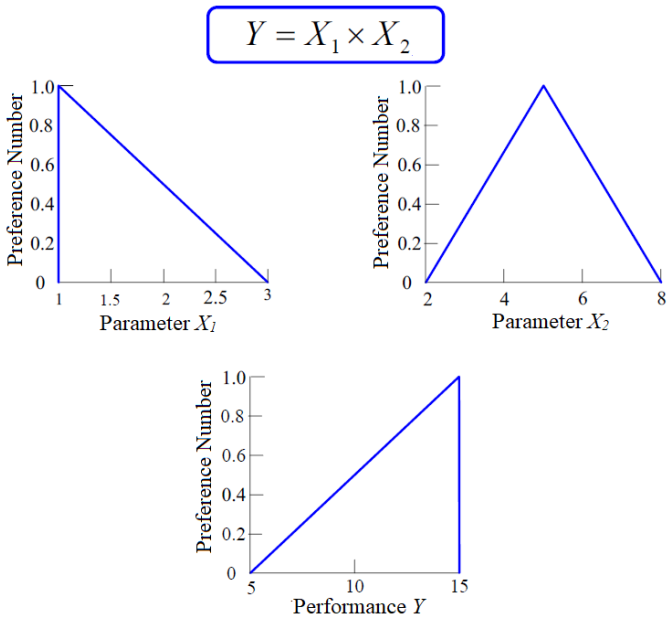

Figure 2.19. Example of a set representation

2.2.2.3. Set propagation phase

The “set propagation” is the computational phase that searches for achievable performance sets under the conditions configured by the initial combination of each design parameter (Figure 2.20).

The set propagation phase employs extended interval arithmetic, such as the Interval Propagation Theorem [44, 45], or optimization methods like the Swarm Optimization Method [46, 47], at each priority value level. These techniques are utilized to calculate the performance spaces achievable within the given original design space. Subsequently, if all performance parameter spaces exhibit a common space, referred to as an acceptable performance space, between the required performance space and the possible representation space, it indicates the existence of feasible design alternatives within the original design space. Figure 2.21 shows the set propagation phase of the example depicted in Figure 2.19.

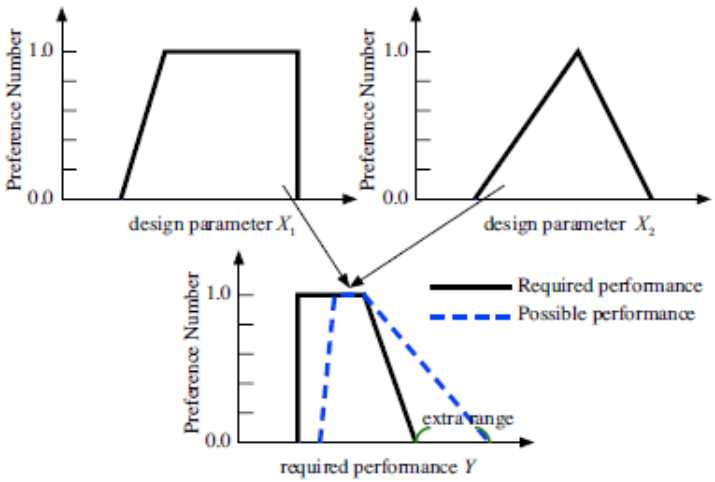

Figure 2.20. Set propagation phase

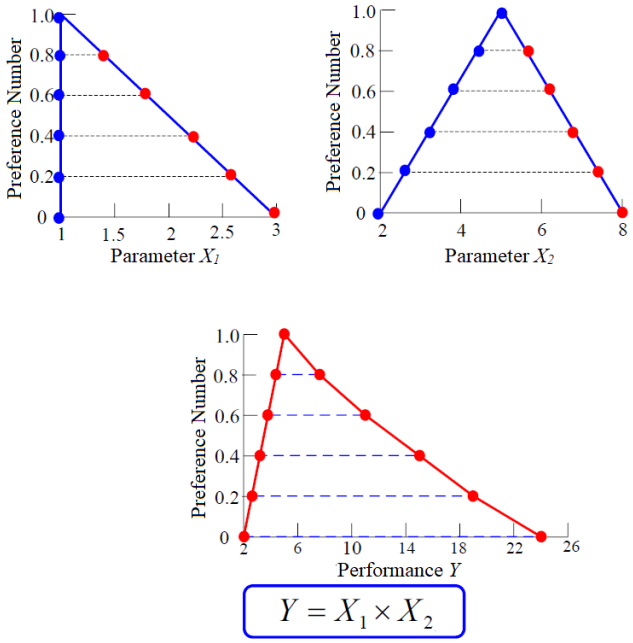

Figure 2.21. Example of a set propagation

2.2.2.4. Set narrowing phase

In the “set narrowing” phase, the sets are narrowed by removing the parts that do not meet the designer’s requirements from design parameter sets using the preference of each design parameter configured in the “set representation” phase (Figure 2.22). The process of quantitatively evaluating the preference and robustness of the proposal is repeated until there are no inefficient sets. When all performances meet the requirements, the allowable range of design parameters is finally given with the highest satisfaction indexes and robustness, reflecting the designer’s intent. The details of the PSD method are given in Refs. [38] and [48].

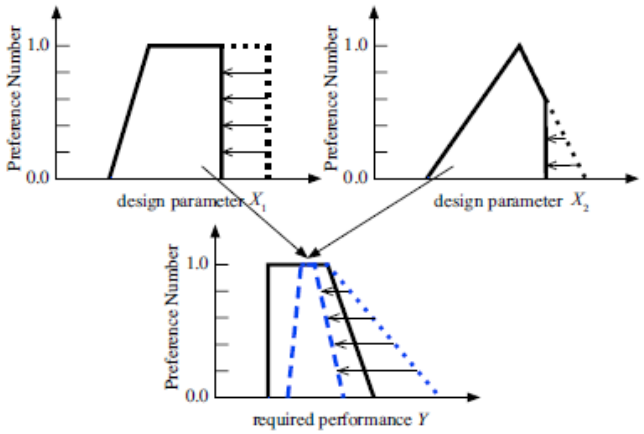

Figure 2.22. Narrowed set

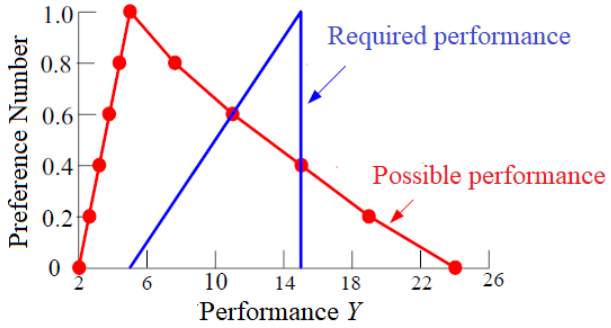

Figure 2.23. Compare the result of required performance and possible performance

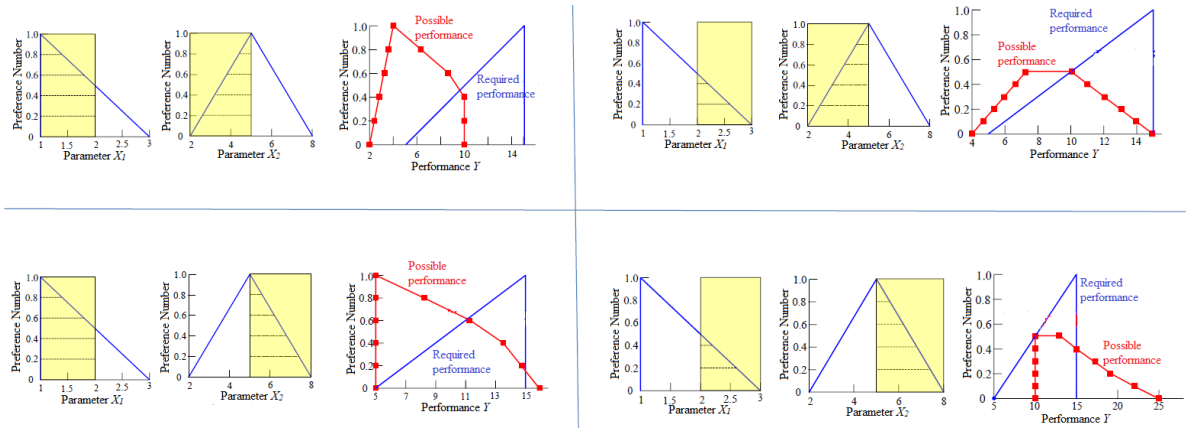

Figure 2.24. Some examples to narrow the parameter range

With the examples in Figures 2.19 and 2.21, the results of the required performance and set propagation phase are compared in Figure 2.23. During the set narrowing phase, the parameter range is progressively narrowed down to obtain a result that matchs with the specified requirement. Figure 2.24 shows a few examples of parameter narrowing by dividing two ranges. The division width is gradually reduced, ensuring that the possible distribution remains entirely within the required performance distribution.

2.3. Polynomial Chaos Method

2.3.1. Overview

Evaluation of signal integrity and EMC often requires statistical analysis due to the inherent nature of the problem under investigation [49] - [54]. Indeed, design specifications, such as wire placement and routing, or manufacturing tolerances, affect the electrical performance of interconnects in ways that are difficult or even impossible to predict with certainty determined. As a result, even with the most accurate simulation models, actual performance can differ largely from early-stage predictions due to uncalculated variations in design parameters.

The traditional approach to handling a stochastic problem is to perform deterministic simulations for a large number of random parameter variations to collect random response samples [51]. This approach, known as the MC method, converges very slowly. It requires several samples, usually of order 10^4, and thus makes it very inefficient or even prohibitive when a single numerical solution requires a little time [8]. The MC method can directly obtain highly accurate statistical information from a large number of samples but has the disadvantages of requiring many computations and poor computational efficiency as the number of samples increases [7].

The inefficiency of the MC method in many circuit simulators, has fueled widespread interest in efficient stochastic techniques for generating circuit model and transmission line design. This section provides an overview of recent methods, based on polynomial chaos [55], [56] that have been proposed for efficient statistical analysis of electronic circuits. The Polynomial Chaos (PC) method is a mathematical technique used for uncertainty quantification and propagation in computational models. It is particularly applied in fields such as engineering, physics, and finance, where there are uncertainties in the input parameters of a model, and the goal is to understand the effect of these uncertainties on the model’s output.

The PC method represents uncertain parameters as random variables and approximates their probability distributions using orthogonal polynomials. These orthogonal polynomials, such as Legendre, Hermite, or Chebyshev polynomials, form a basis set that allows for efficient representation of the random variables [57]. By expanding the uncertain quantities as a series of these polynomials, the PC method constructs a polynomial chaos expansion (PCE).

The PCE expresses the model's output as a polynomial of the uncertain parameters, where each term in the expansion corresponds to a specific combination of the polynomial basis functions. The coefficients of these terms capture the contributions of different orders of uncertainty. Typically, the PCE is truncated after a certain order to balance accuracy and computational efficiency. PCE coefficients can be calculated using different approaches and directly provide relevant statistical information such as the mean and variance of the output [58]. Furthermore, PCE can be used more commonly as an inexpensive but computationally accurate macro model to extract other statistical properties such as higher statistical moments or distribution functions.

2.3.2. Polynomial chaos expansion

The basic idea of PC is to represent random unknowns as PCE. The method is based on a spectral representation of the uncertainty where the basis polynomials contain the randomness, described by random variables ξ and the unknown expansion coefficients are deterministic, resulting in deterministic equations.

Let consider a stochastic process $Y(x, t, \xi)$ with finite second-order moments, depending on the normalized random variables collected in the vector ξ [59]:

$$Y(x,t,\xi) = L(x,t,\xi) \tag{2.29}$$

where $t \in [0, T]$ represents the time, x is the state vector, and L is an operator (linear or nonlinear). Now, Y can be expressed as an infinite series of orthogonal basis functions ϕ_i with suitable coefficients y_i as [55, 60, 61]:

$$Y(t,\xi) = \sum_{i=0}^{\infty} y_i(t)\phi_i(\xi) \tag{2.30}$$

The orthogonal polynomials ϕ_i by inner product are:

$$\langle \phi_m, \phi_n \rangle = \int_{-\infty}^{+\infty} \phi_m(\xi)\, \phi_n(\xi) w(\xi) d\xi = \delta_{mn} \tag{2.31}$$

that is, the above integral is only non-zero when $m = n$.

The function $w(\xi)$ in Equation (2.31) is the probability density function (PDF) of ξ, determined by the statistical model corresponding to the stochastic parameters in the problem. Examples of PDF for some random variables are described in Table 2.2 [59].

Table 2.2. Polynomials for some random variables

Distribution	Orthogonal Polynomials	PDF	Weight Function	Support Range
Gaussian	Hermite $H_{e_k}(\xi)$	$\frac{1}{\sqrt{2\pi}}e^{\frac{-x^2}{2}}$	$e^{\frac{-x^2}{2}}$	$[-\infty,\infty]$
Uniform	Legendre $P_k(\xi)$	$\frac{1}{2}$	1	$[-1,1]$
Gamma	Laguerre $L_k^a(\xi)$	$\frac{x^a e^{-x}}{\Gamma(a+1)}$	$x^a e^{-x}$	$[0,\infty]$
Beta	Jacobi $J_k^{a,b}(\xi)$	$\frac{(1-x)^a(1+x)^b}{2^{a+b+1}\beta(a+1,b+1)}$	$(1-x)^a(1+x)^b$	$[-1,1]$

The representation in (2.30) is exact, however, for practical applications, Equation (2.30) must be truncated to a limited number of basis functions *M +1* via suitable truncation schemes, as [62]:

$$M+1=\frac{(N+P)!}{N!P!} \tag{2.32}$$

with *N* is the number of random variables considered and *P* is the maximum order of the polynomials in Equation (2.30). Equation (2.30) is truncated as:

$$Y(t,\xi)\approx\sum_{i=0}^{M}y_i(t)\phi_i(\xi) \tag{2.33}$$

The advantage of using a PCE is that its coefficients are often calculated much faster than running a MC simulation. The representation of Equation (2.26) is then used as a cheap computational and analytical macro model to quickly obtain many actual response samples, from which statistical information such as stochastic moments or distribution functions can be calculated. Example, the first two statistical moments are the expected value, or mean, and the variance, which are given by follows [8]:

$$E\{(Y(t)\}=y_o(t) \tag{2.34}$$

i.e., the first coefficient, and:

$$Var\{Y(t)\}=\sum_{i=1}^{M}y_i^2(t) \tag{2.35}$$

i.e., the sum of the squares of all remaining coefficient.

In Equation (2.33), the higher the expansion order, the better the accuracy but, the lower the computational efficiency. According to [8], quadratic expansion is usually precise enough in most cases. Therefore, this dissertation will use the second-order expansion of PCE with the randomness problem. In Equation (2.33), in order to determine the stochastic *Y*, it is necessary to determine the basis functions ϕ_i and the coefficients of PCE y_i.

2.3.2.1. Building of the polynomial chaos basis

An orthogonal polynomial sequence is a family of polynomials satisfying condition (2.31). The set of classical orthogonal polynomials is known as Askey scheme [63], which includes Hermite, Legendre, Jacobi and Lagurere as Table 2.2. Each class of them provides an optimal basis for a specific continuous probability distribution type.

Example Normal distribution and Uniform distribution, two types often assumed for the distribution of the uncertain parameters in the engineering problems [64]. With the input variable having a uniform distribution, the first six orthonormal Legendre polynomials are as follows:

$$\begin{aligned}
\phi_0 &= 1 \\
\phi_1 &= \sqrt{3}\xi \\
\phi_2 &= \frac{1}{2}\sqrt{5}(3\xi^2 - 1) \\
\phi_3 &= \tfrac{1}{2}\sqrt{7}(5\xi^3 - 3\xi) \\
\phi_4 &= \tfrac{1}{8}\sqrt{9}(35\xi^4 - 30\xi^2 + 3) \\
\phi_5 &= \tfrac{1}{8}\sqrt{11}(63\xi^5 - 70\xi^3 + 15\xi)
\end{aligned} \tag{2.36}$$

In the case of normal distribution of the variable ξ, the Hermite polynomials are used and the first six orthonormal Hermite polynomials are:

$$\begin{aligned}
\phi_0 &= 1 \\
\phi_1 &= \xi \\
\phi_2 &= \frac{1}{\sqrt{2}}(\xi^2 - 1) \\
\phi_3 &= \tfrac{1}{\sqrt{6}}(\xi^3 - 3\xi) \\
\phi_4 &= \tfrac{1}{\sqrt{24}}(\xi^4 - 6\xi^2 + 3) \\
\phi_5 &= \tfrac{1}{\sqrt{120}}(\xi^5 - 10\xi^3 + 15\xi)
\end{aligned} \tag{2.37}$$

With multiple variables, a basis made of multivariate polynomials can be built up by tensorization, that is by multiplying the univariate polynomials. For example, the basis of

multivariate polynomials for a second-order expansion in each of two random dimension (ξ_1 = ξ_2 = 2) as follows [57]:

$$\begin{aligned}
\phi_0(\xi) &= \phi_0(\xi_1)\phi_0(\xi_2) \\
\phi_1(\xi) &= \phi_1(\xi_1)\phi_0(\xi_2) \\
\phi_2(\xi) &= \phi_0(\xi_1)\,\phi_1(\xi_2) \\
\phi_3(\xi) &= \phi_2(\xi_1)\phi_0(\xi_2) \\
\phi_4(\xi) &= \phi_1(\xi_1)\phi_1(\xi_2) \\
\phi_5(\xi) &= \phi_0(\xi_1)\,\phi_2(\xi_2)
\end{aligned} \tag{2.38}$$

2.3.2.2. Computation of the coefficients of PCE

There are many methods that can be used to calculate the coefficient of PCE. This dissertation uses projection methods to calculate the coefficients of PCE. These methods take benefit of the orthonormality of the PC basis. By multiplying the expansion in Equation (2.33) by $\phi_i(\xi)$ and by integrating with respect to the joint PDF of ξ, one gets:

$$y_i = \int Y(\xi)\,\phi_i(\xi) w(\xi) d\xi \tag{2.39}$$

Equation (2.39) has many solutions, such as using estimation by classical methods for numerical integration, which consist in approximating multi-dimensional integral by a weighted sum or several techniques based on the choice of the integration point ξ and weights w. These methods are presented in the document [58].

In Chapter 2, the dissertation presented basic theories about the problem encountered, including EMC solutions, the PSD method, and the PC method. From there, the dissertation proposes a method of solving problems encountered and tests in the following chapters.

Chapter 3
Multi-objective Design for EMC Solutions

3.1. Proposed Idea

The dissertation aims to present a multi-objective design method for EMC solutions, specifically addressing the challenges posed by uncertain parameters encountered in practical cases. By developing the proposed method, the aim is to offer effective solutions that can accommodate and mitigate the impact of uncertainties in practical situations. The dissertation seeks to contribute to the EMC field by providing a robust design approach that considers the uncertainties inherent in practical applications.

In recent years, the PSD approach has been extensively applied in the mechanical and automotive fields and is being explored in electronic fields. This method has significant advantages over traditional point-based design methods, helping to reduce product development costs and time. By considering design parameters within a range instead of exact values, the PSD method demonstrates robustness, accounting for deviations during actual production. Thus, the dissertation propose the application and evaluation of the PSD method in conjunction with EMC solutions.

The flowchart of the proposed method is shown in Figure 3.1, outlining its main phases. The initial step involves preparing an initial data set for the PSD method - Preliminary Phase. This initial data set is established based on the theories, preferences, and experiences of the designers. However, there are always random variables in practice, so the dissertation uses a statistical method to handle this challenge - the PC method. The PC method generates the necessary initial data set for applying the PSD method.

Applications of the PC method have been widely used in recent years to overcome the disadvantages of the traditional Monte Carlo method. The PC method helps to increase the calculation efficiency and still ensures accuracy by the requirements.

Consequently, our proposed method comprises two essential steps. The first is to use the PC method to simulate random variables (if any) and generate an initial data set for the preliminary phase of the PSD method. The second is to use the PSD method with the EMC problems posed. If the conditions and initial values of the input have been precisely determined with no random variables, it is not necessary to use the PC method.

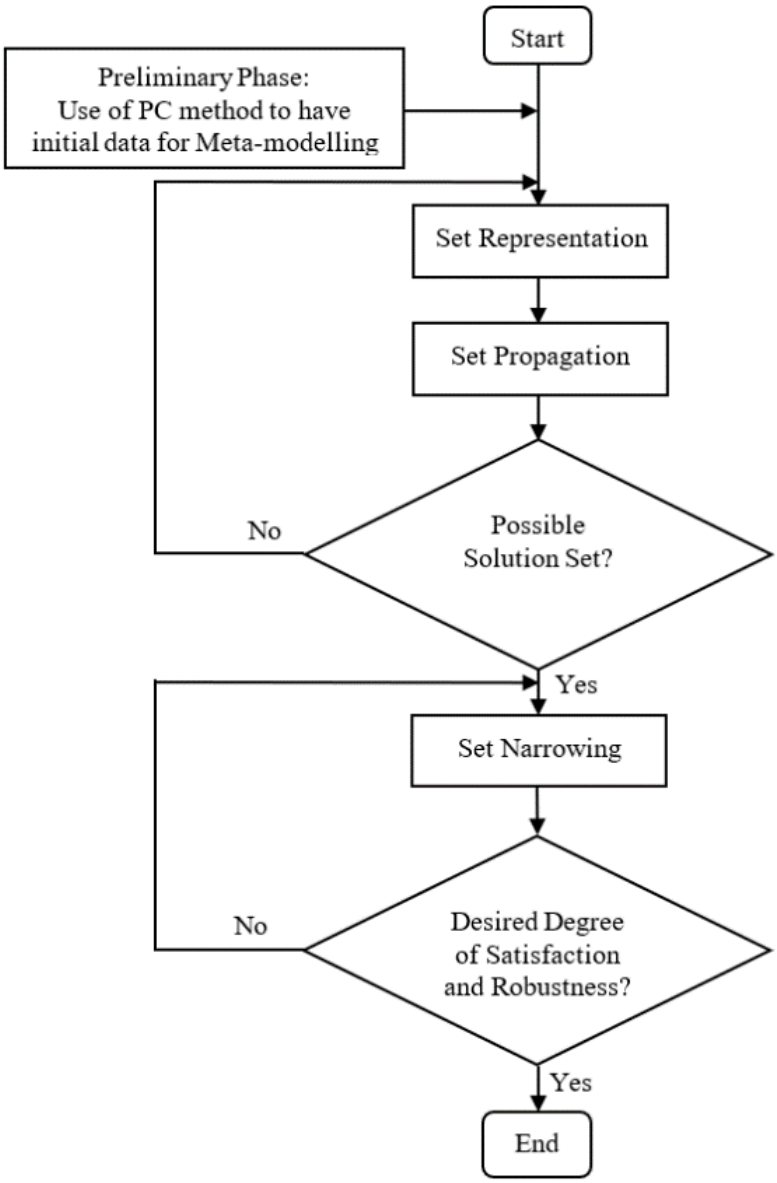

Figure 3.1. Flowchart of the proposed method

3.2. Literature Reviews

In essence, EMC deals with interference and the prevention of it through the design of electronic systems [9]. EMC topics have become an essential subdiscipline in the design of electrical and electronic devices. EMC-related courses have also been incorporated into university curricula since the early 1980s. This shows the importance of applying EMC solutions in the design of electronic devices. Many EMC solutions have been published and used.

The EMI filter is a fundamental EMC solution for noise suppression and is widely employed in high-speed differential signal wires, power supply lines, and so on (for example,

[4]). With the EMC problem, the design of the EMI filter should simultaneously satisfy the required performances for both Differential Mode (DM) and Common Mode (CM). Many EMI filter design methods have been studied, proposed, and tested, such as those using analytic electromagnetic fields, trial-and-error tests through experiments, and design using Particle Swarm Optimization, a super simulation method [5].

Another EMC solution is the shielding method, which is also commonly used. An example of a shielding method is enclosure. An example of a shielding method is enclosure. The enclosure is constructed from multiple metal sheets for the purpose of isolating the device or electronic components inside from the external electromagnetic environment and vice versa. The theory and design methods of enclosures and metal sheets are given in many documents, such as [9, 30, 31]. The shielding method provides high protection for electronic components or devices from the electromagnetic field.

To meet multiple performance requirements and to reduce product development costs and time, concurrent design techniques for meeting multiple performance requirements have been proposed. Notable examples include the Taguchi method [1] and set-based design [2]. Among these approaches, the PSD method [3] stands out, widely adopted in mechanical engineering. The PSD method allows designers to incorporate their intent by quantitatively evaluating performance requirements and design variables using a preference set and frequency. By obtaining design variables within a range rather than specific values, the PSD method exhibits robust design capabilities, accommodating deviations during actual production [6]. It should be noted that the PSD method is not an optimization technique but a design method for concurrently satisfying multi-objective performances.

The possibility of applying the PSD method to electric and electronic systems have been studying, and so far, filters [6, 35, 36, 65, 66], EMI filters [32, 37, 67, 68], transmission lines [69], differential-paired lines [70], cantilever for electrical contact [71] and radio absorbers [48]. These investigations have shown good utility, indicating that the PSD method can deliver a design solution (within a specified range) satisfying multiple performance requirements.

In the context of the multi-objective problem for EMI filters, references [32], [67], and [68] investigate the feasibility of designing EMI filters using the PSD method in an ideal case, taking into account mutual inductance (coupling factor) between inductors. However, in practical cases, circuits inherently present uncertain parameters arising from manufacturing tolerances, parasitic elements, improper impedance matching, and other factors. The challenge lies in the presence of these uncertain parameters making it difficult or impossible to predict circuit performance deterministically. Even with highly accurate simulation models, the actual performance may differ largely from predictions at an early stage due to this uncalculated variation. Hence, the use of statistical simulation becomes essential to evaluate the EMC performance considering variations in characteristics caused by unintended fluctuations in these uncertain numerical parameters.

Reference [37] used Monte Carlo method to simulate source and load resistor fluctuation statistically. Fifty combinations of resistors are calculated to obtain the initial data set for PSD. However, the test is not performed with more random samples, and there is no guarantee that fifty samples are enough to ensure the convergence of the simulation. As the number of samples increases, the computational efficiency of the MC method will decrease rapidly. The MC method allows for obtaining highly accurate statistical information from a large number of samples but has the disadvantages of requiring many computations and poor computational efficiency as the number of samples increases [7].

Another statistical method is used to increase computational efficiency, the PC method. In recent years, the PC method has been proposed for highly efficient statistical simulation [8]. PC looks for an approximate response to a system's performance as an expansion in orthogonal polynomials. PCE coefficients can be calculated using different approaches, such as the stochastic testing method and stochastic Galerkin method [8, 72], and directly provide relevant statistical information such as mean and variance. PC expansion can commonly be used as a cheap but computationally accurate macro model. The PC method analyzes faster than the MC method, although it may be slightly less accurate. The PC method has been applied and reviewed in circuit design, such as for transmission lines [7, 8, 73], modern integrated circuits [59, 74], and RC filters [75, 76]. Previous works on the PC method have mainly focused on stochastic analysis, while this dissertation attempts to apply the PC method to design methodology, specifically for EMI filters.

3.3. Proposed Method

In this dissertation, a design method for EMC solutions is proposed by combining the PC and PSD methods. With the use of the PC method to simulate multiple uncertain parameters and generate initial data for the Preliminary Phase of the PSD method, the proposed method will have higher computational efficiency than previous work in Ref. [37]. And the PSD method will satisfy the multi-objective requirement. For applications that do not need to handle the randomness problem, only use the PSD method to obtain the final results.

The procedure for designing EMC solutions using the combination of PC and PSD methods proposed is outlined as follows:

1. Determine design specifications: Identify the design parameters, required performances, and uncertain parameters based on the EMC requirements. This step involves understanding the performance criteria and the variables that influence the EMC solution.

2. Utilize the PC method to obtain an initial data set: When uncertain parameters are present, the PC method is employed to generate an initial data set by considering the ranges of design parameters, mathematical formulas relevant to the application, and the designer's experience.

3. Design the application with PSD using the initial data from step 2: Use the PSD method to configure the design parameters and required performances, thereby calculating the narrow range of the design parameters and obtaining final results that satisfy the required performances. This step involves an iterative process of refining the design based on the PSD method.

4. Evaluate the obtained performances: Consider the validity of the obtained range of design parameters by calculating the performances and comparing them against the required performances. This evaluation ensures that the EMC solution meets the specified criteria and identifies any discrepancies or areas for further refinement.

Following this procedure, the proposed method combines the PC and PSD methods to design EMC solutions, considering both deterministic and uncertain parameters. For applications that do not involve uncertain parameters, the PSD method alone can be utilized to obtain the final results.

Chapter 4

Experiment with the Proposed Design for EMC Solutions

Chapter 4 experiments with the proposed method with two common EMC solutions, a shielding metal sheet and an EMI filter. The final results obtained as a range will be validated, and then the feasibility of the proposed method in the field of EMC will be evaluated.

4.1. Experiment with the Proposed Method for Shielding Design

The first application related to shielding design, specifically focusing on the design of a metal sheet design for the enclosure.

Theoretically, *SE* of a metal sheet in the ideal condition is very high [9] and meets the necessary requirements. However, in practical applications, metal sheets always have apertures and holes, which compromise the SE, as depicted in Figure 4.1. Unlike water or gas pipelines, electromagnetic field leakage through holes does not behave by "spraying" internally or externally when under pressure. Instead, when an electromagnetic field encounters a shielding metal sheet, an electric current is induced on the surface of the sheet. In Figure 4.1a, the resulting surface currents flow within the shield. These currents and related fields create new fields, that counteract or reduce the impact of incident fields. The incident field generated a surface current, which can be thought of as generating a reflected field. The reflected field tends to cancel the radiated field in order to satisfy the boundary condition that the total electric field tangential to the conductor must be zero. In order for the shield to perform this cancellation, the surface current must be allowed to flow unimpeded. When the surface currents encounter a hole, they must change direction to flow around it (Figure 4.1b,c) [9]. This change in current direction introduces inductance, along with associated magnetic fields, which propagate through the hole, thus reducing the SE of the sheet metal. As the surface current flows through the inductance created by the deviation around the hole, a voltage difference is generated across this inductance, appearing across the hole. The difference in voltage generates new electric fields (E), ontribute to the degradation of *SE* value.

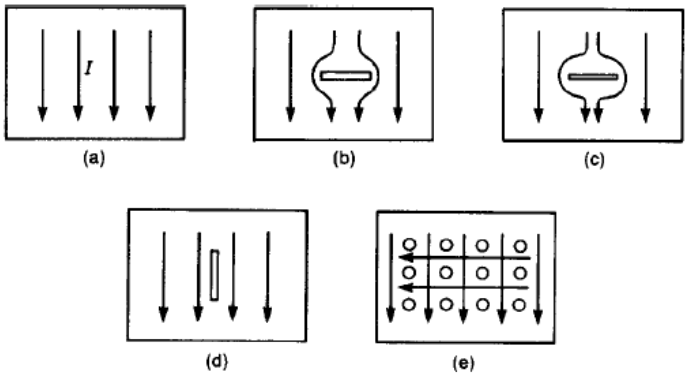

Figure 4.1. Effect of holes with the surface current on the metal sheet

Typically, in low-frequency fields, the SE of the enclosure is primarily determined by the material used. However, at higher frequencies, factors such as joints, openings, and I/O ports on the enclosure become decisive in determining *SE*. For the purpose of this discussion, a simple case with a metal sheet is considered, including holes for screw jointing.

4.1.1. Specification

The design specification of the metal sheet of enclosure includes:

- Material: Aluminum with $\gamma = 2700$ kg/m^3,
- Dimension: 2 m x 3 m (a common size),
- $\sigma_r = 0.61$, $\mu_r = 1$,
- Frequency range: 100 MHz ~ 10 GHz.

The design parameters are the thickness *t* of the metal sheet and the radius *r* of hole on metal sheet. The required performances are the shielding effectiveness *SE* and weight *W* of the metal sheet as follows:

- $W \leq 40$ kg (depends on designer's intention),
- $SE \geq 80$ dB (a typical performance of enclosure).

4.1.2. Research methodology

a. Determination of the initial element values

In the enclosure design procedure, a designer determines the configuration by considering the required specification and then uses the design formulation in subsection (2.1.3.4). To satisfy the requirements, the designer will specify the element parameters in generating numerical values of the performances.

Table 4.1. Initial element value of metal sheet

Level	*t* (mm)	*r* (mm)
1	1	4
2	2	5
3	3	6

The data for meta-modeling is obtained with the characteristics calculated by combining three values at the minimum (level 1), intermediate (level 2), and maximum (level 3) of the initial range of each parameter, as shown in Table 4.1. The design parameters in this study are *t* and *r*.

b. Generation of initial data

For a round hole with diameter *d* in mm and *t* is the depth of hole in mm, the SE can be calculated as [31]:

$$SE(dB) \approx 102 - 20\log(df_{Mhz}) + 30(\frac{t}{d}) \text{ when } d \leq \lambda/2 \quad (4.1)$$

The hole here will be considered in the case of jointing using screws, so assume a leak value of 10% of the hole size. In the case of multiple holes, because the holes are used for coupling, the distance is usually above 10 cm, i.e., more significant than a half wavelength $\lambda/2$, it can be ignored, and only the effect of one hole can be taken into account. The final *SE* of the sheet metal is calculated as [31]:

$$\frac{1}{SE_{total}} = \frac{1}{SE_1} + \frac{1}{SE_2} + \cdots \quad (4.2)$$

where SE_1 is SE of metal sheet in the ideal condition and is calculate by Eqs. (2.8), (2.9) and (2.13).

The weight of the metal sheet is calculated as:

$$W = 2 \times 3 \times t \times 10^{-3} \times \gamma \quad (4.3)$$

with γ = 2700 kg/m^3 is the specific weight of aluminum.

Since *SE* varies with frequency, the dissertation takes the worst-case data values of *SE* (minimum value) as the initial data.

c. Design of metal sheet by PSD method

Next, the obtained initial data is used with the PSD method to obtain the design parameters for the metal sheet. First, the response surface methodology will use the initial data for meta-modeling. The response surfaces are represented as quadratic models taken from the initial data. The meta-modeling equation of *SE* and *W* has been obtained as a quadratic polynomial expressed as the sum of the quadratic, linear, and alternating terms.

The three levels shown in Table 4.1 are set as the initial range. The preference functions of the design parameters and the required performances are shown in Figures 4.2 and 4.3.

Design parameters are combined in the preliminary phase to generate a feasible set as the possibility distribution set, which is the “set propagation” phase, as explained in subsection 2.2.2.3. Then the feasible set is narrowed by the "set narrowing" process to obtain the narrowed distribution in the final phase. The dissertation uses the PSD software to accomplish this task [77].

Finally, the responses of obtained ranges of design parameters are calculated to consider the validity of the proposed method.

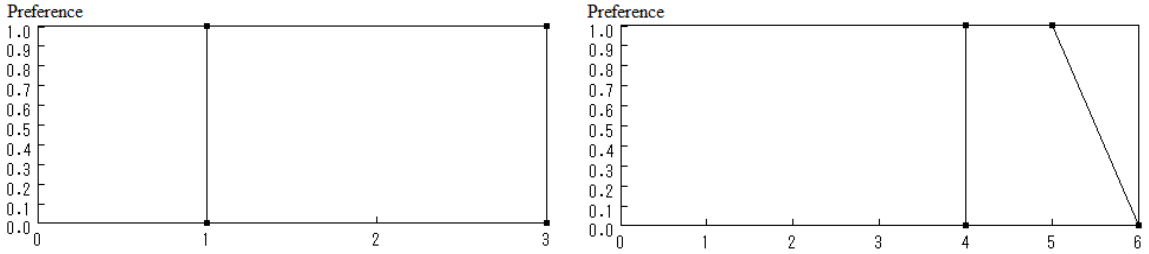

(a). *t* (b). *r*

Figure 4.2. Preference functions of metal sheet’s design parameters

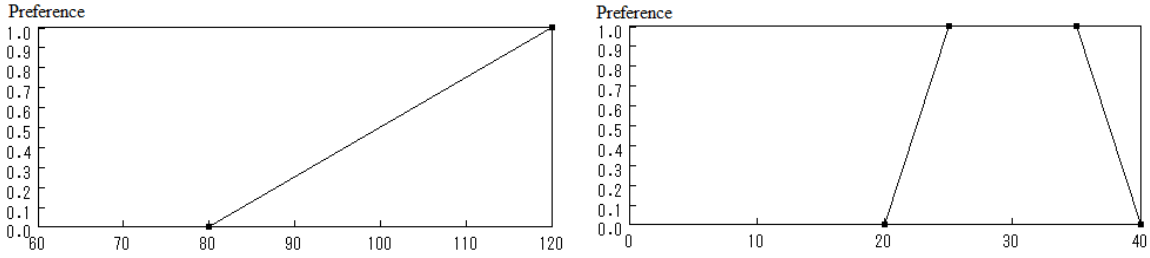

(a). *SE* (b). *W*

Figure 4.3. Preference functions of metal sheet’s required performances

4.1.3. Calculated results and discussion

Figure 4.4 shows a scatter diagram (predicted values by RSM and actual values). The correspondence between the theoretically calculated values and meta-modeling equations obtained by the response surface methodology can be seen. The horizontal axis is the theoretically calculated value when the element value is changed. The vertical axis is the value calculated by the meta-modeling formula according to the response surface methodology. In the ideal response surface methodology, the actual value and the calculated value by RSM perfectly match, leading to a straight line with slope one and intersection zero (red-solid line in Figure 4.4). However, in practice, if there is a slight error and correlation coefficient of the meta-modeling equation, i.e., a low degree of approximation, then the range solution may not satisfy the required performance depending on the preference [65]. In this model, a high correlation is obtained with 0.99 or more.

The preference distributions as the final results and obtained range solution of the design parameters and required performances are shown in Table 4.2, Figures 4.5 and 4.6, which describes the relationship between the “Initial set” and “Narrowed set”. In Figure 4.5, the black-dot and red-solid lines are “Initial set” and “Narrowed set”, respectively. In Figure 4.6, the black-dot, the blue-solide and red-solid lines are “Required performance”, “Possibility distribution”, and “Narrowing distribution”, respectively. The final results indicate that obtained ranges of the design parameters satisfy the required performance sets.

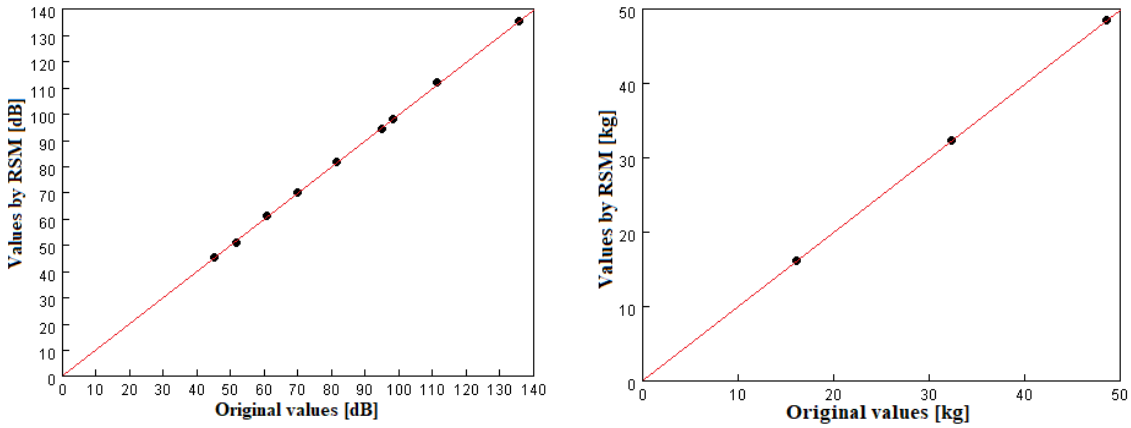

(a). *SE* (b). *W*

Figure 4.4. Scatter diagram is calculated with theoretically calculated values of *SE* and *W* compared with meta-modeling formula

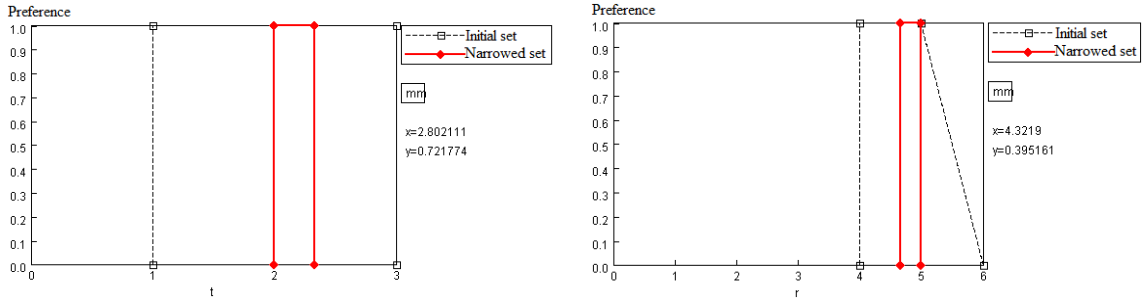

(a). *t* (b). *r*

Figure 4.5. Preference set of metal sheet's design parameters

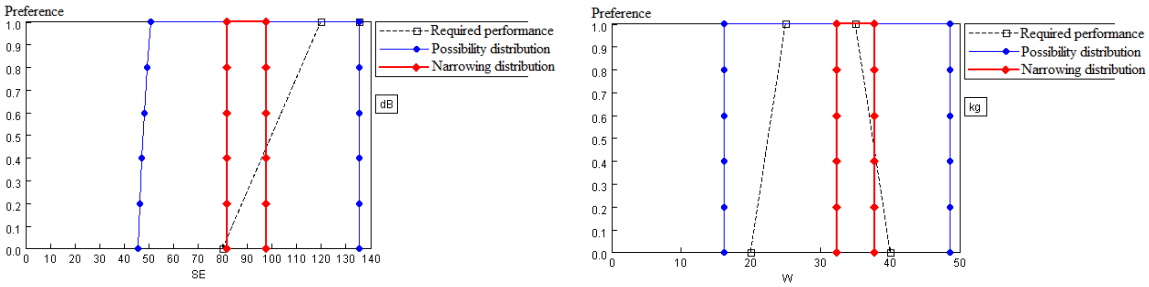

(a). *SE* (b). *W*

Figure 4.6. Preference set of metal sheet's required performances

Table 4.2. Narrowed set of metal sheet obtained by PSD

Elements	*t* (mm)	*r* (mm)
Narrowed set	2 ~ 2.33	4.67 ~ 5

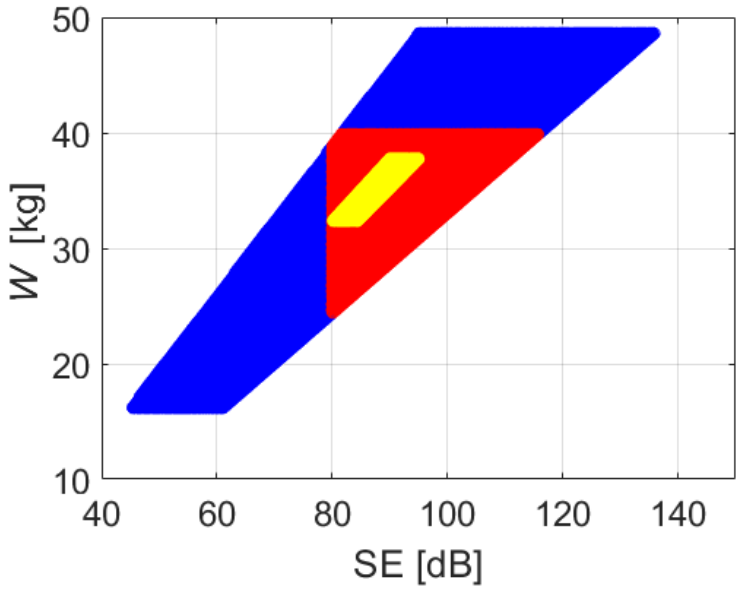

Figure 4.7. Pareto front diagram of metal sheet's performances

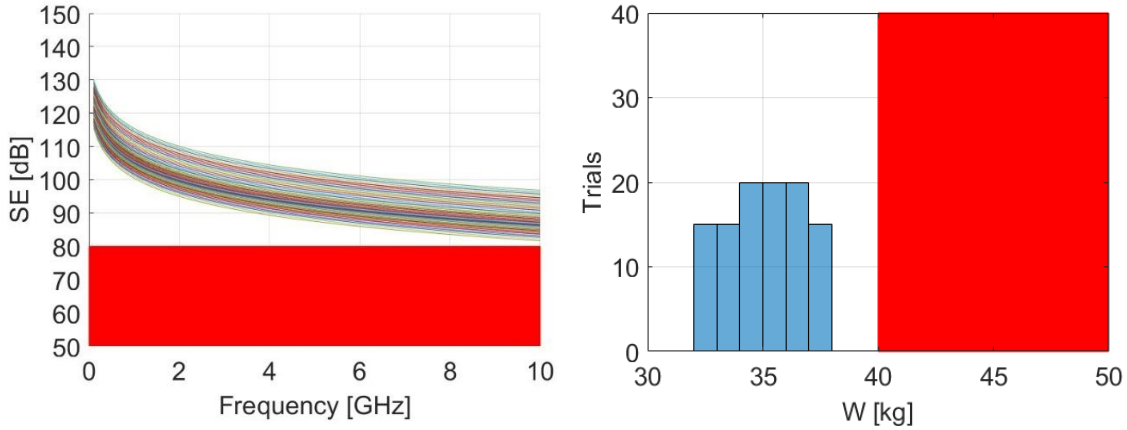

(a). *SE* (b). *W*

Figure 4.8. Required performances of metal sheet are calculated based on design parameters in the range obtained by PSD

Figure 4.7 depicts a Pareto front diagram for a more precise assessment of the multi-objective optimization problem. Where the blued area is calculated results with the initial range of design parameters, red area is the feasible area satisfied with required performances, and the yellow area is the performance area for the range obtained from PSD with preference function as intended by the designer. This demonstrates PSD's powerful design capabilities to be able to meet many designers' criteria.

To consider the validity of the obtained ranges of design parameters, the required performances are calculated. Design parameters are selected in the range obtained by the PSD method from the minimum value to the maximum value to produce about 100 combinations of design parameters, and *SE* and *W* are calculated and shown in Figure 4.8. Multicolored curves represent the minimum to maximum values of the metal sheet’s performances for the range obtained. The area filled with red indicates out of range for the required performances.

Figure 4.8 shows that the characteristics are satisfied with the required performances, and therefore the validity of the design parameters is demonstrated. As a result, it is confirmed that all required performances are met, and the proposed method can be applied for the metal sheet of enclosure.

4.2. Experiment with the Proposed Method for EMI Filter Design

The second application considered is the EMI filter. The EMI filter will be tested in three cases: the ideal case, the case with one stochastic parameter, and the case with multiple stochastic parameters.

Since normal distribution spreads to infinity, it is difficult to determine the worst-case data for EMC evaluation. In this application, I assume that the resistor value is random with equal probability within 5% of the mean value. So I use a uniform distribution for stochastic variables, a distribution commonly used in engineering problems.

The circuit diagram of the EMI filter is shown in Figure 4.9. The filter is considered in three cases, from simple to complex, as follows:

- Case 1 - Ideal case:

  + $R_{g1} = R_{g2} = R_{L1} = R_{L2}$, i.e., a balanced circuit, no stochastic parameter.

- Case 2 - One stochastic parameter:

  + $R_{g1} = R_{L1} = 50 \pm 2.5\ \Omega$,

  + $R_{g2} = R_{L2} = 50\ \Omega$,

  + Resistor R_{g1} and R_{L1} are same stochastic parameters with uniform distribution. The average value of resistors is 50 Ω, and the standard deviation is equal to 5% of the average.

- Case 3 - Multiple stochastic parameters:

  + Resistors R_{g1}, R_{g2}, R_{L1}, and R_{L2} are stochastic parameters with uniform distribution. The average value of resistors is 50 Ω, and the standard deviation is equal to 5% of the average.

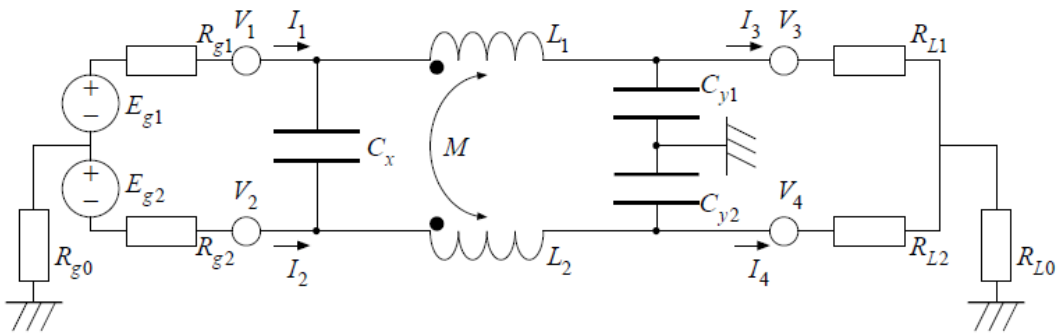

Figure 4.9. Circuit model for EMI filter

4.2.1. EMI filter in the ideal case

The ideal case, $R_{g1} = R_{g2} = R_{L1} = R_{L2}$, i.e., a balanced circuit, was studied and tested, and the validity of the PSD method was proven in [37]. To show the generality of the research, the dissertation will reconsider this work.

4.2.1.1. Specification

The design specification of the circuit in Figure 4.9 includes:

- E_{g1} = 0.5 V, E_{g2} = -0.5 V,
- $R_{g0} = R_{L0}$ = 0 Ω,
- $R_{g1} = R_{L1} = R_{g2} = R_{L2}$ = 50 Ω.

The required performances are the attenuation of DM A_{DM} and CM A_{CM} at the output terminal of the EMI filter as follows:

- $f \leq f_p$ = 10 kHz: $A_{DMpb} \leq$ 1.0 dB,
- $f \geq f_s$ = 200 kHz: $A_{DMsb} \geq$ 60 dB,
- $f_p \leq f \leq f_s$: $A_{CMpb} \geq$ 6 dB,
- $f \geq f_s$: $A_{CMsb} \geq$ 40 dB.

First, when converting to the normalized frequency region and calculating the filter order according to Equation (2.17), N_{DM} = 2.53 for DM and N_{CM} = 1.35 for CM , i.e., DM and CM require a third-order circuit and second-order, respectively. Therefore, the circuit configuration is obtained, as shown in Figure 4.10.

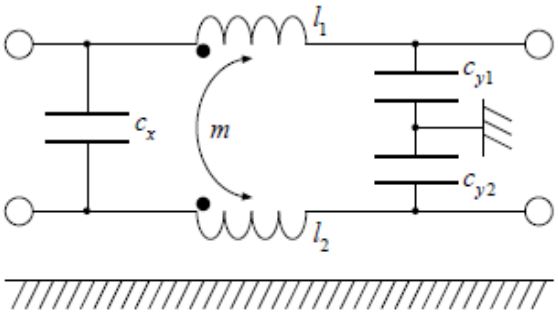

(a). Lowpass prototype filter

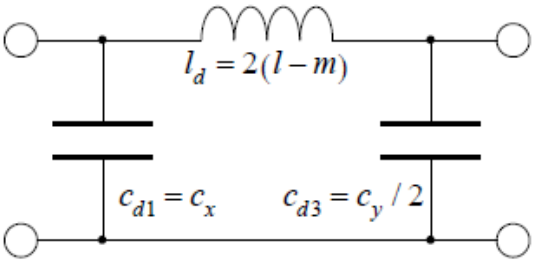

(b). Third-order equivalent circuit model for DM

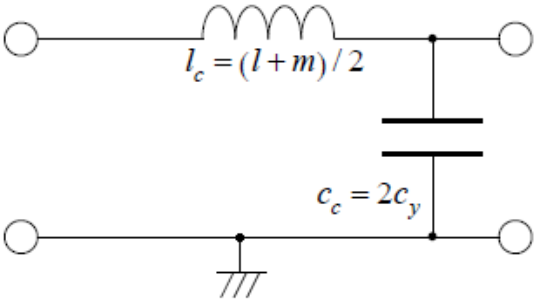

(c). Second-order equivalent circuit model for CM

Figure 4.10. Equivalent circuit model for EMI filter: $l = l_1 = l_2$, $c_y = c_{y1} = c_{y2}$, $m = k\sqrt{l_1 l_2}$, where k is coupling coefficient

4.2.1.2. Research methodology

a. Determination of the initial element values

During the filter design procedure, a designer selects the configuration by taking into account the required specifications, as well as the source and load terminals. Subsequently, the designer employs the design formulation or table. To meet the requirements, the designer will specify the element parameters in generating numerical values of the performances.

Table 4.3. Initial element value of EMI filter

Level	$l_1 = l_2$	k	c_x	$c_{y1} = c_{y2}$
1	1.0	0.5	0.2	1.0
2	1.5	0.7	0.6	1.5
3	2.0	0.9	1.0	2.0

The data for meta-modeling is obtained with the characteristics calculated by combining three values at the minimum (level 1), intermediate (level 2), and maximum (level 3) of the initial range of each parameter, as shown in Table 4.3. The design parameters in this study are $l = l_1 = l_2$, k, c_x, and $c_y = c_{y1} = c_{y2}$. The region of variables may be determined by theory, preference, and limitation of the design target. As described in subsection 2.1.3.5, the element values l_1, c_x, and c_{y1} are between 0.1 and 2.0 in the normalized frequency range, and k is the coupling coefficient and with value between 0 and 1. The values of levels 1 and 3 of the design parameters are selected based on the designer's experience to maintain the limits of the design target. The values of level 2 are generally selected as the middle between levels 1 and 3 because the selection is appropriate for obtaining the equation for the response surface methodology. The same three-level initial values as the former design in Ref. [37] were used in this study.

b. Generation of initial data

Design parameters are $l = l_1 = l_2$, k, c_x, and $c_y = c_{y1} = c_{y2}$. The required performances are the attenuation of the DM A_{DM} and CM A_{CM} at the output terminal of the EMI filter can be obtained by solving the EMI filter equations from the ABCD matrix in subsection 2.1.3.5. Since the design parameters in Table 4.3 vary in 81 combinations (3^4), and EMI filter performances also vary with frequency, the dissertation takes the worst-case data values of the A_{DM} and A_{CM} performance as the initial data. The worst-case here means the maximum value of attenuation for the DM in the passband and minimum value in the stopband, as well as the minimum value of attenuation for the CM in both the passband and stopband.

c. Design of EMI filter by PSD method

After obtaining the initial data, it is utilized in the PSD method to determine the design parameters for the EMI filter. Firstly, the response surface methodology employs the initial data for meta-modeling. In this process, response surfaces are represented as quadratic

models derived from the initial data. These quadratic models capture the relationships between the design parameters and the EMI filter's performance characteristics. In Refs. [40] and [41], the meta-modeling equation of attenuation of the DM voltage and CM current has been obtained as a quadratic polynomial expressed as the sum of the quadratic, linear, and alternating terms. In this model, all 81 combinations are calculated for circuit analysis (numerical computation) with low computational costs. However, DOE, such as L9 orthogonal arrays [42], can be applied as in Ref. [66] to reduce the computational cost of the meta-modeling.

The three levels in Table 4.3 are set as the initial range. The preference functions of the design parameters are given as isosceles triangles between the maximum and minimum values as Figure 4.11 [37]. The preference functions of the required performances are linear diagonals with the value PN = 0 corresponding to the limit value of the required performances as Figure 4.12.

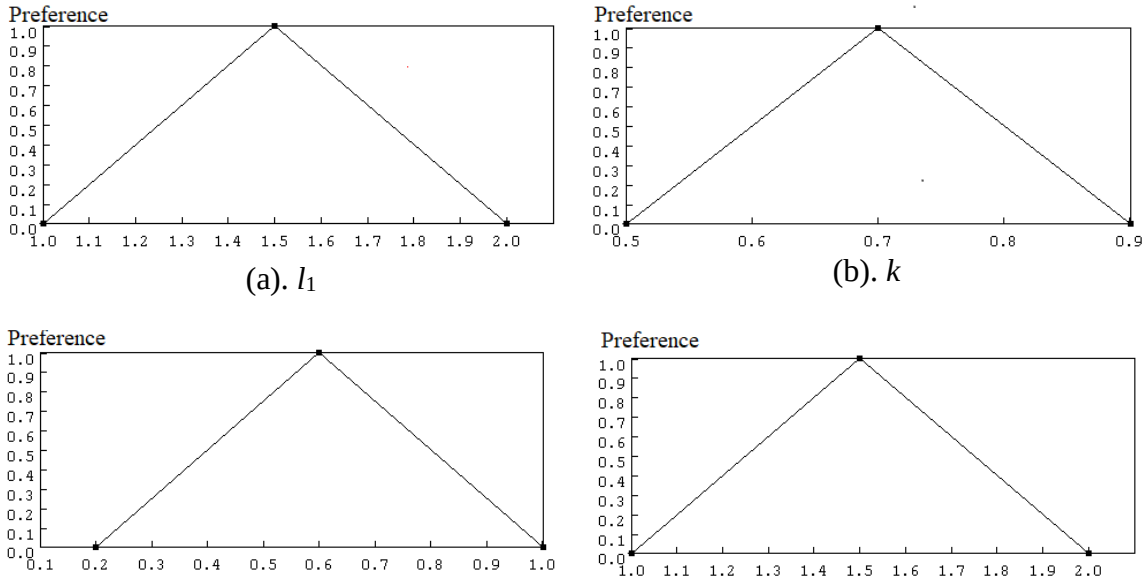

(a). l_1 (b). k

(c). c_x (d). c_{y1}

Figure 4.11. Preference functions of EMI filter's design parameters in case 1

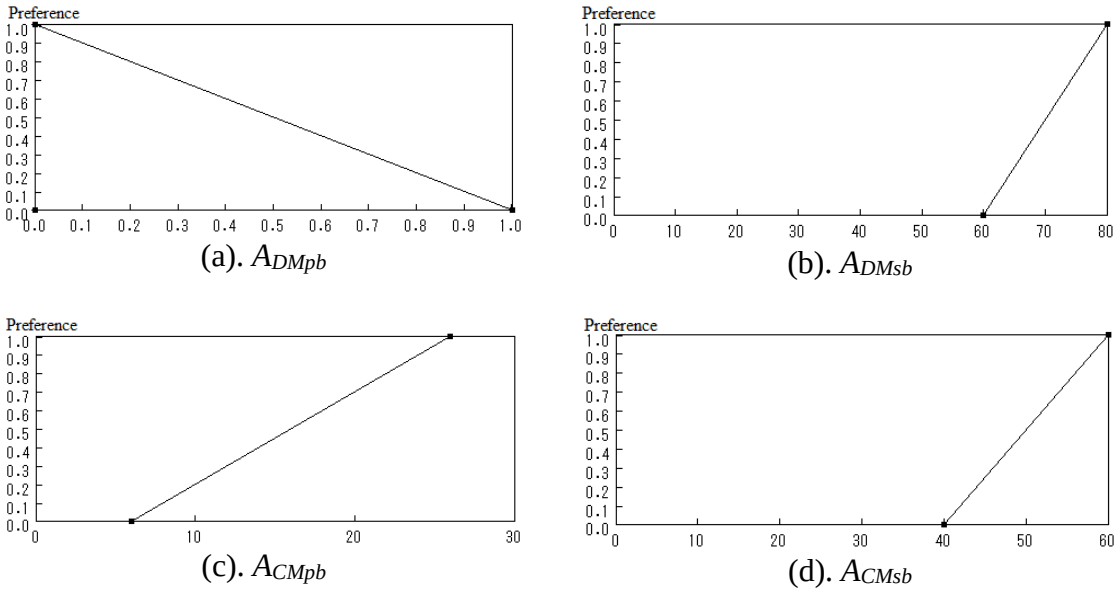

(a). A_{DMpb} (b). A_{DMsb}

(c). A_{CMpb} (d). A_{CMsb}

Figure 4.12. Preference functions of EMI filter's required performance in case 1

The design parameters are combined to create a feasible set, which serves as the possibility distribution set. This set propagation phase is explained in subsection 2.2.2.3. The feasible set is then narrowed through the "set narrowing" process, resulting in the narrowed distribution in the final phase. The PSD software is employed to carry out these tasks efficiently. Lastly, the frequency responses of the obtained ranges of design parameters are calculated to assess the validity of the proposed method. This analysis allows the designer to evaluate how well the EMI filter meets the required specifications and ensures that the design is capable of meeting the intended objectives.

4.2.1.3. Calculated results and discussion

Figure 4.13 displays a scatter diagram that compares the predicted values obtained by RSM and the actual values. The correspondence between the theoretically calculated values and the meta-modeling equations derived using RSM is evident in the plot. The horizontal axis represents the theoretically calculated values obtained when the element value is changed, while the vertical axis represents the values calculated using the meta-modeling formula based on the response surface methodology. In the ideal RSM, the actual value and the calculated value by RSM perfectly match, leading to a straight line with slope one and intersection zero (red-solid line in Figure 4.13). However, in practice, if there is a slight error and correlation coefficient of the meta-modeling equation, i.e., a low degree of approximation, then the range solution may not satisfy the required performance depending on the preference [65]. In this model, a high correlation is obtained with 0.98 or more.

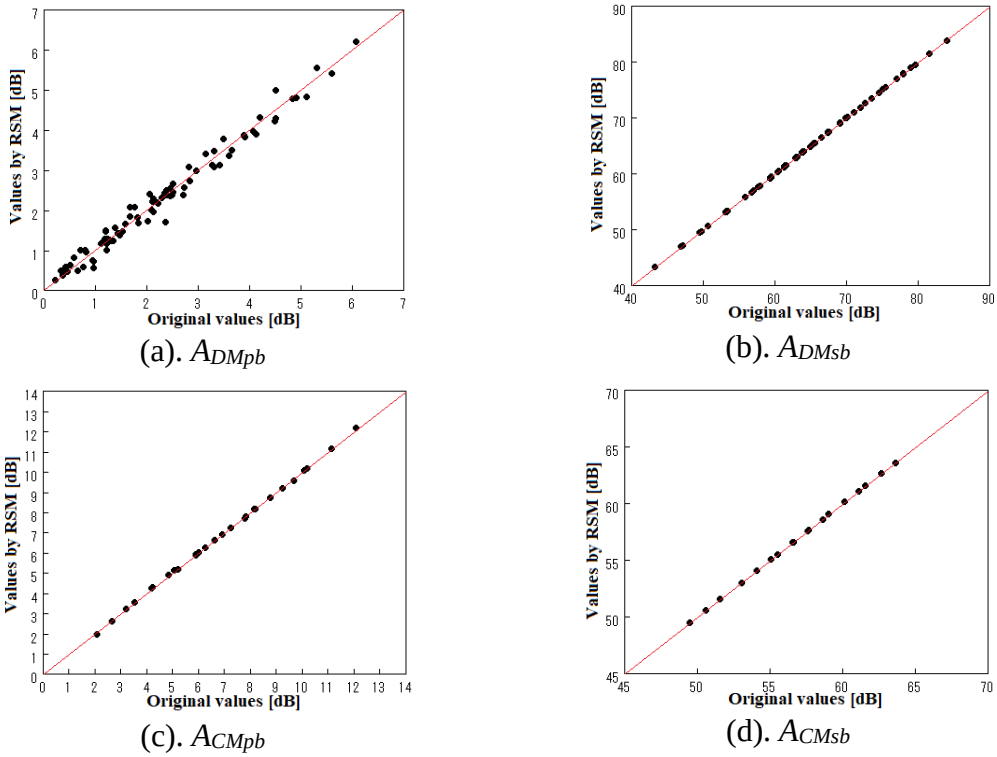

(a). A_{DMpb} (b). A_{DMsb}

(c). A_{CMpb} (d). A_{CMsb}

Figure 4.13. Scatter diagram is calculated with theoretically calculated values of attenuation of DM and CM compared with meta-modeling formula in case 1

The preference distribution as the final result and obtained range solution of the design parameters are shown in Table 4.4, Figures 4.14 and 4.15, which describes the relationship between the “Initial set” and “Narrowed set”. In Figure 4.14, the black-dot and red-solid lines are “Initial set” and “Narrowed set”, respectively. In Figure 4.15, the black-dot, the blue-solide and red-solid lines are “Required performance”, “Possibility distribution”, and “Narrowing distribution”, respectively. The final results indicate that obtained ranges of the design parameters satisfy the required performance sets.

Table 4.4. Narrowed set of EMI filter obtained by PSD in case 1

	Normalized frequency			
Elements	$l_1 = l_2$	k	c_x	$c_{y1} = c_{y2}$
Narrowed set	1.875 ~ 2.000	0.65 ~ 0.70	0.3 ~ 0.4	1.000 ~ 1.125
	Real frequency			
Real elements	$L_1 = L_2$ [mH]	k	C_x [μF]	$C_{y1} = C_{y2}$ [μF]
Narrowed set	1.49 ~ 1.59	0.65 ~ 0.70	0.096 ~ 0.127	0.32 ~ 0.36

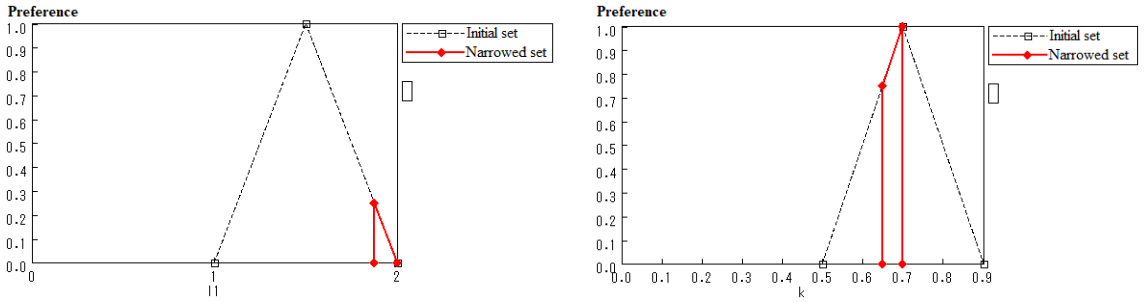

(a). l_1 (b). k

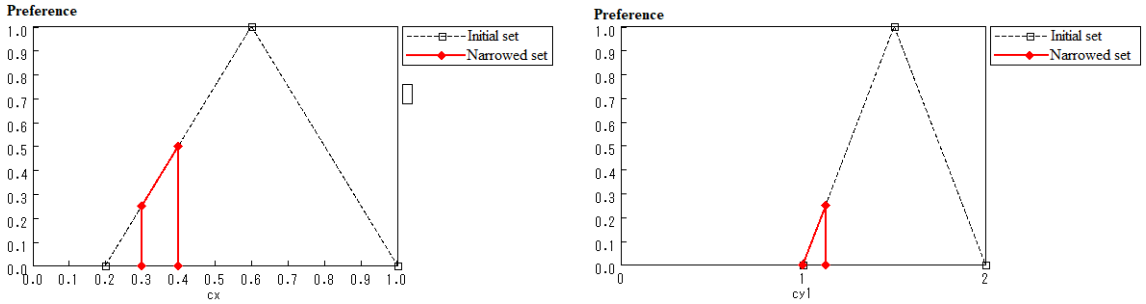

(c). c_x (d). c_{y1}

Figure 4.14. Preference set of EMI filter's design parameters in case 1

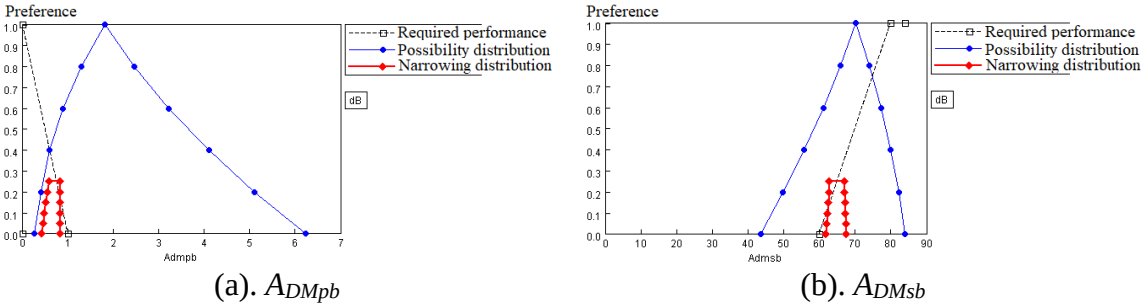

(a). A_{DMpb} (b). A_{DMsb}

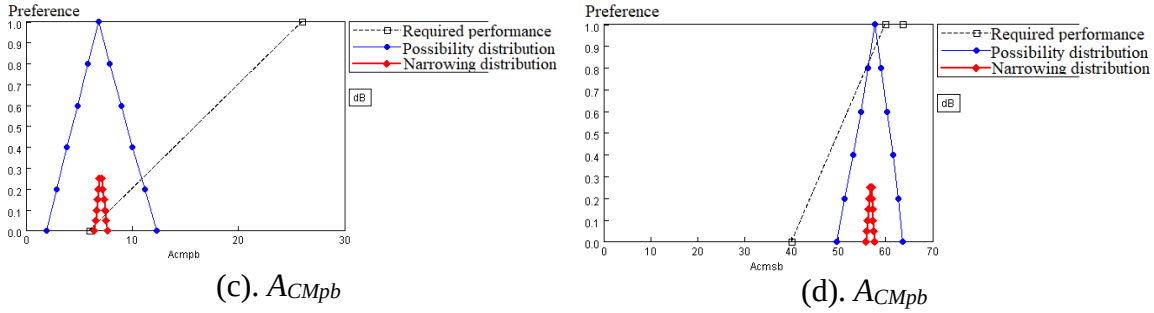

(c). A_{CMpb} (d). A_{CMpb}

Figure 4.15. Preference set of EMI filter's required performances in case 1

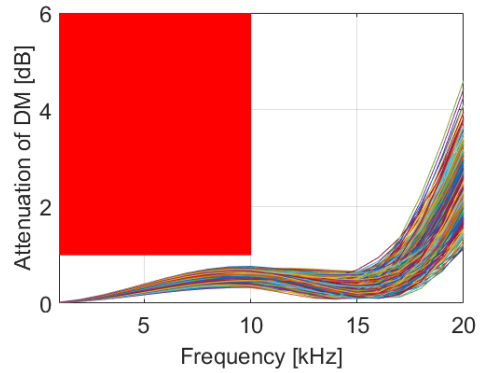

(a). Attenuation of DM at passband

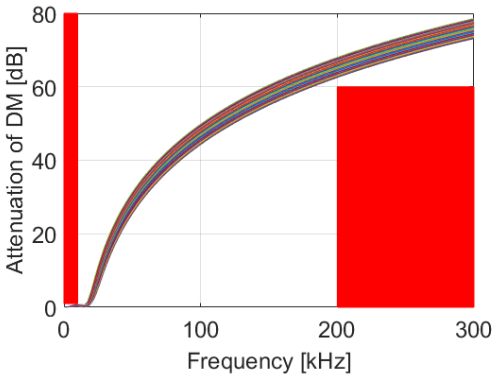

(b). Attenuation of DM at stopband

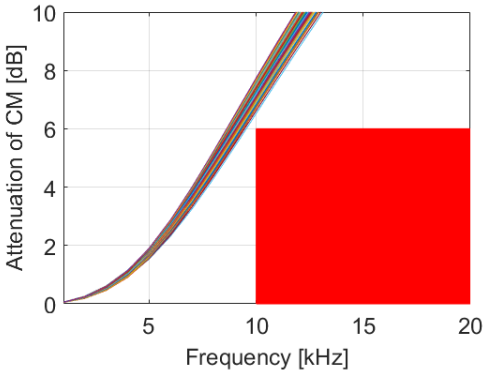

(c). Attenuation of CM at passband

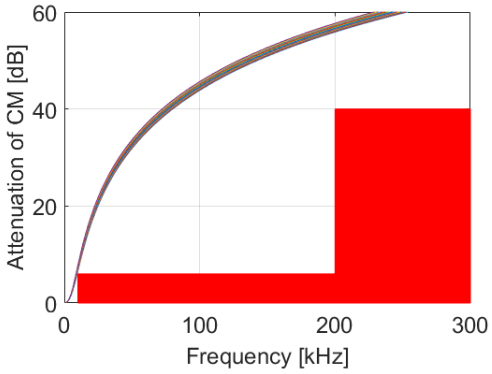

(d). Attenuation of CM at stopband

Figure 4.16. Frequency response of EMI filter is calculated based on design parameters in the range obtained by PSD in case 1

Figure 4.16 displays the calculated frequency responses for the EMI filter design parameters obtained within the range derived from the PSD method. The design parameters are selected from the minimum to the maximum values, resulting in around 1000 combinations. The plot illustrates the attenuation of DM and CM, and the multicolored curves represent the minimum to maximum values of the EMI filter's performances within the obtained range. The area filled with red indicates values that are out of range for the required performances. In this filter configuration, the order of DM is 3, and the order of CM is 2, so the attenuation characteristic of DM is better than the attenuation characteristic of CM in the stopband.

Figure 4.16 demonstrates that the characteristics of the filter meet the required performances, as the curves remain within the specified performance range. This confirms the validity of the design parameters obtained through the proposed method, and the proposed method is suitable for the EMI filter in an ideal case.

4.2.2. EMI filter with one stochastic parameter

The proposed method with an EMI filter in the ideal case have been demonstrated and tested. However, in practice, such an EMI filter is always imbalanced due to the impedance difference between lines. This subsection considers a simple case study with an uncertain parameter for a line of source and load circuit to demonstrate the validity of the proposed method [78, 79].

4.2.2.1. Specification

It is assumed that randomness occurs with the circuit in Figure 4.9 because the source and load resistors fluctuate with a maximum error of 5%. Hence, CM will appear because the difference in impedance leads to an imbalance. Although parasitic components such as the capacitor ESL are in the actual design, they are neglected in this preliminary study. The design specification includes:

- E_{g1} = 0.5 V, E_{g2} = -0.5 V,
- $R_{g0} = R_{L0} = 0\ \Omega$,
- $R_{g2} = R_{L2} = 50\ \Omega$,
- $R_{g1} = R_{L1} = 50 \pm 2.5\ \Omega$.

The required performances are the attenuation of DM voltage A_{VDM} and the value of CM current I_{CM} at the output terminal of the EMI filter as follows:

- $f \leq f_p$ = 10 kHz: $A_{VDMpb} \leq 1.0$ dB,
- $f \geq f_s$ = 200 kHz: $A_{VDMsb} \geq 46$ dB,
- $f_p \leq f \leq f_s$: $I_{CMpb} \leq 60$ dBμA,
- $f \geq f_s$: $I_{CMsb} \leq 0$ dBμA.

4.2.2.2. Research Methodology

a. Determination of the initial element values

The same three-level initial values as subsection 4.2.1 are used in this subsection (Table 4.3).

b. Generation of initial data by PC

Similar to subsection 4.2.1, the attenuation of the DM voltage and CM current in 81 combinations (3^4) are calculated using Equations (2.25) and (2.27) correspond to the design parameters in Table 4.3. The difference here is that it is necessary to determine the output voltage and current corresponding to the change of the stochastic parameter.

With voltage, an expansion of the function $v(\xi)$ with ξ is a standardized random variable with zero mean and unit variance, in the form of a predefined orthogonal polynomial, for example [8]:

$$v(\xi) \approx v_0\phi_0(\xi) + v_1\phi_1(\xi) + v_2\phi_2(\xi) + \ldots \tag{4.4}$$

where v_0, v_1, and v_2 are undetermined PC expansion coefficients and ϕ_0, ϕ_1, ϕ_2, … are polynomials used according to the probability distribution of the random variable ξ. The orthogonal polynomials ϕ_k by inner product are:

$$\langle \phi_m, \phi_n \rangle = \int_{-\infty}^{+\infty} \phi_m(\xi)\, \phi_n(\xi) w(\xi) d\xi = \delta_{mn} \tag{4.5}$$

that is, the above integral is only non-zero when $m = n$.

The function $w(\xi)$ in Equation (4.5) is the probability density function (PDF) of ξ, determined by the statistical model corresponding to the stochastic parameters in the problem.

The stochastic parameters here are the values of the source and load resistors varying according to a Uniform distribution with PDF as $w(\xi) = 1/2$. This subsection uses the second-order expansion of PCE with the randomness problem.

The corresponding orthonormal polynomials satisfying Equation (4.5) are the normalized Legendre polynomial. With PC expansion of the second order, the first three polynomials are:

$$\begin{aligned} \phi_0 &= 1 \\ \phi_1 &= \sqrt{3}\xi \\ \phi_2 &= \frac{1}{2}\sqrt{5}(3\xi^2 - 1) \end{aligned} \tag{4.6}$$

Various techniques can define PCE coefficients in Equation (4.4). Specifically, this dissertation uses the stochastic Galerkin method. This method determines the expansion

coefficient of order k from the orthogonal by taking the inner product ϕ_k on both sides of PCE.

The source and load resistors are expressed by PCE as:

$$R(\xi) \approx R_0\phi_0(\xi) + R_1\phi_1(\xi) + R_2\phi_2(\xi) \tag{4.7}$$

The expansion coefficients in Equation (4.7) are calculated by the projection of the analytic expressions of the source and load resistors into basic functions as:

$$R_k = \langle R(\xi), \phi_k \rangle = \int_{-1}^{+1} R(\xi)\,\phi_k(\xi) \times 0.5 \times d\xi \tag{4.8}$$

with k = 0, 1, 2.

Auxiliary matrices are used to get resistor value as a matrix:

$$\boldsymbol{R} = R_0\boldsymbol{A_0} + R_1\boldsymbol{A_1} + R_2\boldsymbol{A_2} \tag{4.9}$$

with the auxiliary matrix $\boldsymbol{A_k}$ having the coefficients $A_{kmn} = \alpha_{kmn}$ as follows:

$$\alpha_{kmn} = \langle \phi_k, \phi_m, \phi_n \rangle = \int_{-1}^{+1} \phi_k(\xi)\phi_m(\xi)\phi_n(\xi)w(\xi)d\xi \tag{4.10}$$

For the normalized Legendre polynomials in Equation (4.6), these auxiliary matrices are:

$$\boldsymbol{A_0} = \begin{bmatrix} 1 & 0 & 0 \\ 0 & 1 & 0 \\ 0 & 0 & 1 \end{bmatrix} \tag{4.11a}$$

$$\boldsymbol{A_1} = \begin{bmatrix} 0 & 1 & 0 \\ 1 & 0 & 2/\sqrt{5} \\ 0 & 2/\sqrt{5} & 0 \end{bmatrix} \tag{4.11b}$$

$$\boldsymbol{A_2} = \begin{bmatrix} 0 & 0 & 1 \\ 0 & 2/\sqrt{5} & 0 \\ 1 & 0 & 2\sqrt{5}/7 \end{bmatrix} \tag{4.11c}$$

Next, voltage and current are represented by PCE as:

$$V = V_0\phi_0(\xi) + V_1\phi_1(\xi) + V_2\phi_2(\xi) \tag{4.12}$$

$$I = I_0\phi_0(\xi) + I_1\phi_1(\xi) + I_2\phi_2(\xi) \tag{4.13}$$

The expansion coefficients of Equations (4.12) and (4.13) can be obtained by solving the EMI filter equations from the ABCD matrix in subsection 2.1.3.5, and the voltage and current values are obtained. Next, using Equations (2.25) and (2.27) will get the attenuation of DM voltage and the value of CM current as initial data for PSD. Since the source and load

resistors in Equation (4.6) vary with ξ and EMI filter performances also vary with frequency and design parameters, the dissertation takes the worst-case data values of A_{VDM} and I_{CM} performance as the initial data.

c. Design of EMI filter by PSD method

The obtained initial data is used with the PSD method to obtain the design parameters for the EMI filter similar to subsection 4.2.1.

In Table 4.3, the initial range is defined by three levels. The preference functions for the design parameters are represented as isosceles triangles, with the maximum and minimum values defining the base of each triangle. This representation is similar to the concept shown in Figure 4.11.

Additionally, the preference functions for the required performances are depicted as linear diagonals, with the value PN = 0 corresponding to the limit value of the required performances. This visual representation is similar to the depiction in Figure 4.17.

The following steps of the PSD method are performed similarly to subsection 4.2.1.

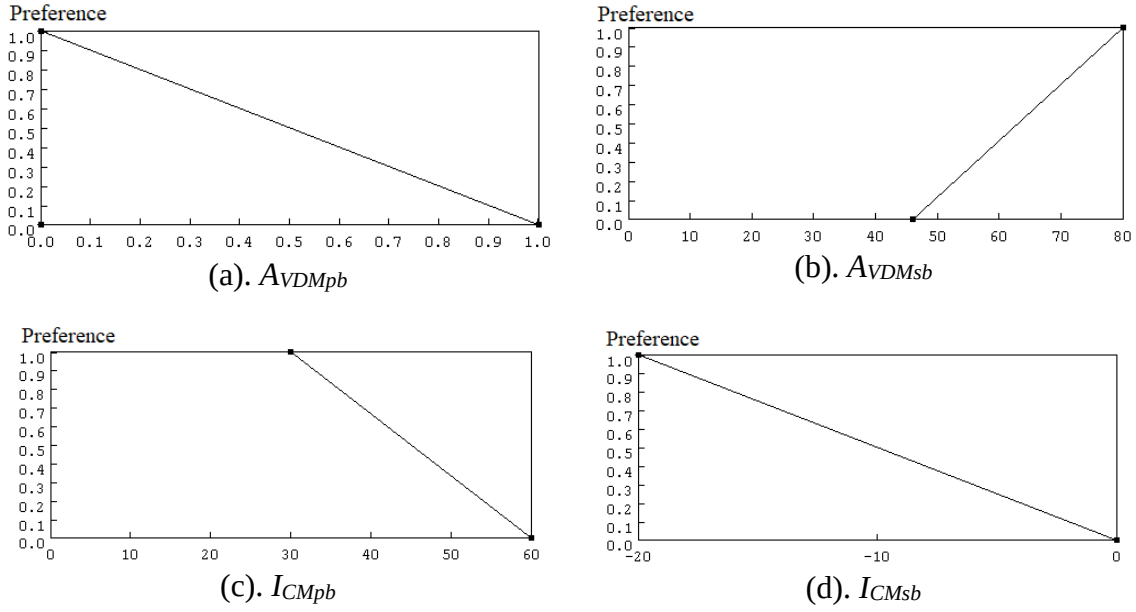

(a). A_{VDMpb} (b). A_{VDMsb}

(c). I_{CMpb} (d). I_{CMsb}

Figure 4.17. Preference functions of EMI filter's required performance in case 2

4.2.2.3. Calculated results and discussion

a. Generation of initial data by PC

Suppose resistor R_{g1} and R_{L1} are stochastic parameters that fluctuate around the value R_0 = 50 Ω with a uniform distribution expressed as:

$$R_{g1} = \mu_R + \sigma_R \xi \tag{4.14}$$

where μ_R is the average value of R_{g1}, that is, 50 Ω in the absence of fluctuation. σ_R is the maximum error of R_{g1}, equal to 5% of the average, equivalent to 2.5 Ω. The resistor value R_{L1} is also set the same.

Substituting Equation (4.14) into Equation (4.8) to calculate the second order PCE coefficient of resistors R_{g1} and R_{L1} as in [22], the result is as follows:

R_0 = 50, R_1 = 1.4434, R_2 = 2.2204 x 10^{-15} [Ω] (4.15)

Combining PCE coefficients in Equation (4.15) with Equations (4.9) and (4.11) to get the augmented matrices of resistors R_{g1} and R_{L1} (collectively, R) as follows [79]:

$$\boldsymbol{R} = \begin{bmatrix} 50 & 1.4434 & 2.2204 \times 10^{-15} \\ 1.4434 & 50 & 1.291 \\ 2.2204 \times 10^{-15} & 1.291 & 50 \end{bmatrix} [\Omega] \tag{4.16}$$

The augmented matrices of R_{g1} in Equation (4.16) are used to find the PCE coefficients of the voltage and current in Equations (4.12) and (4.13). Then, Equations (2.25) and (2.27) are used to calculate the attenuation of DM voltage and the value of CM current.

Figure 4.18 compares the results obtained by the MC and PC methods for the DM voltage and CM current at f = 10 kHz, with the value ξ varying step-by-step between -1 and 1. The value ξ = 0 in Figure 4.18b corresponds to the ideal case, so the CM current is almost zero. The maximum differences between the MC and PC methods are 0.6 µV for the DM voltage and 0.007 dB for the CM current.

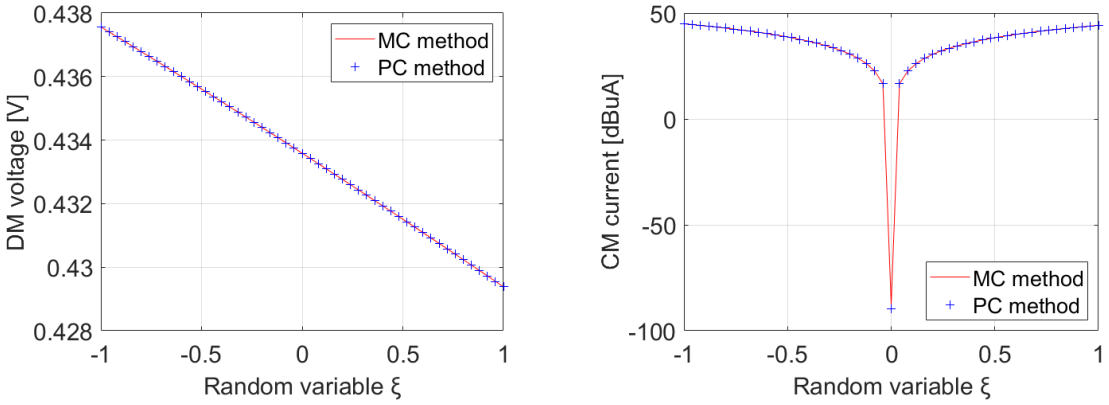

(a). DM voltage (b). CM current

Figure 4.18. Variation of DM voltage and CM current in ξ in case 2

Figure 4.19 shows a comparison of the results obtained by the MC and PC methods for the mean values of the DM voltage and CM current of 50 resistor trials with frequencies between 1 kHz and 300 kHz. The maximum differences between the MC and PC methods are 0.4 mV for the mean of the DM voltage and 4.2 dB for the mean of the CM current. As the number of random samples increases is 5000, the maximum difference between the MC and PC methods of the mean of the CM current decrease is 0.47 dB. The design parameters in Figures 4.18 and 4.19 are for the $l_1 = l_2 = 2$, $k = 0.7$, $c_x = 0.2$ and $c_{y1} = c_{y2} = 1.5$ case.

Table 4.5 compares the initial data generation times and maximum differences for the mean of DM voltage amd CM current of MC and PC methods. The MC method generates a random set of n input values of the resistors R_{g1} and R_{L1}. The MC program repeats n times the calculation process of the attenuation of DM voltage and CM current at the output terminal of the EMI filter, whereas the PC method only performs almost the whole calculation process once. The PC program generates n random values of ξ and repeats n times the calculation of the attenuation of DM voltage and CM current at the output terminal of the EMI filter only with Equations (4.11), (4.12), (2.25), and (2.27). Therefore, the PC method has a shorter initial data generation time than the MC method. As the number of random samples increases, the difference in computational efficiency of two methods becomes more significant, from 10 times with 50 samples to 36 times with 5000 samples.

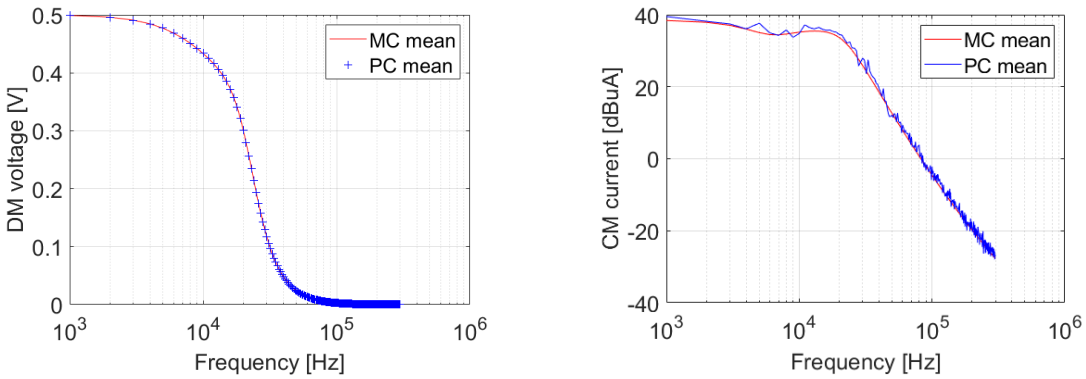

(a). DM voltage (b). CM current

Figure 4.19. Comparison of mean of DM voltage in case 2

Table 4.5. Comparison of initial data generation time of MC and PC in case 2

	Number of samples					
	50	100	500	1000	2000	5000
Generation time of PC (s)	1.8	2.3	6.24	11.2	21	50.7
Generation time of MC (s)	18	42	184	364	710	1805
Speed-up	x10	x18	x29	x32.5	x34	x36
Maximum difference for mean of DM voltage (mV)	0.4	0.15	0.1	0.06	0.04	0.02
Maximum difference for mean of CM current (dB)	4.2	3.48	1.48	0.99	0.73	0.47

Since the design parameters in Table 4.3 vary in 81 combinations (3^4), the resistors fluctuate with *n* random values, and EMI filter performances also vary with frequency, the dissertation takes the worst-case value of the EMI filter performances as initial data for PSD. The worst-case here means the maximum value of attenuation for the DM voltage in the passband and minimum in the stopband, as well as the maximum value of the CM current in both the passband and stopband.

b. Design of EMI filter by PSD

The EMI filter is designed using the PSD method with the initial data obtained from the PC method. First, the response surface methodology will use the initial data for meta-modeling. In this model, all 81 combinations are calculated for circuit analysis (numerical computation) with low computational costs.

Figure 4.20 shows a scatter diagram (predicted values by RSM and actual values). In this model, a high correlation is obtained with 0.93 or more.

The preference distribution as the final result and obtained range solution of the design parameters are shown in Table 4.6, Figures 4.21 and 4.22, which describes the relationship between the "Initial set" and "Narrowed set". In Figure 4.21, the black-dot and red-solid lines are "Initial set" and "Narrowed set", respectively. In Figure 4.22, the black-dot, the blue-solide and red-solid lines are "Required performance", "Possibility distribution", and "Narrowing distribution", respectively. The final results indicate that obtained ranges of the design parameters satisfy the required performance sets.

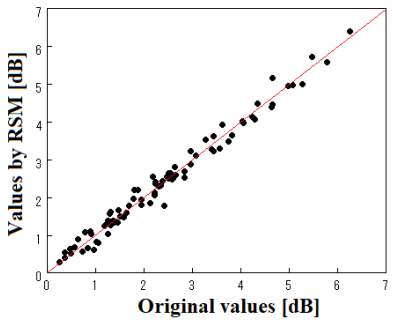

(a). Attenuation of DM voltage at passband

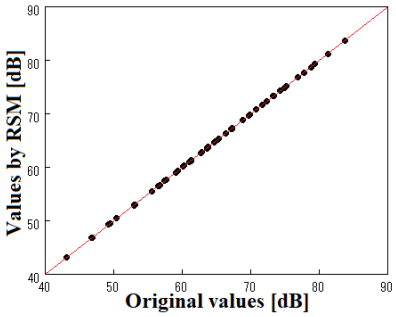

(b). Attenuation of DM voltage at stopband

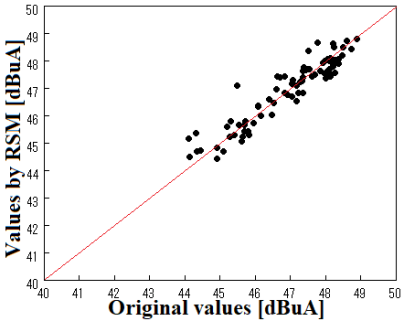

(c). CM current at passband

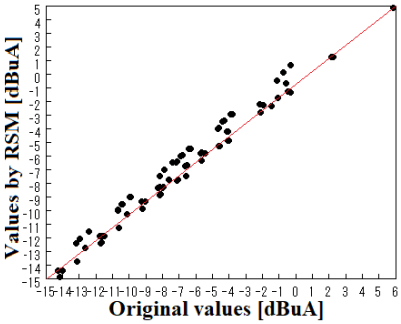

(d). CM current at stopband

Figure 4.20. Scatter diagram is calculated with theoretically calculated values of attenuation of DM voltage and CM current compared with meta-modeling formula in case 2

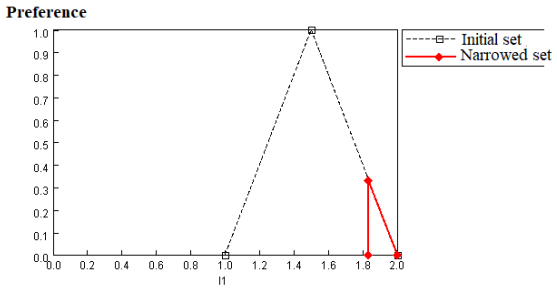

(a). l_1

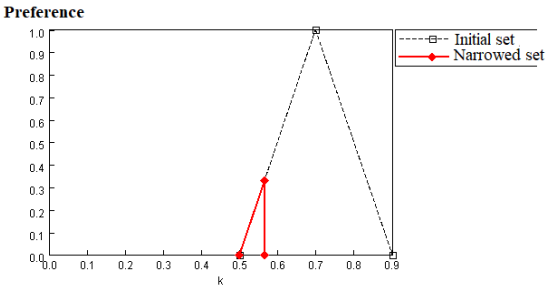

(b). k

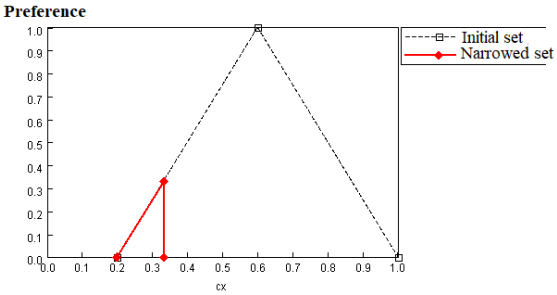

(c). c_x

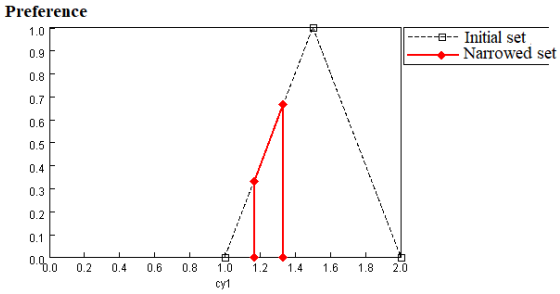

(d). c_{y1}

Figure 4.21. Preference set of EMI filter's design parameters in case 2

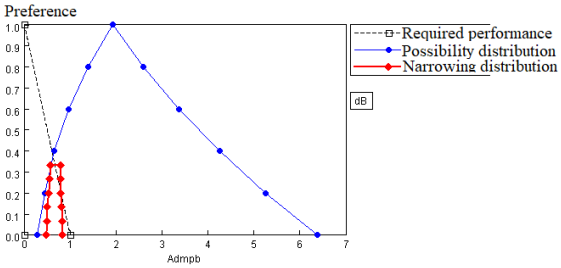

(a). A_{VDMpb}

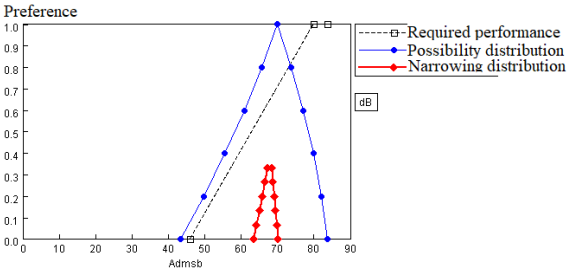

(b). A_{VDMsb}

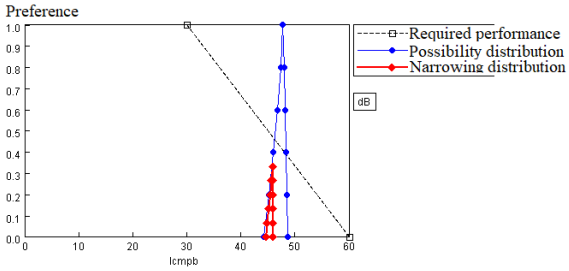

(c). I_{CMpb}

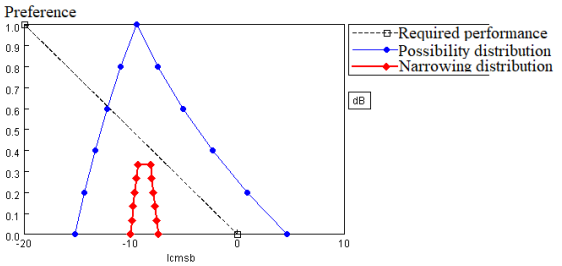

(d). I_{CMsb}

Figure 4.22. Preference set of EMI filter's required performances in case 2

Table 4.6. Narrowed set of EMI filter obtained by PSD in case 2

	Normalized frequency			
Elements	$l_1 = l_2$	k	c_x	$c_{y1} = c_{y2}$
Narrowed set	1.83 ~ 2	0.5 ~ 0.57	0.2 ~ 0.33	1.17 ~ 1.33
	Real frequency			
Real elements	$L_1 = L_2$ [mH]	k	C_x [µF]	$C_{y1} = C_{y2}$ [µF]
Narrowed set	1.46 ~ 1.59	0.5 ~ 0.57	0.064 ~ 0.105	0.372 ~ 0.423

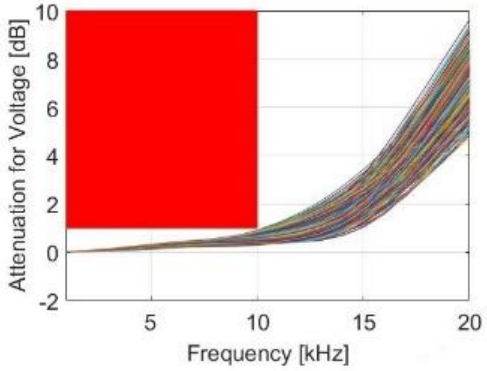

(a). Attenuation of DM voltage at passband

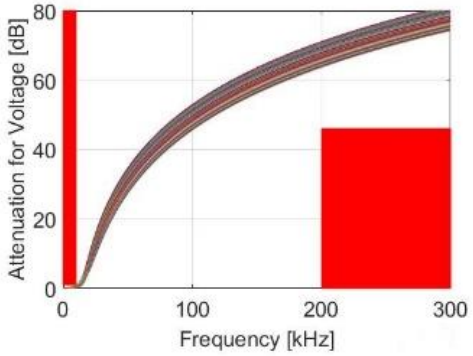

(b). Attenuation of DM voltage at stopband

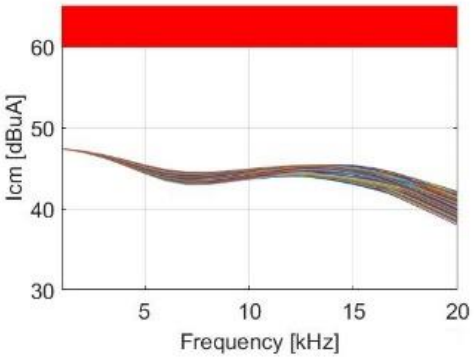

(c). CM current at passband

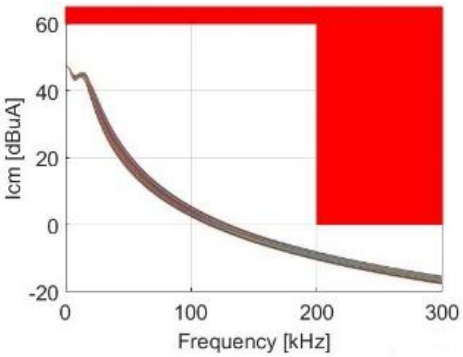

(d). CM current at stopband

Figure 4.23. Frequency response of EMI filter is calculated based on design parameters in the range obtained by PSD in case 2

The initial data generated by the MC method are also tested with the PSD method and had the same results as in Table 4.6. Since the design parameters are given in a range, not

specific numbers, a designer can apply arbitrary values of design parameters in a set. This is one of PSD's advantages for robustness.

To consider the validity of the obtained ranges of design parameters, frequency responses are calculated. Design parameters are selected in the range obtained by the PSD method from the minimum value to the maximum value to produce about 1000 combinations of design parameters. Value of variable ξ is step-by-step generated in the range of -1 and 1. Attenuation of DM voltage and CM current are calculated and shown in Figure 4.23. Multicolored curves represent the minimum to maximum values of EMI filter's performances for the range obtained. The area filled with red indicates out of range for the required performances.

c. Discussion

In Figures 4.18 and 4.19, there are some errors between the MC and PC methods, but the deviation is not significant and it can be seen that the PC method generates initial data for PSD with high enough accuracy and several times higher computational efficiency. As the number of random samples increases, the maximum difference between the MC and PC methods of the mean of the DM voltage and the CM current decreases. This suggests that increasing the number of random samples improves the accuracy and convergence of the PC method toward the MC results.

The PC method has a shorter initial data generation time than the MC method. As the number of random samples increases, the difference in computational efficiency of two methods becomes more significant.

From Figure 4.18, the worst-case value of the attenuation of the DM voltage can be predicted at ξ = -1 and CM current at ξ = -1 or 1. The reason is that this subsection considers only a simple case study, only one uncertain parameter (resistor) for a line of the source and load circuit, and the remaining resistor values are fixed (50Ω). In the case where R_{g1}, R_{g2}, R_{L1}, and R_{L2} are uncertain parameters, there is no guarantee that the worst-case value is at the boundary points of ξ. This subsection focuses on handling stochastic problems so that chooses the worst-case value from among many stochastic values.

Figure 4.23 show that the characteristics are satisfied with the required performances, and therefore the validity of the design parameters is demonstrated. As a result, it is confirmed that all required performances are met, and the proposed method can be applied even in an actual case where asymmetry exists in the power supply and the load.

4.2.3. EMI filter with many stochastic parameters

This subsection considers a more complex and general case study with multiple uncertain parameters to demonstrate the validity of the proposed method [80, 81].

4.2.3.1. Specification

Assume the circuit in Figure 4.9 experiences randomness due to fluctuations in the source and load resistors with maximum errors of 5%. Consequently, this difference in impedance gives rise to imbalances and the appearance of CM. The design specification includes:

- E_{g1} = 0.5 V, E_{g2} = -0.5 V,
- $R_{g0} = R_{L0} = 0$ Ω,
- $R_{g1} = 50 \pm 2.5$ Ω,
- $R_{g2} = 50 \pm 2.5$ Ω,
- $R_{L1} = 50 \pm 2.5$ Ω,
- $R_{L2} = 50 \pm 2.5$ Ω.

The required performances are the attenuation of DM voltage A_{VDM} and the value of CM current I_{CM} at the output terminal of the EMI filter as follows:

- $f \leq f_p$ = 10 kHz: $A_{VDMpb} \leq 1.0$ dB,
- $f \geq f_s$ = 200 kHz: $A_{VDMsb} \geq 46$ dB,
- $f_p \leq f \leq f_s$: $I_{CMpb} \leq 60$ dBµA,
- $f \geq f_s$: $I_{CMsb} \leq 0$ dBµA.

4.2.3.2. Research methodology

a. Determine initial element value

In this subsection, the same three-level initial values are utilized as in subsections 4.2.1 and 4.2.2 (Table 4.3).

b. Generation of initial data by PC

The method is similar to subsection 4.2.2. This subsection highlight the differences. The corresponding orthonormal polynomials satisfying Equation (4.5) are the normalized Legendre polynomial. With PC expansion of the second order and four stochastic variables,

use Equation (2.32), total number of polynomials are fifteen and the orthonormal polynomials as follows:

$$\phi_0 = 1$$

$$\phi_1 = \xi_1\sqrt{3}$$

$$\phi_2 = \xi_2\sqrt{3}$$

$$\phi_3 = \xi_3\sqrt{3}$$

$$\phi_4 = \xi_4\sqrt{3}$$

$$\phi_5 = \frac{1}{2}\sqrt{5}(3\xi_1^2 - 1)$$

$$\phi_6 = 3\xi_1\xi_2 \quad (4.17)$$

$$\phi_7 = 3\xi_1\xi_3$$

$$\phi_8 = 3\xi_1\xi_4$$

$$\phi_9 = \frac{1}{2}\sqrt{5}(3\xi_2^2 - 1)$$

$$\phi_{10} = 3\xi_2\xi_3$$

$$\phi_{11} = 3\xi_2\xi_4$$

$$\phi_{12} = \frac{1}{2}\sqrt{5}(3\xi_3^2 - 1)$$

$$\phi_{13} = 3\xi_3\xi_4$$

$$\phi_{14} = \frac{1}{2}\sqrt{5}(3\xi_4^2 - 1)$$

The source and load resistors are expressed by PCE as:

$$R(\xi) = \sum_{k=0}^{14} R_k\, \phi_k(\xi) \quad (4.18)$$

The expansion coefficients in Equation (4.18) are calculated by the projection of the analytic expressions of the source and load resistors into basic functions as:

$$R_k = \langle R(\xi), \phi_k \rangle = \int_{-1}^{1}\int_{-1}^{1}\int_{-1}^{1}\int_{-1}^{1} R(\xi)\, \phi_k(\xi) \times 0.5^4 \times d\xi_1 d\xi_2 d\xi_3 d\xi_4 \quad (4.19)$$

with k = 0, 1, 2, …, 14.

Auxiliary matrices are used to get resistor value as a matrix:

$$\boldsymbol{R} = \sum_{k=0}^{14} R_k \, \boldsymbol{A_k} \tag{4.20}$$

with the auxiliary matrix $\boldsymbol{A_k}$ having the coefficients $A_{kmn} = \alpha_{kmn}$ as follows:

$$\alpha_{kmn} = \langle \phi_k, \phi_m, \phi_n \rangle = \int_{-1}^{1} \int_{-1}^{1} \int_{-1}^{1} \phi_k(\xi)\phi_m(\xi)\phi_n(\xi) \times 0.5^4 \times d\xi_1 d\xi_2 d\xi_3 d\xi_4 \tag{4.21}$$

Next, voltage and current are represented by PCE as:

$$V = \sum_{k=0}^{14} V_k \, \phi_k(\xi) \tag{4.22}$$

$$I = \sum_{k=0}^{14} I_k \, \phi_k(\xi) \tag{4.23}$$

The expansion coefficients in Equations (4.22) and (4.23) can be determined by solving the EMI filter equations using the ABCD matrix, as described in subsection 2.1.3.5. This process yields voltage and current values. Subsequently, Equations (2.25) and (2.27) are employed to calculate the attenuation of DM voltage and the value of CM current, which serve as initial data for PSD. Considering that the source and load resistors in Equation (4.18) vary with ξ, and EMI filter performance depends on frequency and design parameters, the dissertation adopts the worst-case data values of A_{VDM} and I_{CM} performance as the initial data.

c. Design of EMI filter by PSD method

The initial data, as obtained from the previous steps, is now utilized with the PSD method to obtain the design parameters for the EMI filter, similar to subsection 4.2.2.

4.2.3.3. Calculated results and discussion

a. Generation of initial data by PC

In the given scenario, the resistor R_{g1}, R_{g2}, R_{L1} and R_{L2} are stochastic parameters that exhibit fluctuations around the value R_0 = 50 Ω with a uniform distribution expressed as:

$$R_{g1} = \mu_R + \sigma_R \xi_1 \tag{4.24a}$$

$$R_{g2} = \mu_R + \sigma_R \xi_2 \tag{4.24b}$$

$$R_{L1} = \mu_R + \sigma_R \xi_3 \tag{4.24c}$$

$$R_{L2} = \mu_R + \sigma_R \xi_4 \tag{4.24d}$$

where μ_R represents the average value of resistors, which is 50 Ω in the absence of fluctuation. σ_R is the maximum error of resistors, equivalent to 5% of the average, i.e., 2.5 Ω. ξ_1, ξ_2, ξ_3, and ξ_4 are random variables, with values between -1 and 1.

Substituting Equation (4.24) into Equation (4.19) to calculate the second order PCE coefficient of resistors R_{g1}, R_{g2}, R_{L1} and R_{L2} as in [75], similar to subsection 4.2.2.

Once PCE coefficients of resistors are determined, they can be combined with Equations (4.20) and (4.21) to obtain the augmented matrices of resistors R_{g1}, R_{g2}, R_{L1}, and R_{L2}.

Then with the augmented matrices of resistors, the PCE coefficients of the voltage and current in Equations (4.22) and (4.23) can be found. Finally, using Equations (2.25) and (2.27), the attenuation of DM voltage and CM current can be calculated.

Unlike case 2, case 3 has four uncertain parameters. Therefore, this case cannot directly compare the results of DM voltage and CM current. Figures 4.24 and 4.25 provide a comparison between the results obtained using the MC and PC methods for the mean values of the DM voltage and CM current of 50 resistor trials. The frequency range considered is from 1 kHz and 300 kHz. The maximum differences between the MC and PC methods are 0.94 mV for the mean of the DM voltage and 3.52 dB for the mean of the CM current. As the number of random samples increases to 5000, maximum difference between the MC and PC methods for the mean of the CM current decrease to 0.37 dB. Design parameters used in Figures 4.24 and 4.25 are for the case where $l_1 = l_2 = 2$, $k = 0.7$, $c_x = 0.2$ and $c_{y1} = c_{y2} = 1.5$.

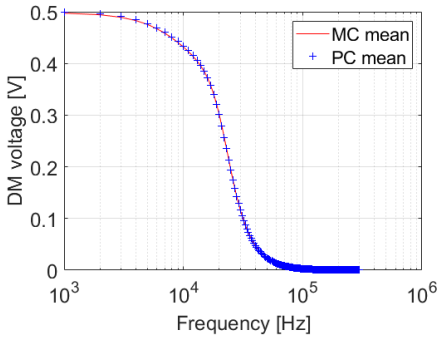

Figure 4.24. Comparison of mean of DM voltage in case 3

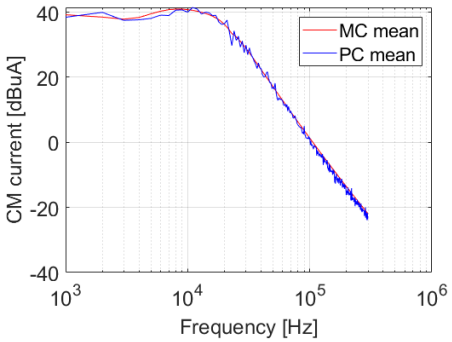

Figure 4.25. Comparison of mean of CM current in case 3

Table 4.7. Comparison of initial data generation time of MC and PC in case 3

	Number of samples					
	50	100	500	1000	2000	5000
Generation time of PC (s)	10	12	28	44	74	170
Generation time of MC (s)	16	29	142	288	578	1500
Speed-up	x1.6	x2.2	x5.1	x6.5	x7.8	x8.8
Maximum difference for mean of DM voltage (mV)	0.94	0.61	0.3	0.22	0.12	0.07
Maximum difference for mean of CM current (dB)	3.52	2.84	1.12	0.77	0.65	0.37

Table 4.7 presents a comparison of the initial data generation times and maximum difference for mean of DM voltage and CM current between MC and PC methods. As the number of random samples increases, the difference in computational efficiency between two methods becomes more significant. With 50 random samples, the PC method is 1.6 times faster than the MC method for generating initial data. However, as the number of random samples increases to 5000, the PC method becomes 8.8 times faster than the MC method.

Since the design parameters in Table 4.3 vary in 81 combinations, and the resistors fluctuate with *n* random values, along with EMI filter performances varying with frequency, the dissertation adopts the worst-case approach for selecting initial data for PSD. In this context, the worst-case value of EMI filter performances is chosen as the initial data.

The worst-case value in this scenario refers to selecting the maximum value of attenuation for the DM voltage in the passband and the minimum value in the stopband. Similarly, the maximum value of the CM current in both the passband and stopband is also chosen. This approach ensures that the PSD method considers the most challenging conditions and provides robust results that satisfy the required performance criteria even under the worst-case scenarios.

b. Design of EMI filter by PSD

EMI filter is designed using the PSD method, with initial data obtained from the PC method. Firstly, RSM leverages the initial data for meta-modeling. In this model, all 81 combinations undergo circuit analysis with low computational costs, allowing for efficient numerical computation. Figure 4.26 presents a scatter diagram comparing the predicted values from RSM with the actual values. Notably, a strong correlation of 0.92 or higher is observed, indicating the accuracy of the predictions.

The preference distribution, as the final result, and the range solution of the design parameters are illustrated in Table 4.8, Figures 4.27 and 4.28, delineating the relationship between the "Initial set" and the "Narrowed set". In Figure 4.27, the black-dot and red-solid lines represent "Initial set" and "Narrowed set", respectively. In Figure 4.28, the black-dot, the blue-solide and red-solid lines symbolize "Required performance", "Possibility distribution", and "Narrowing distribution", respectively. The final results indicate that obtained ranges of the design parameters satisfy the required performance sets.

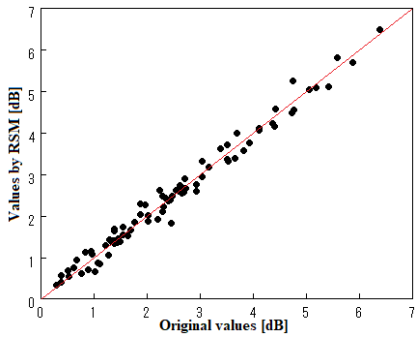

(a). Attenuation of DM voltage at passband

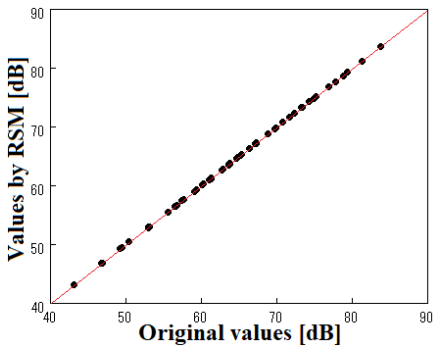

(b). Attenuation of DM voltage at stopband

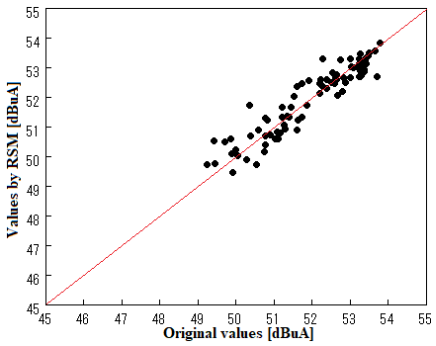

(c). CM current at passband

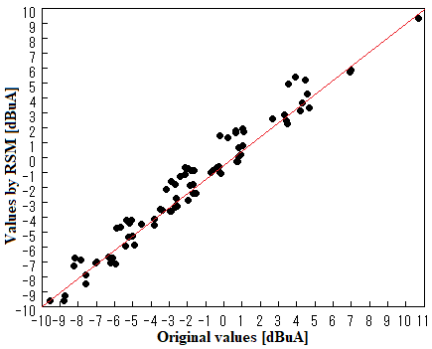

(d). CM current at stopband

Figure 4.26. Scatter diagram is calculated with theoretically calculated values of attenuation of DM voltage and CM current compared with meta-modeling formula in case 3

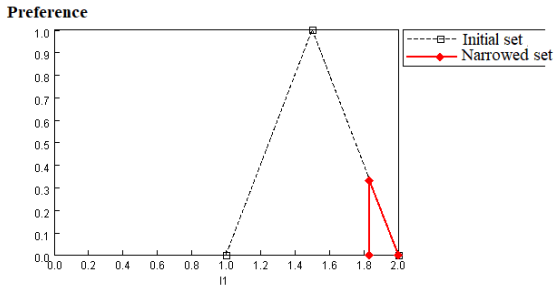

(a). l_1

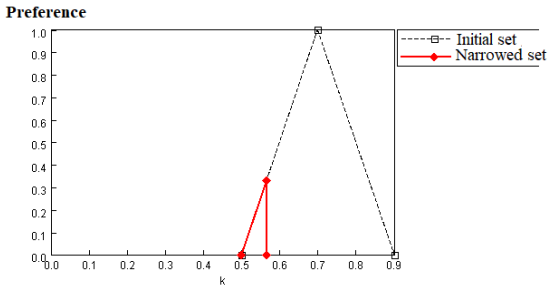

(b). k

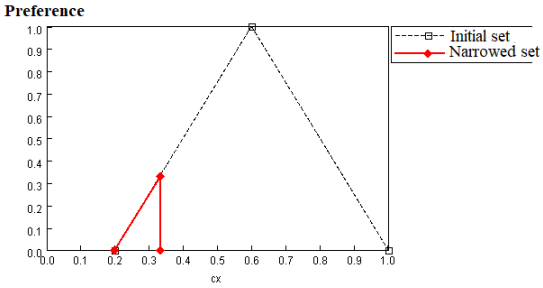

(c). c_x

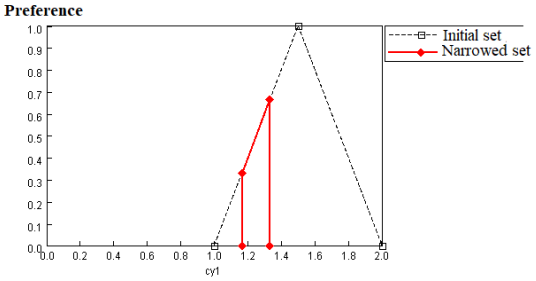

(d). c_{y1}

Figure 4.27. Preference set of EMI filter's design parameters in case 3

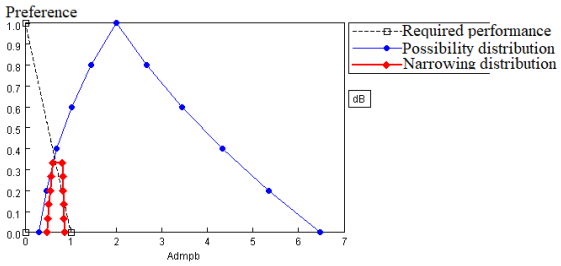

(a). A_{VDMpb}

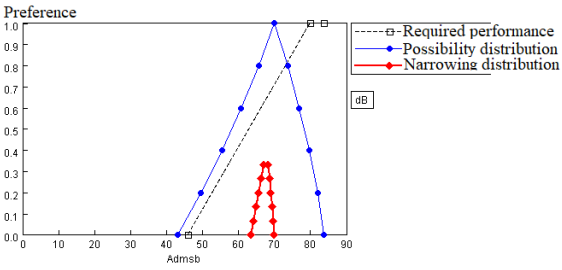

(b). A_{VDMsb}

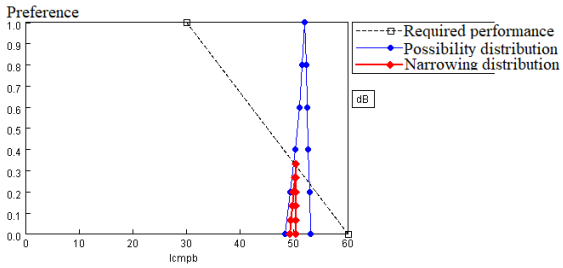

(c). I_{CMpb}

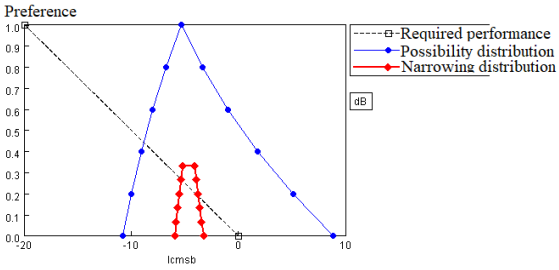

(d). I_{CMsb}

Figure 4.28. Preference set of EMI filter's required performances in case 3

Table 4.8. Narrowed set of EMI filter obtained by PSD in case 3

	Normalized frequency			
Elements	$l_1 = l_2$	k	c_x	$c_{y1} = c_{y2}$
Narrowed set	1.83 ~ 2	0.5 ~ 0.57	0.2 ~ 0.33	1.17 ~ 1.33
	Real frequency			
Real elements	$L_1 = L_2$ [mH]	k	C_x [µF]	$C_{y1} = C_{y2}$ [µF]
Narrowed set	1.46 ~ 1.59	0.5 ~ 0.57	0.064 ~ 0.105	0.372 ~ 0.423

The initial data generated by the MC method is also subjected to testing using (PSD method, yielding the same results as presented in Table 4.8. This confirms the consistency and reliability of the obtained ranges of design parameters through both methods.

An advantage of the PSD method is its ability to handle ranges of design parameters rather than a point value, providing flexibility for the designer to apply arbitrary combinations of design parameters within a defined set. This characteristic enhances the robustness of the EMI filter design, allowing for the exploration of various design scenarios under uncertainties and variable conditions.

To further assess the validity of the obtained design parameter ranges, frequency responses are calculated. Design parameters are selected within the range obtained by the PSD method, producing approximately 1000 combinations of design parameter sets. The variables ξ_1, ξ_2, ξ_3, and ξ_4 are randomly generated within the range of -1 and 1, reflecting the variability of the uncertain parameters. The attenuation of DM voltage and the value of CM current is then calculated and depicted in Figure 4.29. The multicolored curves represent the minimum to maximum values of the EMI filter's performance for the obtained range of design parameters. The area filled with red indicates values that fall outside the required performance range.

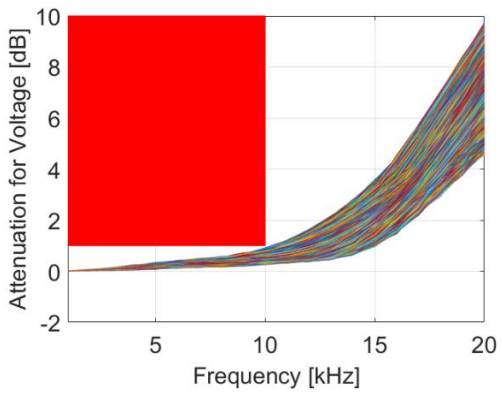

(a). Attenuation of DM voltage at passband

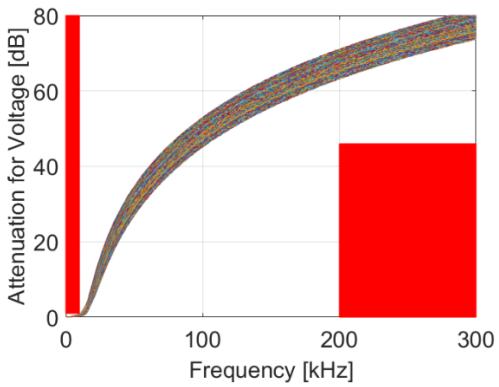

(b). Attenuation of DM voltage at stopband

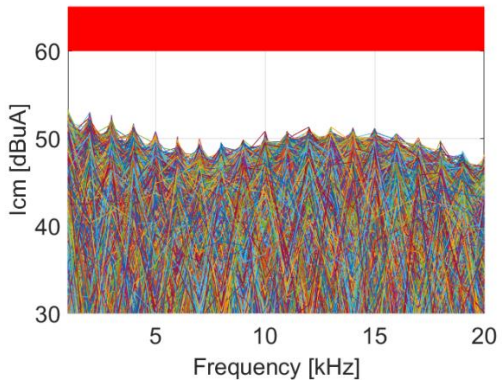

(c). CM current at passband

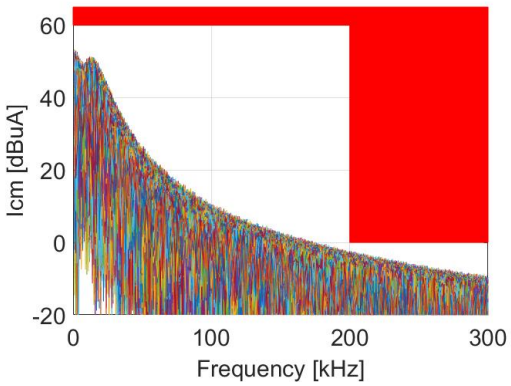

(d). CM current at stopband

Figure 4.29. Frequency response of EMI filter is calculated based on design parameters in the range obtained by PSD in case 3

c. Discussion

Figures 4.24 and 4.25 demonstrate that although there are some discrepancies between MC and PC methods, the deviation is not significant. The PC method generates initial data for the PSD method with high accuracy and significantly higher computational efficiency compared to the MC method. Moreover, as the number of random samples increases, the maximum difference between the MC and PC methods for the mean of the DM voltage and CM current decreases. The comparison between the MC and PC methods demonstrates that the PC method provides reliable results with good agreement with the MC method, particularly when a sufficient number of random samples are considered. These results reinforce the reliability and efficiency of the PC method for handling uncertainties in EMI filter design.

Notably, the PC method exhibits shorter initial data generation times than the MC method. As the number of random samples increases, the difference in computational efficiency between the two methods becomes even more pronounced. This indicates that the PC method becomes increasingly advantageous over the MC method as the number of samples grows, making it a more efficient choice for handling a larger number of random values. Besides, compared with the results in subsection 4.2.2, when the number of stochastic parameters increases, the computational efficiency of the PC method will decrease.

Figure 4.29 shows that the design parameters obtained through the PSD method satisfy the required performances. The characteristics of the EMI filter meet the desired specifications, validating the effectiveness of the proposed method. It is confirmed that all required performances are met, demonstrating the robustness of the proposed method even in practical cases where asymmetry exists in the power supply and load.

4.3. Summary

In Chapter 4, the dissertation experimented with the proposed method in Chapter 3 with different applications, such as the metal sheet of enclosure and EMI filter. With the EMI filter, the dissertation has tested different cases, from simple to complex, including uncertain parameters. The final results obtained as a set from the PSD method are validated. In addition, initial data and the results obtained when using the PC method in the proposed method are also compared with the MC method and show an improvement in the calculation efficiency but still keep the required accuracy.

Overall, the combination of the PC method and the PSD method provides a powerful and efficient approach for designing EMI filters with multiple uncertain parameters. The method enables the exploration of design spaces, considering uncertainties and meeting performance objectives while ensuring computational efficiency and robustness.

Chapter 5
Conclusion

In the framework of this dissertation, the author attempt to propose a design method for electronic devices, with the main application being EMC solutions, to meet multi-objective requirements. The dissertation also consider problems closest to practical scenarios, including multiple uncertain parameters ranging from simple to complex cases. To address the stated problem, the dissertation has handled the following two main contents:

+ Firstly, employ the PC method to simulate uncertain parameters and generate initial data for applications.

+ Secondly, utilize the PSD method to find the design parameter values within a range that meets multi-objective requirements.

Subsequently, the obtained design solution has also been validated. The results of the proposed design could be obtained within a range, not a specific number, and the design met the required performances. This demonstrates a strong attribute of the proposed method.

By using the PC method in the preliminary phase of the design process, the dissertation have addressed the randomness issue and obtained the necessary data with high computational efficiency and good accuracy compared to traditional methods based on the MC method. When combined with the PSD method, the final results produced by the PC and MC methods are the same (in the form of a range). The use of the PC method helps accelerate the computation speed several times, depending on the required number of samples, uncertain parameters, and the original computation process. The difference ranges from a few times to several tens or even hundreds of times. The results demonstrate the potential of using the PSD method in the field of electronics, particularly concerning EMC. By combining the PC and PSD methods, the proposed method also addresses the drawback of the PSD method, which is the lack of appropriate input data for the requirements.

The dissertation still has some limitations, including:

+ When the number of uncertain parameters increases, the computational efficiency decreases. This is due to the increased number of polynomials required. Additionally, multiple integral functions are also needed to compute the coefficients of the PCE.

+ If the problem requires high accuracy, the order of the polynomial must also increase to ensure the desired accuracy, leading to an increase in the number of polynomials, thus reducing the computational efficiency.

Future work will focus on addressing the aforementioned limitations. The use of techniques to approximate multiple integral functions will be considered. Furthermore, I will continue to explore the application of the proposed method (PSD combined with PC) in electronics and EMC domains (the lower level of the EMC pyramid).

References

[1] K. Tatebayashi, *Taguchi Method (in Japanese)*, JUSE Press, 2004.

[2] A. C. Ward, J.K. Likker, J.J. Cristiano and D.K. Sobek, “The Second Toyota Paradox: How Delaying Decisions Can Make Better Cars Faster”, Sloan Management Review, pp. 43-61, 1995.

[3] H. Ishikawa, *Set-Based Design Approach Multi-Objective Optimum Design (in Japanese)*, Corona, 2010.

[4] H. Inoue, et al., *Electromagnetic Noise in Electronic System - EMC Evaluation and Solution (in Japanese)*, Chapter 5.1 Passive Element and Filter, pp. 129-141, Ohm, 2012.

[5] F. Viani, F. Robol, M. Salucci and R. Azaro, “Automatic EMI Filter Design Through Particle Swarm Optimization”, IEEE Transactions on Electromagnetic Compatibility, vol. 59, no. 4, pp. 1079-1094, August 2017.

[6] M. Kawakami, H. Ishikawa, Y. Kami, and F. Xiao, “An Application of the Preference Set-based Design Method to Filter Designs”, 2015 IEEE International Symposium on Electromagnetic Compatibility (EMC), Dresden, Germany, pp. 1315-1318, 2015.

[7] I. S. Stievano, P. Manfredi, and F. G. Canavero, “Stochastic Analysis of Multiconductor Cables and Interconnects”, IEEE Transactions on Electromagnetic Compatibility, vol. 53, no. 2, pp. 501-507, May 2011.

[8] P. Manfredi, D. V. Ginste, I. S. Stievano, D. D. Zutter, and F. G. Canavero, “Stochastic Transsmission Line Analysis via Polynomial Chaos Methods: An Overview”, IEEE Electromagnetic Compatibility Magazine, vol. 6, no. 3, pp. 77-84, November 2017.

[9] C. R. Paul, *Introduction to Electromagnetic Compatibility*, John Wiley & Sonc Inc., 2006.

[10] “CISRP-22”, edition 6.0, IEC, 2009.

[11] “IEC EN 61000”, IEC.

[12] “MIL-STD-461F”, 10 December 2007.

[13] F. Szoncsó, “Introduction to EMC”, CERN SC.

[14] M. I. Montrose, *Printed Circuit Board Design Techniques For EMC Compliance: A*

Handbook for Designers, Second Edition, IEEE Press Series on Electronics Technology, 2000.

[15] M. I. Montrose, "Introduction to Printed Circuit Board Design For EMC Compliance", Wiley/IEEE Press, 2000.

[16] J. Delaballe, "Cahier Technique no. 149 EMC", Schneider Electric, 2001.

[17] "EMI Shielding Design Guide", Tecknit, 2005.

[18] E. Benedict, "PCB Design for EMI/EMC Compliance", WEMPEC Seminar, 2000.

[19] J. Colotti, "EMC Design Fundamentals", Telephonics - Command Systems Division, 2003-2005.

[20] T. C. Lun, "Designing for Board Level Electromagnetic Compatibility", Freescale Semiconductor, Inc., 2005.

[21] T. Williams, *EMC for Product Designers*, Elsevier's Science & Technology Rights Department in Oxford, UK, 1992.

[22] M. Aamir and M. F. Saleem, "Analysis of Noise Reduction Techniques in Embedded Systems", National Conference on Emerging Technologies, 2004.

[23] "Design For EMI", Intel, 1999.

[24] M. I. Montrose, L. Enxiao, and E-P. Li, "Analysis on the Effectiveness of Printed Circuit Board Edge Termination Using Discrete Components Instead of Implementing the 20-H Rule", 2004 International Symposium on Electromagnetic Compatibility, Silicon Valley, CA, USA, vol. 1, pp. 45-50, 2004.

[25] "EMC Design Guide for Printed Circuit Boards", Engineering Specification, Ford Motor Company, 2002.

[26] E.B. Joffe and K-S. Lock, *Grounds for Grounding: A Circuit to System Hanbook*, Wiley-IEEE Press, 2010.

[27] E. Coca and D. Alexa, "Power Line Filters For Switching Power Supplies", 1999.

[28] N. Y. Nasser, "Practical Approach in Designing Conducted EMI Filter to Mitigate Common Mode and Differential Mode Noises in SMPS", Journal of Engineering and Development, vol. 16, no. 1, pp. 164-183, March 2012.

[29] P. Huang, Z. Liu, and J. Qi, "Simulation Analysis of Electromagnetic Shielding

Effectiveness in Ventilation Window of Waveguide", Journal of Residuals Science & Technology, vol. 13, no. 7, pp. 142-149, 2016.

[30] L. H. Hemming, *Architectural Electromagnetic Shielding Handbook: A Design and Specification Guide*, The Institute of Electrical and Electronics Engineers, Inc., 1992.

[31] X. C. Tong, *Advanced Material and Design for Electromagnetic Interference Shielding*, CRC Press, 2008.

[32] Y. Kayano, M. Kawakami, Y. Kami, H. Ishikawa, F. Xiao and H. Inoue, "Multi-Objective Design of EMI Filter for Differential Paired-Lines by Preference Set-based Design", EMC Sapporo & APEMC, pp. 812-815, June 2019.

[33] M. Berman, "All about EMI filters", Electronic Products, 2008.

[34] H. Watanabe, *Theory and Design of Passive Network*, Ohmsha, 1968.

[35] Y. Kayano, Y. Kami, H. Ishikawa, F. Xiao and H. Inoue, "A Study on Design Methodology of Transmission Line Type Filter by Preference Set-based Design Method", IEICE Technical Report, EMCJ2017-60, November 2017.

[36] Y. Kayano, Y. Kami, H. Ishikawa, F. Xiao and H. Inoue, "Design Methodology of Transmission Line Type Filter by Preference Set-based Design Method", IEICE Transactions on Communications, vol. J102-B, no. 3, pp. 237-247, March 2019.

[37] Y. Kayano, M. Kawakami, Y. Kami, H. Ishikawa, F. Xiao and H. Inoue, "A Study on Multi-Objective Design of EMI Filter by Preference Set-based Design Method", IEICE Technical Report, EMD2018-14, pp. 1-6, July 2018.

[38] Y. E. Nahm and H. Ishikawa, "A New 3D-CAD System for Set-based Parametric Design", The International Journal of Advanced Manufacturing Technology, vol. 29, pp.137-150, May 2006.

[39] D. K. Sobek, A. C. Ward and J. K. Liker, "Toyota's Principles of Set-based Concurrent Engineering", Sloan Management Review 40(2), pp. 67-83, 1999.

[40] R. H. Myers, D. C. Montgomery and C. M. Anderson-Cook, *Response Surface Methodology - Process and Product Optimization Using Designed Experiments*, Wiley, 2008.

[41] A. I. Khuri and S. Mukhopadhyay, "Response Surface Methodology", Wiley Interdisciplinary Reviews: Computational Statistics, vol. 2, no. 2, pp. 128-149, 2010.

[42] D. C. Montgomery, *Design and Analysis of Experiments*, Wiley, 2012.

[43] S. H. Hall and H. L. Heck, *Advanced Signal Integrity For High-Speed Digital Designs*, Chapters 14, John Wiley & Sonc Inc., 2008.

[44] W. W. Finch and A. C. Ward, "Quantified Relations: A Class of Predicate Logic Design Constraint among Sets of Manufacturing, Operating and Other Variables", ASME Design Engineering Technical Conference, Irvine, CA, pp. 18-22, 1996.

[45] W. W. Finch and A. C. Ward, "A Set-based System for Eliminating Infeasible Design in Engineering Problems dominated by Uncertainty.", ASME Design Engineering Technical Conference, Sacramento, CA, pp. 55-66, 1997.

[46] J. Kennedy and R. Eberhart, "Particle Swan Optimization", Proceedings of International Conference on Neural Networks, Perth, WA, Australia, vol. 4, pp. 1942-1948, 1995.

[47] M. Clerc and J. Kennedy, "The Particle Swarm - Explosion, Stability, and Convergence in a Multi-Dimensional Complex Space", IEEE Transactions on Evolutionary Computation, vol. 6, no. 1, pp. 58-73, February 2002.

[48] Y. Kami, Y. Kayano, H. Ishikawa, and F. Xiao, "On Techique of Preference Set-based Design", IEICE Technical Report, EMCJ2017-59, November 2017.

[49] G. Capraro and C. R. Paul, "A Probabilistic Approach to Wire Coupling Interference Prediction", Proceedings of International Zurich Symposium on Electromagnetic Compatibility, Zurich, Switzerland, pp. 267-272, March 1981.

[50] S. Shiran, B. Reiser, and H. Cory, "A Probabilistic Model for The Evaluation of Coupling Between Transmission Lines", IEEE Transactions on Electromagnetic Compatibility, vol. 35, no. 3, pp. 387-393, August 1993.

[51] A. Ciccolella and F. G. Canavero, "Stochastic Prediction of Wire Coupling Interference", Proceedings of International Symposium on Electromagnetic Compatibility, Atlanta, GA, USA, pp. 51-56, August 1995.

[52] D. Bellan and S. A. Pignari, "A Prediction Model for Crosstalk in Large and Densely-packed Random Wire Bundles", Proceedings of International Symposium on Electromagnetic Compatibility., Wrocław, Poland, pp. 267-269, 2000.

[53] D. Bellan, S. A. Pignari, and G. Spadacini, "Characterization of Crosstalk in Terms of Mean Value and Standard Deviation", IEE Proceedings - Science, Measurement and

Technology, vol. 150, no. 6, pp. 289-295, November 2003.

[54] M. Wu, D. G. Beetner, T. H. Hubing, H. Ke, and S. Sun, “Statistical Prediction of “Reasonable Worst-case” Crosstalk in Cable Bundles”, IEEE Transactions on Electromagnetic Compatibility, vol. 51, no. 3, pp. 842-851, August 2009.

[55] D. Xiu and G. E. Karniadakis, “The Wiener-Askey Polynomial Chaos for Stochastic Differential Equations,” SIAM Journal on Scientific Computing, vol. 24, no. 2, pp. 619-644, 2002.

[56] D. Xiu, “Fast Numerical Methods for Stochastic Computations: a Review,” Communications in Computational Physics, vol. 5, no. 2-4, pp. 242-272, February 2009.

[57] M. Cesnovar, “Implementation of an Uncertatin Quantification Tool in MATLAB”, Technique University Munich, 2016.

[58] J. Baroth, D. Breysse, and F. Schoefs, *Construction Reliability: Safety, Variability and Sustainability*, Chapter 8, Wiley, 2013.

[59] A. Kaintura, T. Dhaene, and D. Spina, “Review of Polynomial Chaos-Based Methods for Uncertainty Quantification in Modern Integrated Circuits”, Electronics, vol. 7, no. 3, 2018.

[60] G. Blatman and B. Sudret, “An Adaptive Algorithm to Build Up Sparse Polynomial Chaos Expansions for Stochastic Finite Element Analysis”, Probabilistic Engineering Mechanics, vol. 25, no. 2, pp. 183-197, 2010.

[61] M. S. Eldred, “Recent Advances in Non-Intrusive Polynomial Chaos and Stochastic Collocation Methods for Uncertainty Analysis and Design”, Processdings of the 50th AIAA/ASME/ASCE/AHS/ASC Structures, Structural Dynamics, and Materials Conference, Palm Springs, CA, USA, AAIA 2009-2274, May 2009.

[62] C. Lacor and E. Savin, “General Introduction to Polynomial Chaos and Collocation Methods”, Springer International Publishing AG, Uncertainty Management for Robust Industrial Designin Aeronautics, Notes on Numerical Fluid Mechanics and Multidisciplinary Design 140, 2019.

[63] R. Askey and J. Wilson, “Some Basic Hypergeometric Polynomials that Generalize Jacobi Polynomials”, Memoirs of the American Mathematical Society, vol. 34, no. 319, Providence, RI, 1985.

[64] B. Sudret, “Uncertainty Propagation using Polynomial Chaos Expansion”, GRK1462 Summer School - Weimar, 2016.

[65] M. Kawakami, Y. Kami, H. Ishikawa, and F. Xiao, “Application of the Preference Set-based Design Method to Filter Design”, IEEJ Transactions on Fundamentals and Materials, vol. 136, no. 10, pp. 621-628, Oct. 2016.

[66] Y. Kayano, Y. Kami, H. Ishikawa, F. Xiao, and H. Inoue, “A Study on Design Methodology of Transmission Line Type Filter by Preference Set-based Design Method - (Part 2) Design of Experiments for Metamodeling”, IEICE Technical Report, EMCJ2017-106, March 2018.

[67] M. Kawakami, Y. Kami, H. Ishikawa, and F. Xiao, “Application of the Preference Set-based Design Method to EMI Filter Design”, IEICE Technical Report, EMCJ2015-105, pp.13-18, January 2016.

[68] Y. Kayano, M. Kawakami, Y. Kami, H. Ishikawa, and F. Xiao, H. Inoue, “Multi-Objective Design of EMI Filter by Preference Set-based Design”, IEICE Transactions on Electronics, vol. J102-C, no. 5, pp. 166-169, May 2019.

[69] K. Matsuishi, Y. Kayano, and F. Xiao, “Multi-Objective Design of Transmission Line Referenced to Meshed Ground Planes by Preference Set-based Design”, 2019 International Symposium on Electromagnetic Compatibility - EMC EUROPE, pp. 486-491, 2019.

[70] Y. Kayano, Y. Kami, H. Ishikawa, F. Xiao, and H. Inoue, “A Study on Design of Differential-Paired Lines with Meander Delay Line by Preference Set-based Design Method”, 2018 IEEE International Symposium on Electromagnetic Compatibility and 2018 IEEE Asia-Pacific Symposium on Electromagnetic Compatibility (EMC/APEMC), pp. 536-541, 2018.

[71] Y. Kayano, K. Miyazaga, H. Inoue, and Y. Kami, “Novel Multi-Objective Design Approach for Cantilever of Relay Contact using Preference Set-based Design Method”, IEICE Transactions on Electronics, vol. E103-C, no, 12, pp. 713-717, December 2020.

[72] R. Ghanem and P. Spanos, *Stochastic Finite Elements - A Spectral Approach*, Springer Verlag, 1991.

[73] K. Kawamura, Y. Kayano, Y. Kami, and F. Xiao, “Statistical Analysis of Transmission

Characteristics of Differential-Paired lines using Polynomial Chaos Methods", IEICE Technical Report, MW2019-86, pp. 109-114, October 2019.

[74] Z. Zhang, T. Dhaene, and D. Spina, "Calculation of Generalized Polynomial-Chaos Basis Functions and Gauss Quadrature Rules in Hierarchical Uncertainty Quantification", IEEE Transactions on Computer-Aided Design of Integrated Circuits and Systems, vol. 33, no. 5, pp. 728-740, May 2014.

[75] P. Manfredi, D. V. Ginste, D. D. Zutter and F. G. Canavero, "On the Passivity of Polynomial Chaos-Based Augmented Models for Stochastic Circuits," IEEE Transactions on Circuits and Systems I: Regular Papers, vol. 60, no. 11, pp. 2998-3007, November 2013.

[76] S. Vrudhula and J. M. Wang, "Hermite Polynomial Based Interconnect Analysis in the Presence of Process Variations", IEEE Transactions on Computer-Aided Design of Integrated Circuits and Systems, vol. 25, no. 10, pp. 2001-2011, October 2006.

[77] H. Ishikawa, Y. Kayano, N. Sasaki and Y. Fukunaga, *Preference Set-based Design*, Morikita, 2019.

[78] D. C. Bui, Y. Kayano, F. Xiao, and Y. Kami, "Multi-Objective Design of EMI Filter by Preference Set-based Design Method and Polynomial Chaos Method", IEICE Society Conference, B-4-6, p. 176, September 2022.

[79] D. C. Bui, Y. Kayano, F. Xiao, and Y. Kami, "Multi-Objective Design of EMI Filter with Uncertain Parameters by Preference Set-based Design Method and Polynomial Chaos Method", IEICE Transactions on Communications, vol. E106-B, no. 10, pp. 959-968, October 2023.

[80] D. C. Bui, Y. Kayano, F. Xiao, and Y. Kami, "Multi-Objective Design of EMI Filter with Multiple Uncertain Parameters by Preference Set-based Design Method and Polynomial Chaos Method", IEICE Society Conference, B-4-48, p. 228, September 2023.

[81] D. C. Bui, Y. Kayano, F. Xiao, and Y. Kami, "Enhanced EMI Filter Design by a Combination of Preference Set-based and Polynomial Chaos Methods under Multiple Uncertain Parameters", IEICE Technical Report, EST2023-93, pp. 158-163, October 2023.

Appendix A

Publication List

A. 1. Journal

[1] D. C. Bui, Y. Kayano, F. Xiao, and Y. Kami, “Multi-Objective Design of EMI Filter with Uncertain Parameters by Preference Set-based Design Method and Polynomial Chaos Method”, IEICE Transactions on Communications, vol. E106-B, no. 10, pp. 959-968, October 2023 (related to Chapter 4).

A. 2. Conference

[1] D. C. Bui, Y. Kayano, F. Xiao, and Y. Kami, “Multi-Objective Design of EMI Filter by Preference Set-based Design Method and Polynomial Chaos Method”, IEICE Society Conference, B-4-6, p. 176, September 2022.

[2] D. C. Bui， Y. Kayano, F. Xiao, and Y. Kami, “Multi-Objective Design of EMI Filter with Multiple Uncertain Parameters by Preference Set-based Design Method and Polynomial Chaos Method”, IEICE Society Conference, B-4-48, p. 228, September 2023.

[3] D. C. Bui， Y. Kayano, F. Xiao, and Y. Kami, “Enhanced EMI Filter Design by a Combination of Preference Set-based and Polynomial Chaos Methods under Multiple Uncertain Parameters”, IEICE Technical Report, EST2023-93, pp. 158-163, October 2023.

Author Biography

Bui Duc Chinh graduated from Hanoi University of Science and Technology (HUST), Hanoi, Vietnam and received Degree of Engineer in Electronics and Telecommunications B.Sc degree in 2013 and Degree of Master in Telecommunications Engineering in 2016. He is currently participating in a Doctoral course in Information and Network Engineering at the University of Electro-Communications (UEC), Tokyo, Japan, in 2020. He is also a Researcher at the Institute of Cryptographic Science and Technology - Vietnam Government Information Security Commission, Hanoi, Vietnam.

THE END